AD

Technical Report ECOM-01698-F

LONG-LIFE COLD CATHODE STUDIES FOR CROSSED-FIELD TUBES

FINAL REPORT

by

L. Lesensky
H. H. Miller
D. K. Das
K. W. Dudley
M. Arnum
C. R. McGeogh
R. A. Handy

SEPTEMBER, 1969

ECOM

UNITED STATES ARMY ELECTRONICS COMMAND · FORT MONMOUTH, N.J.

Contract DA28-043-AMC-01698 (E)

SPONSORED BY: ADVANCED RESEARCH PROJECTS AGENCY
ARPA ORDER NO. 345

RAYTHEON COMPANY
MICROWAVE AND POWER TUBE DIVISION
Waltham, Massachusetts

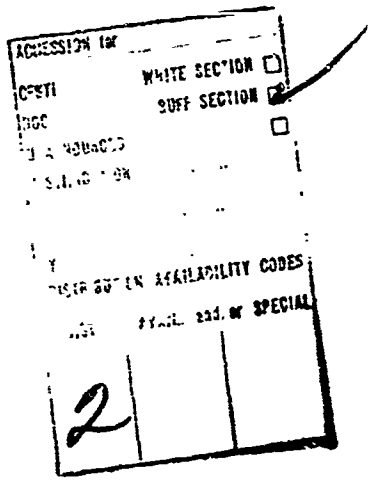

NOTICES

Disclaimers

The findings in this report are not to be construed as an official Department of the Army position, unless so designated by other authorized documents.

The citation of trade names and names of manufacturers in this report is not to be construed as official Government indorsement or approval of commercial products or services referenced herein.

Disposition

Destroy this report when it is no longer needed. Do not return it to the originator.

Reports Control Symbol
OSD-1366

Technical Report ECOM-01698-F

September 1969

LONG-LIFE COLD CATHODE STUDIES FOR CROSSED-FIELD TUBES

Final Report
15 October 1965 to 31 December 1968

Report No. 13
Contract No. DA28-043-AMC-01698(E)
DA Project No. 7900-21-223-12-00

Prepared by

L. Lesensky
H. H. Miller
D. K. Das
K. W. Dudley
M. Arnum
C. R. McGeogh
R. A. Handy

RAYTHEON COMPANY
Microwave and Power Tube Division
Waltham, Massachusetts

For

U. S. Army Electronics Command
Fort Monmouth, N. J.

This research is a part of Project DEFENDER, sponsored by the Advanced Research Projects Agency Department of Defense, under Order No. 345, and is conducted under the technical guidance of the U. S. Army Electronics Command, Fort Monmouth, N. J.

ABSTRACT

The evaluation of prospective materials for long life cold cathodes in crossed-field tubes has involved a materials investigation (Phase A), including secondary emission measurements and the study of electron and ion bombardment effects, and a second phase (Phase B) consisting of the testing of cold cathodes in crossed-field amplifier. (CFA' s) at medium to high power levels.

The main thrust of the program has been to respond to the life-limiting characteristics of the oxide-containing cold cathodes in the electron and ion bombardment environment of a CFA. The pure (unoxidized) metallic cold cathodes have a longer life expectancy but a lower secondary emission ratio (and therefore lower available current) in a CFA.

Both the materials investigation phase and the tube evaluation phase of the program have demonstrated the advantages of thin films of Al_2O_3 and BeO, and impregnated tungsten, although exploratory experiments were also performed on other materials of interest, such as semiconducting diamond, boron nitride, silver-magnesium, and beryllium-copper. It was shown that dissociation of the oxide films caused by electron bombardment in an operating CFA can be overcome by providing a low pressure atmosphere of O_2 and that δ can thereby be stabilized at an acceptably high value over extended periods of time. CFA life tests of up to 1000 hours have confirmed the feasibility of this approach.

Our experiments performed during both phases of the total program indicated a tendency of δ to stabilize at a value intermediate between the maximum and minimum values found as a result of repeated electron bombardment dissociation and O_2-assisted regeneration of the surface oxides. This may be tentatively explained by assuming that, after much surface manipulation, a metal-rich film of only 2-3 atom layers forms at the surface, thus protecting the δ-enhancing oxide layer underneath from further dissociation.

The effects of typical tube gases other than C_2 on Be and Al cold cathodes were also investigated in Phase A. The beneficial effects of H_2, CO_2, and N_2 on δ, observed particularly on Be cathodes, reminded one of the behavior of many metals which show a higher δ prior to degassing The non-specific nature of the effect leads one to discount surface dipole effects but rather to suspect a connection with the known lowering of the photoelectric work function due to gas absorbed perhaps to some depth into the metal.

The work performed on the barium-calcium-aluminate impregnated tungsten cathode demonstrated its stability under electron bombardment and in actual CFA operation. During a 350-hr CFA test the emission current boundary stayed practically constant, the cathode not requiring any initial thermal outgassing and activation. The tungsten cathode impregnated with barium-calcium-aluminate is therefore believed to be activated by electron and/or ion bombardment by releasing Ba from the aluminate and enhancing its diffusion along the tungsten surface. The high stability of the impregnated tungsten cathode implies adequate reactivation kinetics.

Based on the results of this investigation, the following guidelines are presented for the optimum selection of CFA cold cathode materials.

δ Required	Average Emission Current Density Required	Recommended Emitter Type
> 2.4	< 15 mA/cm^2	Oxygen assisted Al or Be
1.9 - 2.5	< 30 mA/cm^2	Barium-calcium-aluminate impregnated tungsten
≤ 1.9	----------	Pt

CFA life tests of up to 1000 hours have demonstrated successful operation of the impregnated W emitter as well as the oxygen-assisted Al and Be cathodes, with no indication of life limitation. Oxygen stabilization can indeed achieve very long cathode life. Oxygen source life of 10,000 hours in a high stress level CFA is believed to be achievable. Both Pt and impregnated tungsten cold cathodes can be reliably employed in applications and tube designs requiring δ' s of up to 1.8 to 2.5, but higher δ requirements call for oxide-film cold cathodes.

FOREWORD

This is the final report of a 3-year program of extensive investigation, sponsored by the Advanced Research Project Agency, with technology guidance provided by the United States Army Command, Fort Monmouth, New Jersey, to determine the secondary emission properties and life expectancy of candidate cold cathode materials in operating microwave crossed-field amplifiers. The total project, consisting of two phases, was supervised by L. Lesensky of Raytheon Company. Principal contributors to Phase A (materials investigation) were D. K. Das, L. Lesensky and H. H. Miller. Phase B (CFA testing) contributors were M. Arnum, K. W. Dudley, R. A. Handy and C. R. McGeogh. F. T. Hill contributed to the writing of the Final Report. D. Dobischek of ECOM contributed significantly to technical discussions and project review.

TABLE OF CONTENTS

TABLE OF CONTENTS (con't)

TABLE OF CONTENTS (con't)

LIST OF ILLUSTRATIONS

LIST OF ILLUSTRATIONS (con't)

LIST OF ILLUSTRATIONS (con't)

LIST OF ILLUSTRATIONS (con't)

LIST OF TABLES

1. PURPOSE

The Materials, Processes, and Techniques Group of the Microwave and Power Tube Division of Raytheon Company has conducted an extensive study of selected cold cathode materials to determine their secondary emission properties and their ability to withstand the environmental conditions in an operating crossed-field amplifier. Raytheon Company had been actively engaged in the research and development of cold cathode materials for crossed-field devices for many years before the initiation of this program of study sponsored by the United States Army Electronics Command, Fort Monmouth, New Jersey, under contract DA-28-043-AMC-01698(E).

The objective of this program is to develop long life cold cathodes capable of enduring bombardment by ions and large concentrations of high voltage electrons over periods of time up to 10,000 hours.

The use of a "cold" cathode is essential for efficient operation of devices being studied in this program. It is necessary that the cathode emit principally by secondary emission, rather than by thermionic emission in these devices. Although the cold cathode does not require thermal energy for secondary electron emission, the cathode may actually be at elevated temperature due to electron bombardment.

2. INTRODUCTION

2.1 Properties of materials for cold cathodes. The choice of cold cathode materials for use in crossed-field amplifiers (CFA's) is predicated upon the long life requirement in the severe environment of this device. A knowledge therefore of the following physical phenomena of materials was considered essential:

a. Secondary emission ratio (δ) as a function of primary energy.

b. The effect of high electron bombardment current density on δ.

c. The sputtering erosion of candidate materials due to ion bombardment.

d. The effect of typical tube gases on δ.

e. The effect of metal vapors on δ.

f. δ as a function of angle of incidence.

Of the above factors, because of their importance, the first three (a, b, c) received the most attention.

2.2 Significant technical areas in support of this program. The discussion of significant technical areas presented below will (1) focus attention on the desirable properties of cold cathode materials and on the principal life-limiting factors in CFA operation, and (2) provide guidelines

for the selection of cold cathode materials. Based on the above motivations, certain areas were selected for intensive investigation. The discussion is based on technical literature and consultation, and consists of the high-lighted technical areas as follows:

a. The relation between CFA performance and secondary emission properties. This is expressed principally in terms of the emission current boundary (ECB) phenomenon in cold cathode crossed-field tubes.

b. The basic mechanisms of secondary emission. High secondary emission ratios (δ's) are desirable and, while attempting to develop long life cold cathode materials, it is well to keep those factors in mind which tend to increase δ.

c. Electron bombardment effects. This is a life limiting factor. Both quantitative data concerning the effect on δ and an understanding of the dissociation processes are desirable.

d. Ion bombardment effects. Sputtering erosion is deemed to be a significant factor in limiting the life of oxide film secondary emitters. A number of the candidate materials under considerations in this program were oxide films.

e. Current transmission. The secondary emitting oxide film cathode must be capable of transmitting large tube currents (an important factor if thick non-conducting films are needed for life).

2.3 The relation between crossed-field amplifier (CFA) performance and secondary emission properties. Crossed-field amplifiers exhibit an emission current boundary which is the locus of emission-limited maximum current termini of operating lines (each operating line is at a constant magnetic field) in the V-I plane. One can understand the basic phenomenon by considering a current balance equation at the emission current boundary (ECB) of the form, $I_a = (\delta-1)I_{bb}$.

With the assumption that the available thermionic current is zero, as appropriate to cold cathode operation, let I_{bb} represent the back-bombardment current,* I_a the anode current, and δ the effective value of secondary emission ratio. If one assumes that I_{bb} is proportional to the characteristic current I_o, then $I_a \propto V_a^{3/2}$. However, the best fit to experimental data found in the literature on cold cathode magnetrons[2,3,4] is a linear relationship $I_a = a(V_a - b)$. The parameter b is positive and represents a threshold voltage for operation determined by the lower crossover (voltage at which δ first exceeds 1) of the δ vs V_p characteristic of the cathode material. The slope of the ECB, a, is proportional to $(\delta-1)$.

It is clear that the larger the δ, the larger will be the available current at a given voltage of operation. This places a premium on high secondary emission ratios. Values of δ significantly larger than that of Pt are not available from metals but must be sought among the semiconductors and insulators. Platinum is not adequate for many present and future CFA designs.

* A theoretical study of back-bombardment parameters has been made by J. M. Osepchuck of Raytheon Research Division and the results are reported in an appendix to Quarterly Report No. 4 of this contract (Technical Report ECOM 01698-4).

One may conclude therefore that large values of δ are needed for future CFA operating levels and that a desirable objective for a long life cold cathode is a δ of ~4-5.

2.4 High secondary emission ratio. This section will describe some of the significant properties of materials which influence the secondary emission ratio of metals, semiconductors, and insulators so that guidelines may be set up for the selection of cold cathode materials for a CFA.

The secondary emission process may be thought of as a two-step process. First, the incident primary electron loses energy as it penetrates the material so that only a small fraction of its initial energy results in the production of secondaries. Second in the process is the escape of secondaries from the surface of the material. The range of the primaries increases with increasing primary energy, while the maximum depth (escape depth) from which low energy secondaries can be extracted from the surface is independent of the primary energy. This phenomenon is responsible for the existence of a maximum in the dependence of δ on primary energy (and the maximum occurs when the primary range is approximately equal to the escape depth).

The secondary emission ratio (δ) for metals (δ_{max} for normal incidence) varies from 0.5 for Li to 1.9 for Ir, and is limited by the scattering of secondaries by conduction electrons. Absence of a temperature dependence of δ for metals indicates the minor role played by lattice vibrations. Contrary to what one might expect, δ_{max} for clean metals (no absorbed surface layer) is found to increase slowly with increasing work function.[5] However, adsorbed surface layers, which can lower the work function (φ) by creating a dipole layer of the proper sense, do in fact increase δ by increasing the escape probability of secondaries. For example, the adsorption of thorium,[6,7] barium,[6,8] or sodium[9] on tungsten increases its secondary emission yield and reduces its work function.

It is known that δ is proportional to the number of electrons per unit volume and increases with the density.[10] Sternglass[11] correlated δ_{max} with the position of metals within the periodic system of the elements, showing that the yield rises in each horizontal line of the periodic chart from the alkali metals to the multivalent ones.

The universal yield curve shows the similarity of the δ vs V_p (primary voltage) characteristic for various materials. This was pointed out by Baroody[12] who plotted δ/δ_{max} vs $V_p/V_{p_{max}}$. Several theoretical expressions for the normalized universal curve have been derived and compared[13] with experimental data. The original Baroody-Bruining derivation was based on Whiddington's Law for the energy loss of primaries. This deviates significantly for $V_p/V_{p_{max}} > 1$ by falling below the experimental data. Better agreement was found for a theoretical curve based on a power law for the practical range of primaries $R_p \sim (V_p)^n$ with a value[14] of the exponent $n = 1.35$. On this basis the secondaries are produced principally near the end of the range. If the scattering of primaries is taken into account, one obtains the "constant loss" curve, for which the energy dissipation is constant throughout the range. The constant loss curve provides good agreement with experimental data and is the one used for comparison with the data presented in this report.

Due to the basic limitations of metals, the quest for high δ materials leads one to semiconductors and insulators. The range of secondaries in insulators is enhanced by the absence of conduction electrons. Small-gap semiconductors have low δ's because of the presence of sufficient conduction electrons for the scattering of secondaries. The criterion for high δ in intrinsic semiconductors or insulators is based on the ratio of electron affinity to band gap (χ/Eg). The high δ for MgO is based on this criterion. A small value of χ/Eg implies a long range for the low energy secondaries and a concomitant increase of the yield as compared to a metal or small-gap semiconductor. Possible mechanisms of energy loss for secondaries in insulators are (1) electron-phonon interaction, (2) interaction with valence electrons (if the excitation energy of the secondaries in the conduction band is greater than the interband gap), and (3) interaction with lattice defects. The second of these is insignificant for wide band gap insulators. The larger dependence of δ on temperature in insulators than in metals implies the greater role of phonon interaction in the case of insulators.

An insulator may be used as a cold cathode in a CFA if it is used as a thin film on a metalic substrate (because of the limited conductivity of the insulator). If the insulator film is thin enough (comparable to secondary escape depth) then the substrate may play a role. It is desirable to use a high atomic number substrate to provide significant back-scattering of the primaries and subsequent increase in secondary generation within the insulating film.

Another factor which may be of significance is the observation that crystalline films have a higher yield than amorphous films (or ones having very small crystallites). Therefore, it would be desirable to process the emitter so as to produce a crystalline insulating film.

On the basis of the above discussion it can be seen that crystalline oxide films on a metallic, high atomic number, refractory substrate represent candidate cold cathode materials. MgO, Al_2O_3, or BeO films on a Pt substrate are examples of this.

Another approach is the use of a cermet or impregnated cathode in which a porous metallic matrix is filled with high δ material. Recently published reports[15, 16] are encouraging in this regard, particularly for the Ni cermet cathode with a measured δ of about 5 and capable of withstanding significant electron bombardment when operated at an optimum temperature of 600° C (warm cathode operation). It should be noted that the requirement for rf shutoff in the CFA may necessitate a compromise with the optimum operating temperature.

Still another approach would consider certain semiconductors, such as heavily p-doped GaAs. According to recent work[17] on the photoemissive properties of cesiated p-doped GaAs, the diffusion-recombination length is ~103Å. It is speculated that the secondary emission ratio of the uncesiated p-doped GaAs may also have a reasonably good δ in terms of the objectives of the present program.

In summary, one may list the following for achieving high δ materials for cold cathodes in a CFA:

a. High δ oxide films on a refractory, high atomic number substrate. The oxide film may be doped to achieve conductivity.

b. Cermet or impregnated cathodes.

c. Semiconductors, such as p-doped GaAs, having a long recombination length.

2.5 Electron bombardment effects. The principal requirements of a cold cathode in a CFA is a sufficiently high secondary electron emission ratio for the energy level of the back-bombardment electrons. Additional requirements are (1) no deterioration of this secondary yield below a desired minimum value, and (2) a depletion rate of the emitter material sufficiently low so that a pre-ascertained life may be achieved.

With the above requirements in mind we may proceed to evaluate the effects of electron bombardment on the various types of secondary emitters, i.e., metals, semiconductors, and insulators.

2.5.1 Metals. The effect on metals is likely to be insignificant. If the backbombardment electrons were to arrive on the cathode at an energy of 1000 volts and a current density of 1 amp/cm^2, and if secondary emission occurred at a δ of 2.0 with energies of approximately 5 electron volts, the balance of power of 990 watts/cm^2 area of the cathode must be removed from the cathode. The rate of removal must be sufficiently fast to keep the surface temperature low. If the temperature is maintained such that the surface of the cathode never exceeds a vapor pressure of 10^{-10} torr, no problem is envisioned. At 10^{-10} torr vapor pressure, the cathode surface will lose a mono-layer in roughly 5 hours due to evaporation. For Pt the temperature is approximately 1100°C for 10^{-10} torr vapor pressure.

As for metals, only three, Pt, Ir, and Os have a chance of becoming serious contenders for consideration. For the purpose of this program the metals may be considered of subsidiary significance, since their δ limit tube design possibilities.

2.5.2 Semiconductors. Elemental semiconductors do not possess high δ's. Their δ's may be improved, however, by depositing mono-layers of low work function elements, such as Na or Cs etc on the surface. But it is extremely unlikely that the cathode could go through bake-out cycles and retain such a coverage. In the event that the coverage is applied after bakeout, then for a cesium mono-layer, the temperature of operation will have to be -10°C for a vapor pressure of 10^{-8} torr and 75°C for Na for the same vapor pressure.

There is a possibility that heavily p-doped GaAs may have a high enough secondary emission ratio to satisfy the needs of the CFA even without a low work function coverage. However, there is a likelihood that it might evaporate during bake-out, since As has a vapor pressure of 10^{-8} torr at 105°C. It would thus be difficult to maintain the cathode intact through the bakeout cycle

unless gallium arsenide is a true chemical compound with an arsenic vapor pressure substantially lower than that of elemental arsenic.

No data on the decomposition of GaAs due to electron bombardment are available. However, it is expected that Ga and As would be released by the bombardment process and subsequently evaporated according to the elemental vapor pressure. It is desirable that the elemental components evaporate at equal rates in order to maintain the δ properties during electron bombardment life.

2.5.3 Insulators. Of the insulators, the best candidates at present are the oxides, such as Al_2O_3, MgO, BeO, and BaO. They do possess high secondary emission ratios, but they also have low electrical and thermal conductivities, and they decompose when bombarded by electrons. These problems can, however, be overcome.

For the moment let us consider the largest problem area, that of chemical decomposition. As early as 1936, Headrick and Lederer[18] showed that oxides such as nickel oxide or copper oxide, on being bombarded by electrons, would release gases and thus render vacuum tubes gassy, causing a resultant low emission of thermionic cathodes. The first quantitative work in this field was reported by Jacobs,[19] who demonstrated that when an electron reaches a critical energy, it is capable of decomposing an oxide into its component metal and oxygen. This critical energy is roughly equivalent to the heat of formation of the oxide. Assuming that 23 kilogram calories/mole is equivalent to 1 electron volt/molecule, we find that it will require no more than 5 to 15 electron volts to decompose such highly refractory oxides as MgO, BeO, ThO_2, etc. Much literature[20-24] has since been published giving similar results as Jacobs' original work. In addition, work done at Raytheon Company[25] to study the effect of back-bombardment on magnetron cathodes revealed extensive decomposition of ThO_2 in thoria tungsten cermet cathodes.

More recent work[26, 27, 28] has shown the dependence of the extent of decomposition on the current density. Claims are made that this dependence varies from the linear to the square of the current density. However, a conservative estimate would be that for 10^7 electron impacts, one molecule will decompose.[27] This seems to be a rather inefficient process, but it is still quite significant from our point of view when the total number of impacts are considered.

Assuming that back-bombardment current density is 1 amp/cm^2 of cathode surface, we can expect a 10,000 hour life at 0.1% duty cycle. With 10^{15} molecules of oxide/mono-layer/cm^2, and a thickness of each layer of about 4Å, the following calculations can be made:

Total No. of electron impacts per cm^2 during 10,000 hours $= 10,000 \times \frac{0.1}{100} \times 3600 \times 6.2 \times 10^{18}$

$= 2.23 \times 10^{23}$

No. of decomposed molecules $= 2.23 \times 10^{23} \times 10^{-7} = 2.23 \times 10^{16}$

Total thickness of decomposition $= 2.23 \times 10^{16} \times 10^{-15} \times 4\text{Å}$

$\approx 100\text{Å}$

A layer 100Å thick is thus estimated to provide 10,000 hr of electron-bombardment depletion life under the assumed limited operating conditions. The back-bombardment current density and duty cycle may each be an order of magnitude larger than assumed. Further, in addition to depletion life requirements, there are additional factors which call for larger film thicknesses.

Besides decomposition of the oxide, a further complication develops from selective evaporation of the decomposition products from the bombarded surface. As shown by Wargo and Shepherd[27] there may be a difference of a factor of 1000 between oxygen evolution and that of the metal. Their example was for SrO with a bombarding energy of 300 volts and a current density of 25 mA/cm^2. Oxygen evolution was approximately 10^{12} atoms/cm^2, whereas evolution of Sr was 10^9 atoms/cm^2. This difference must be due to differences in the vapor pressures of the two components. Oxygen, having a vapor pressure which is orders of magnitude higher than that of the metal, readily leaves the surface, and the metal stays behind. If this process is allowed to continue for very long, the surface of the cathode eventually becomes metallic, and thus becomes a low secondary emission surface. Obviously, if the cathode were to be heated to an elevated temperature, the vapor pressure of the metal would rise and cause the metal atoms to evaporate simultaneously. This has recently been shown in a Russian paper[15] for the case of BaO. There, an optimum temperature was shown to be around 600°C to maintain a high secondary yield on continuous bombardment at a fairly high value of current density (60 mA/cm^2) at 1000 V.

2.6 Ion bombardment effects. Because of the location of the secondary emitting cathode (inside the CFA), it is expected that the cathode surface will be subjected to positive ion bombardment. A rough estimate shows that this can amount to a current density of 5.0 $\mu A/cm^2$ at the cathode surface. It is expected that this ion bombardment will cause a serious limitation in cathode life.

When a surface is bombarded by positive ions, momentum transfer occurs between the bombarding ions and the atoms or molecules on the surface. If sufficient energy is acquired by an atom, it could conceivably leave the surface. This is known as sputtering. The sputtering yields and the threshold energies of almost all metals and some semiconductors when bombarded by He^+, Ne^+, Ar^+, Kr^+, Xe^+, and Hg^+ ions have been measured

by many investigators in the field. An excellent review of the subject has been published by Stuart and Wehner.[29] However, very little has been done or published for insulators, mainly because of the experimental difficulties resulting from surface charging of bulk insulators. Insulators can be readily sputtered by rf techniques,[30] although quantitative results are difficult to obtain. As a result, very little literature on this subject has been published. We have been able to locate only 2 references[31, 32] where dc sputtering was carried out on extremely thin films of insulators to avoide charge buildup. Very limited amounts of data are available from which any kind of an estimate can be made.

It is believed that when an insulator is removed by sputtering, the individual particles leaving the surface go off in the same molecular species as they existed on the bombarded surface. This has no significance in the case of metals or elemental semiconductors, but in the case of compound semiconductors and insulators such as oxides, the implication is that there is no chemical change of a portion of the surface material. We must remember that the sputtering phenomenon described in the literature is based mostly on that due to noble gas ions. Such is not the case for our cold cathode in the CFA. Instead, the positive ions are of the ordinary residual tube gases, such as H_2, N_2, CO, CO_2, etc. Therefore, experimental evaluation of the effect of sputtering by positive ions of these gases on the emitting surfaces were of interest in this program. Ion bombardment studies in N_2 atmosphere have resulted in experimental data about (1) the depletion of surface material due to ion bombardment as a function of current density and ion energy, and (2) the effect on the secondary emission of the surface (before complete depletion).

It is difficult to estimate the sputtering losses of the cathode surface due to ion bombardment inside the CFA because the known values are for noble gas ion bombardment. Some of the published data[33] indicate that with an atom-to-ion ratio of 1 at 5 kV ion energy Pt has a reasonably high sputtering yield. Al, Mg, and Be should not have a ratio more than 0.5 at 5 kV. For the oxides of Al, Mg, and Be it is suspected that the ratio may not be more than 0.1 molecule/ion at 5 kV when ordinary gases are used to produce positive ions. The figures given above are based on rough estimates from charts in reference 33 and values for oxides in reference 32. The simple calculations shown below are carried out to illustrate the depletion of Pt and oxides.

If the platinum is exposed to an ion current density of 5 $\mu A/cm^2$ at 5 kV energy, then:

a. Number of atoms sputtered/sec $= 1 \times 5 \times 10^{-6} \times 6.2 \times 10^{18}$

$= 3.1 \times 10^{13}$/sec

b. Life per mono-layer $= \dfrac{10^{15}}{3.1 \times 10^{13}} = 32$ sec

c. Life for 100 Å layer $= 32 \times \frac{100}{4} = 800$ sec

d. Life for a 0.010 in. layer $0.010 \text{ in.} \times 2.54 \times 10^8 \times \frac{800}{100\text{Å}} =$

$$2.03 \times 10^7 \text{ sec} = \frac{2.03 \times 10^7}{3600} = 5,640 \text{ hours.}$$

A 100 Å layer of an oxide bombarded under the same conditions as quoted for Pt would have a life of 8,000 sec (because the atom-to-ion ratio is only 1/10 of that of Pt).

The above values are for continuous bombardment. If the bombardment were carried out at 0.1% duty cycle, the life expectancy of an oxide layer is 8000×10^3 sec, or 2200 hours. For a 10,000 hour life a thickness of 500Å would be required, and for a 1% duty cycle the required thickness would be 5000Å.

Because of the over-all damage resulting from the combined effects of electron and ion bombardment, it is seen that the thickness of the emitter (for a 0.1% duty cycle) must be around 600Å. However, it should be borne in mind that the rough calculations expressed here were based on estimates only of the decomposition rates resulting from the electron bombardment and of the sputtering yields due to ion bombardment.

2.7 Current transmission. Our study has included an investigation of problems connected with current transmission through thin insulating films. Very thin insulating films (thickness < 100Å) can possess enhanced conductivity due to tunneling and Schottky effects, and as such they may be capable of transmitting the high current density (~ 1-10A/cm^2) required in a CFA. However, thicker films (~500-1000Å) will likely be needed for long-life operation of these thin film cathodes, and therefore problems with the effective conductivity of such films will be created (in extreme cases one has to contend with the bulk conductivity). Assuming a conductivity (σ) = 10^{-12} mho/meter, one can compute the power dissipation and potential drop in a 1000Å thick film of Al_2O_3, 1 cm^2 in area, and transmitting 1 A/cm^2. The power to be dissipated would be 10^9 watts/cm^2 and the potential drop 10^9 volts. Clearly, the conductivity must be much larger than the bulk value for thin insulating films to be feasible. One approach to the solution of this problem is the introduction of metallic doping in the insulating film. Recent work by Spindt and Shoulders[34] indicates that the secondary emission ratio of an alumina film was not significantly degraded by the addition of molybdenum as a dopant for doping levels up to ~30 weight% Mo. That the conductivity of such doped coatings appears to be sufficiently high for the CFA application is encouraging. Variants of Mo-doped Al_2O_3 were considered in this program as a means of achieving the most desirable combination of secondary emission, conductivity, and long-life (resistance to electron and ion bombardment) properties.

Another result of poor conductivity is the presence of charging effects. These occur when electrons bombard an insulator under conditions for which $\delta > 1$. An important parameter to consider in this regard is what might be termed the "time constant" of the material. Consider the "condenser" represented by the insulating film between the vacuum-insulator and the

metal-insulator interfaces. The product of resistance and capacitance is the time constant of the condenser. It is found that RC is equal to $K\epsilon_o/\sigma$ and depends only upon the properties of the insulating film. Thus the time constant of the material is $\tau = K\epsilon_o/\sigma$.

where K = relative dielectric constant

ϵ_o = permittivity of free space

σ = conductivity

If one assumes $K = 10$ and $\sigma = 10^{-12}$ mho/meter for Al_2O_3, one obtains $\tau = 100$ sec. Larger or smaller values of τ are possible (depending on the method of preparation of the alumina film and on its thickness, since they influence the effective value of σ). The effect of introducing metal doping in the insulating film will be to reduce τ so that any localized charge in the insulator will spread out evenly.

We may state in summary that an additional degree of freedom may be attained in solving the current transmission problem by incorporating a metallic component in the film. Accordingly, various forms of metal-metal oxide combinations were considered in this program.

2.8 Summary of guidelines for the selection of cold cathode materials

We have explored the various phenomena and materials properties which determine satisfactory operation with long life in a CFA. It has been pointed out that certain metals, notably Pt, are to be preferred whenever the δ of Pt is sufficient to provide the desired anode current. If higher δ's are required, then the several approaches discussed heretofore may be considered. Therefore, some important factors and guidelines relevant to materials selection are listed below.

a. High secondary emission ratio. A normal incidence maximum value of δ of ~4-5 is considered desirable. Literature values, whenever they existed, and measurements on candidate materials taken in the laboratory were used as a basis for selection.

b. Electron bombardment resistance. The ability to withstand high electron current bombardment is a criterion for the choice of materials. For this purpose, data were taken in the present program on the deterioration of δ due to electron bombardment for various materials.

c. Ion bombardment life. Materials selection must consider sputtering erosion due to ion bombardment. This was evaluated for candidate materials.

d. Crossed-field amplifier performance. In addition to directly measured δ values, information as to effective δ's in the CFA is obtained from the ECB (emission current boundary). In view of the anomalously high effective δ for Al_2O_3 on Al cathodes in the CFA, one must consider insulating films, or more specifically oxide films, in a special category. They were considered for CFA evaluation even if directly measured δ values were only ~ 2-3.

e. Ability to withstand tube processing. Additional criteria are vapor pressure, film adherence, and other pertinent properties which relate the ability of the cathode material to retain its mechanical and chemical integrity through tube bakeout and operation.

3. FACTUAL DATA - PHASE A - MEASURABLE PROPERTIES OF COLD CATHODE MATERIALS

Phase A of this program involved an investigation of the phenomena and material properties of cold cathodes, and the testing of specific materials, semiconductors and insulators. Utilized for these tests were the following primary test vehicles:

a. Secondary Electron Emission Test Vehicle (SEE)

b. Hot and Cold Electron Bombardment Test Vehicle (EBV)

c. Ion Bombardment Vehicle (IBV)

Section 3.1 of this report describes all testing performed in the SEE. Secondary emission ratios of selected materials were evaluated for the following parameters:

a. Chemical composition
b. Film thickness
c. Method of preparation
d. Effect of material outgassing
e. Effect of heat with variations in temperature and time.

Sections 3.2 and 3.3 of this report describe all tests performed for the evaluation of secondary emitters, including those tested in the Electron Bombardment Vehicle.

Secondary emission ratios of selected materials were evaluated under the following conditions:

a. Electron bombardment in the range of 0.15 A/cm^2 to 0.75 A/cm^2

b. Partial gas pressure of O_2, N_2, CO_2, and H_2

c. Constant electron bombardment for varying periods of time.

Section 3.4 describes the tests conducted with the Ion Bombardment Vehicle and the subsequent measurement of secondary emission ratios of the sputtered samples in the Secondary Emission Measurement Vehicle.

The test vehicles are described briefly in the pertinent sections of this report. Detailed descriptions of the test vehicles are contained in the previous quarterly reports referred in the bibliography.

The test results for secondary emission measurements, electron bombardment, and ion bombardment have been categorized into 3 groups: metals, semiconductors and insulators.

The effects on secondary emission ratios due to the phenomena associated with the properties of cold cathode materials is summarized at the end of each section of Phase A.

3.1 Secondary emission measurements. The apparatus used for the measurement of secondary electron emission was described in detail by K. Dudley[35] of this laboratory and is shown by Figure 3-1. Briefly, the secondary emission test vehicle (SEE) is a demountable, stainless steel structure having a glass viewing window and provision for 10 targets. A cross-sectional drawing of the vehicle is shown in Figure 3-2. Indexing of the rotatable target holder is accomplished through the use of a small external magnet, and an electron bombardment heater can be used to outgas or otherwise heat the samples individually. The vacuum system consists of an oil diffusion pump with a cold trap for fast pumpdown, a 1-1/2 inch bakeable isolation valve, and a sputter ion pump with a titanium sublimation booster for a final vacuum of $\sim 1 \times 10^{-9}$ torr. The test vehicle is bakeable at 400° C.

The rotor, on which the 10 targets are mounted, is shown in Figure 3-3. A Pt target is typically included as a "standard" to provide a reference point for normal behavior.

Figure 3-4 shows typical SEE results for secondary emission ratio (δ) vs primary energy for a platinum target. This data was used as a control or standard for subsequent measurement of other materials in the SEE.

3.1.1 Preparation of samples. Whereas the metals and semiconductors could be tested in bulk form, and test samples were therefore comparatively easy to fabricate, the oxides, being insulators, had to be tested in thin film form or impurities had to be deliberately introduced in order to tailor some of the physical properties. Sample preparation of the insulators therefore became a specialized effort in this program. In addition, various analytical studies such as resistivity measurements and chemical and structural analysis were required.

Once we decided to form a thin film oxide on a metallic substrate, a number of preparation approaches were possible. These are briefly described below.

a. Controlled oxidation of the metal (to form a surface layer of the oxide) - As an example, the metal aluminum can be oxidized to form alumina. This can be achieved by either oxidation at elevated temperatures in an oxidizing atmosphere or by electrochemical means, known as anodization.

b. Chemical vapor deposition - The vapor of a chemical compound of the metal is allowed to come in contact with a heated substrate with the result that the compound decomposes and deposits metal on the substrate. The ambient atmosphere can be controlled so as to be oxidizing in nature, in which case the metal would deposit on the substrate in its oxide form.

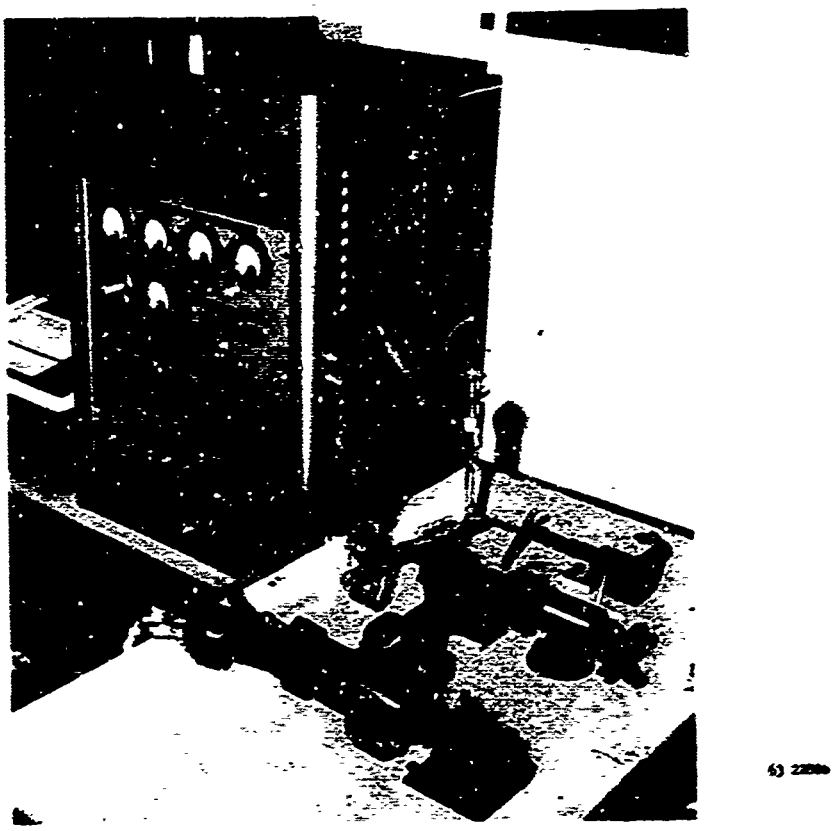

Figure 3-1. Secondary Emission Test Vehicle

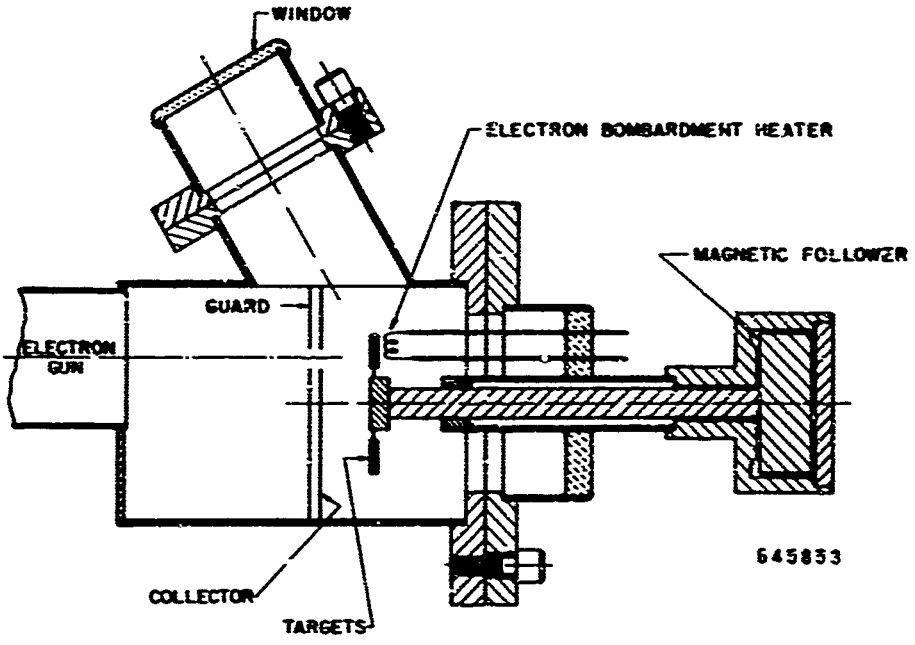

Figure 3-2. Secondary Emission Electron Test Vehicle

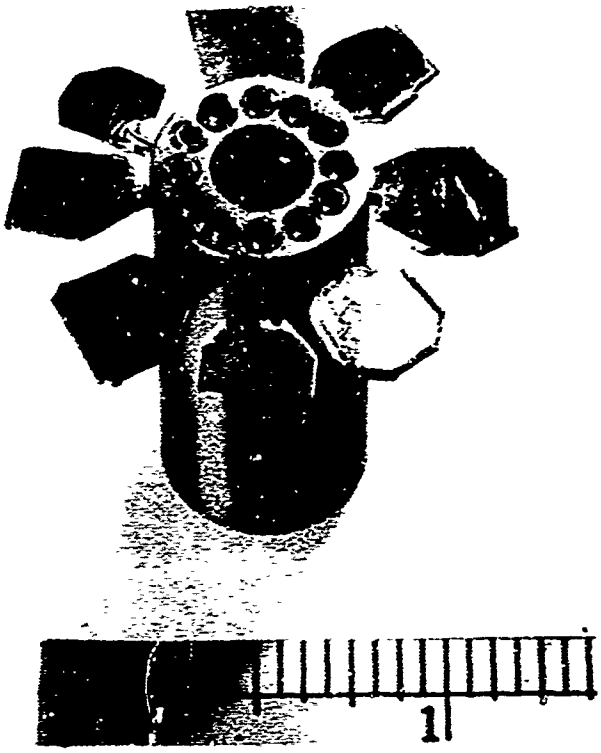

Figure 3-3. Target Assembly

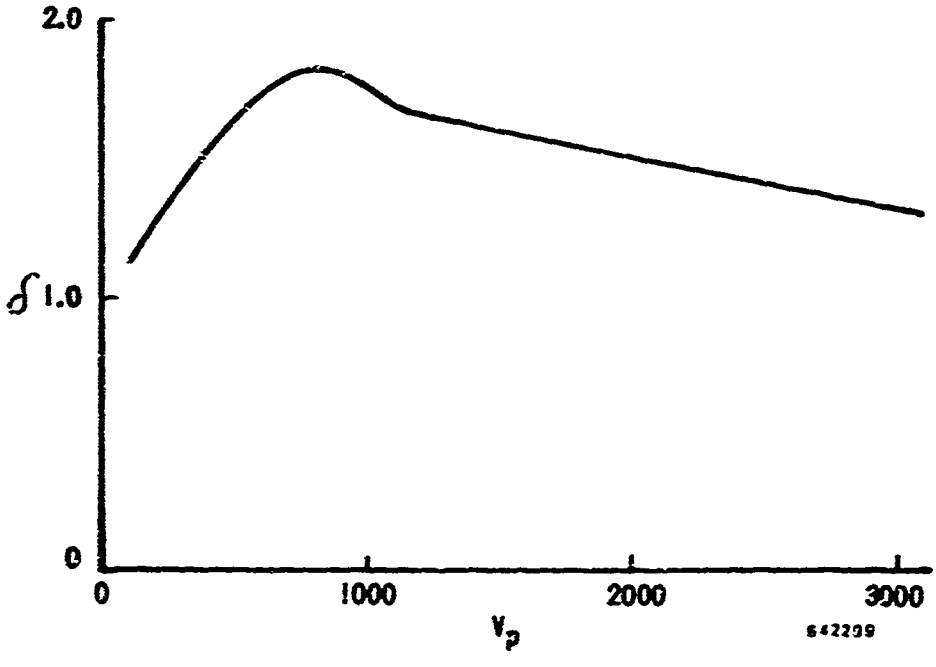

Figure 3-4. δ for Pt as Function of Primary Energy

c. Electron beam evaporation - The insulator to be used is placed in a water-cooled copper crucible and bombarded by electrons to reach evaporation temperatures. The substrate, in position above the crucible, receives the evaporated insulator deposits.

d. Sputtering - In this process the material to be deposited is bombarded by positive ions of an inert gas such as Argon, after which sputtered materials are caught on the surface of the substrate. In the case of insulator bulk materials, ordinary dc sputtering is not possible and rf sputtering has to be employed.

e. Reactive sputtering - Instead of an insulator, the metal can be sputtered by a dc technique in an oxidizing atmosphere. This results in the formation of an oxide layer on the substrate.

Of methods listed above, a and c were used. Figure 3-5 shows the bell jar set-up in which electron beam evaporation is carried out.

3.1.2 Secondary emission ratio as a function of angle of incidence. In conjunction with our interest in resolving the anomaly of the high effective δ of Al when used as a cold cathode in a CFA we investigated the secondary emission ratio of Al cathodes as a function of the incident angle of the primary electrons.

The samples were aluminum oxidized in air at temperatures ranging from room temperatures to 400°C. The thickness of the films formed on the samples were measured by a voltage breakdown technique. Measurements of the air oxidized samples never showed a film thickness exceeding 50Å.

Several Al samples were mounted at different angles to the incident beam in the multiple target holder, and data of δ vs V_p were obtained for $\theta = 0°$ (normal incidence), 20°, 40°, and 70°. Reasonable agreement was obtained for two independent sets of samples in two runs. Data of δ vs V_p are shown in Figure 3-6 for a set of 4 Al samples. The Pt standard was included and showed normal behavior. Apart from the relatively low δ value for the 40° sample, several features of the data are in agreement with theoretical expectations. The measured values of $V_{p_{max}}$ for various values of incidence are tabulated below.

θ (in degrees)	$V_{p_{max}}$ (volts)
0	400
20	500
40	600
70	800

According to simplified theory[10] $V_{p_{max}}$ should be inversely proportional to $(\cos\theta)^{1/2}$. Thus $V_{p_{max}}$ for $\theta = 70°$ should be 1.7 times as large as $V_{p_{max}}$ for $\theta = 0°$. This is close to the observed factor of 2. The δ data for the 0, 20, and 70° samples are in qualitative agreement with the expected increase in δ_{max} with increasing angle of incidence. Although more accurate data for the variation of δ_{max} with θ could be obtained by using a single rotatable sample, our data allows one to conclude that the variation is not greater than the "classical" dependence,[10] as given by:

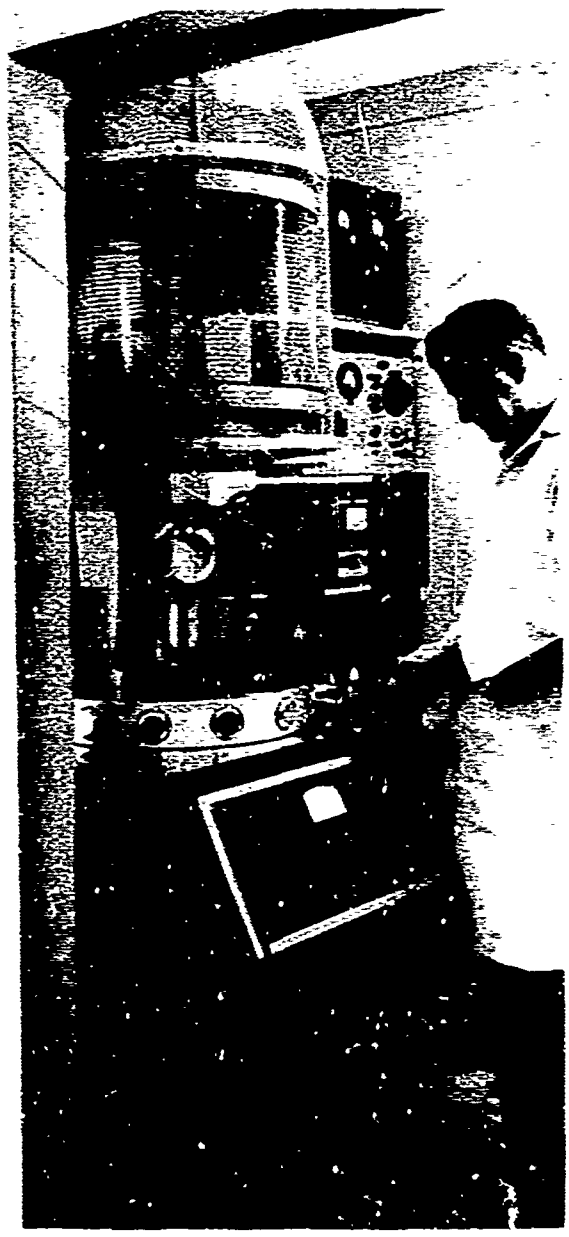

Figure 3-5. Bell Jar Containing Electron Beam Evaporator

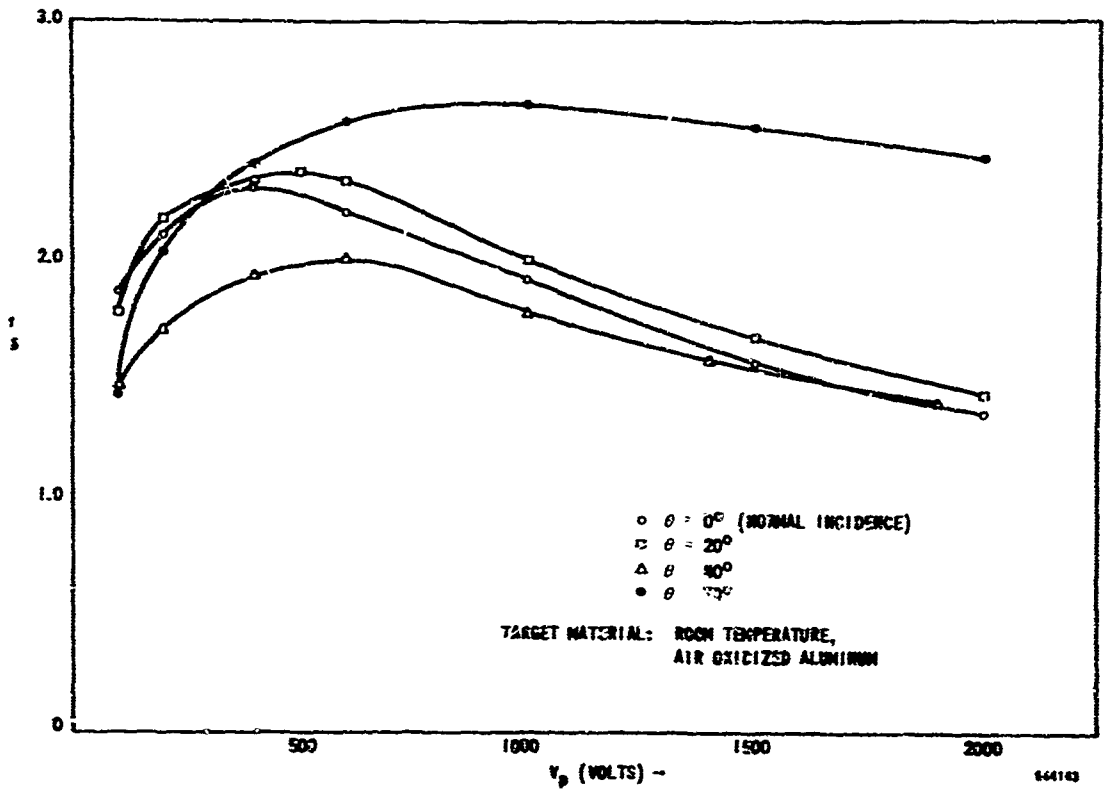

Figure 3-6. Secondary Emission Ratio vs Primary Energy for Aluminum Target for Various Angles of Incidence

$$\ln(\delta_\theta / \delta_o) \sim (1 - \cos\theta) \qquad (1)$$

where: δ_o is δ_{max} for normal incidence,

and δ_θ is δ_{max} for incidence at angle θ.

It is therefore unlikely that the enhanced δ for Al in a CFA can be explained in terms of an anomalous dependence of δ on θ. It is interesting to note that the δ vs V_p data for the 0° and 70° samples are brought into near-coincidence with each other as well as with the constant loss curve when plotted in normalized coordinates as in Figure 3-7.

3.1.3 Aluminum oxide films on metal substrates. A set of Mo-Al_2O_3 samples was prepared with varying compositions and film thicknesses in the following manner: Al_2O_3 and Mo powder were mixed and pressed to form 1/4-inch diameter slugs. These slugs were subjected to electron bombardment and the vapors were deposited on Pt clad Ni flags for δ measurements and on quartz slides for resistivity measurements. The

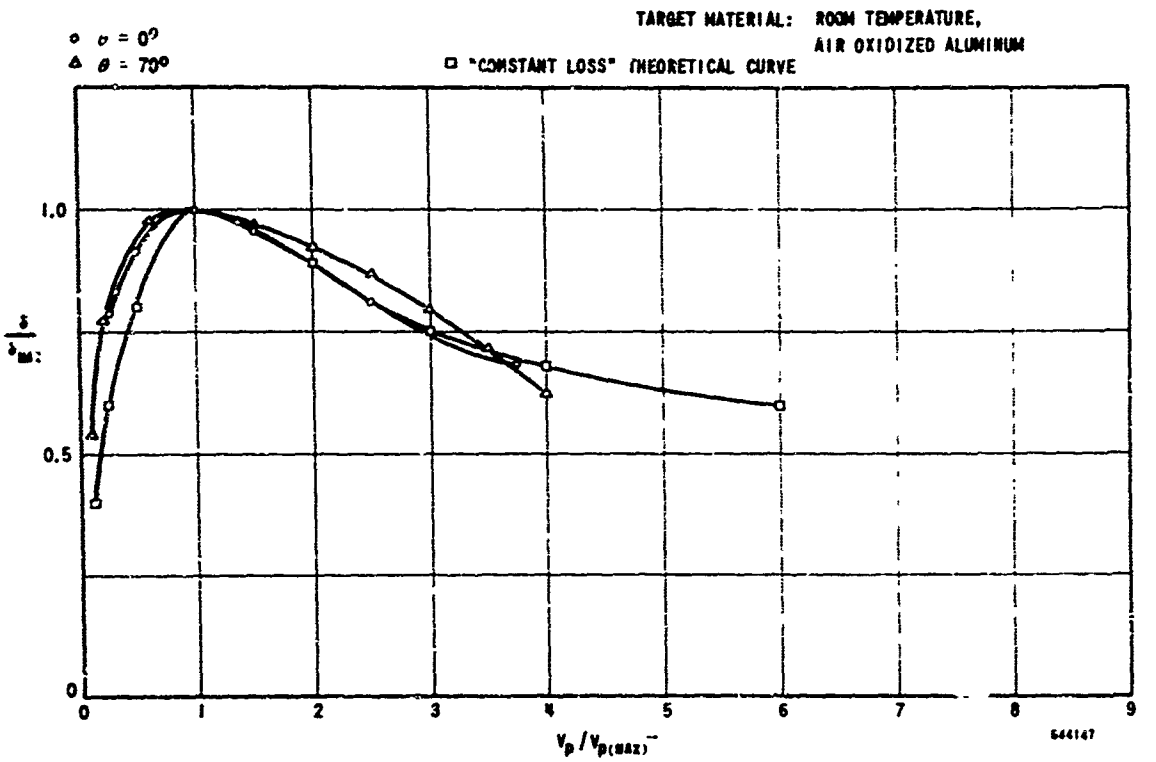

Figure 3-7. Secondary Emission Ratio vs Primary Energy (in Normalized Units) for "Aluminum" Targets at Various Angles of Incidence.

thickness of the films was monitored using a quartz crystal oscillator. Compositions of 10, 20, and 30% Mo were used as vapor source and films were deposited to a thickness of 100 and 1000 Å.

Figure 3-8 shows δ vs V_p data for 1000Å films of 20% Mo - 80% Al_2O_3. The δ_{max} was similar to that of pure Al_2O_3 films on Al. Although the 20% Mo content refers to the evaporator source composition, it was definitely established that some Mo was present in all the composite films of 1000Å thickness. Pure Al_2O_3 films on quartz were transparent, while those obtained from Mo - Al_2O_3 mixtures had a light brown coloration. In addition, the resistance measurements on the quartz substrate samples indicated significantly greater conductivity than that of pure Al_2O_3.

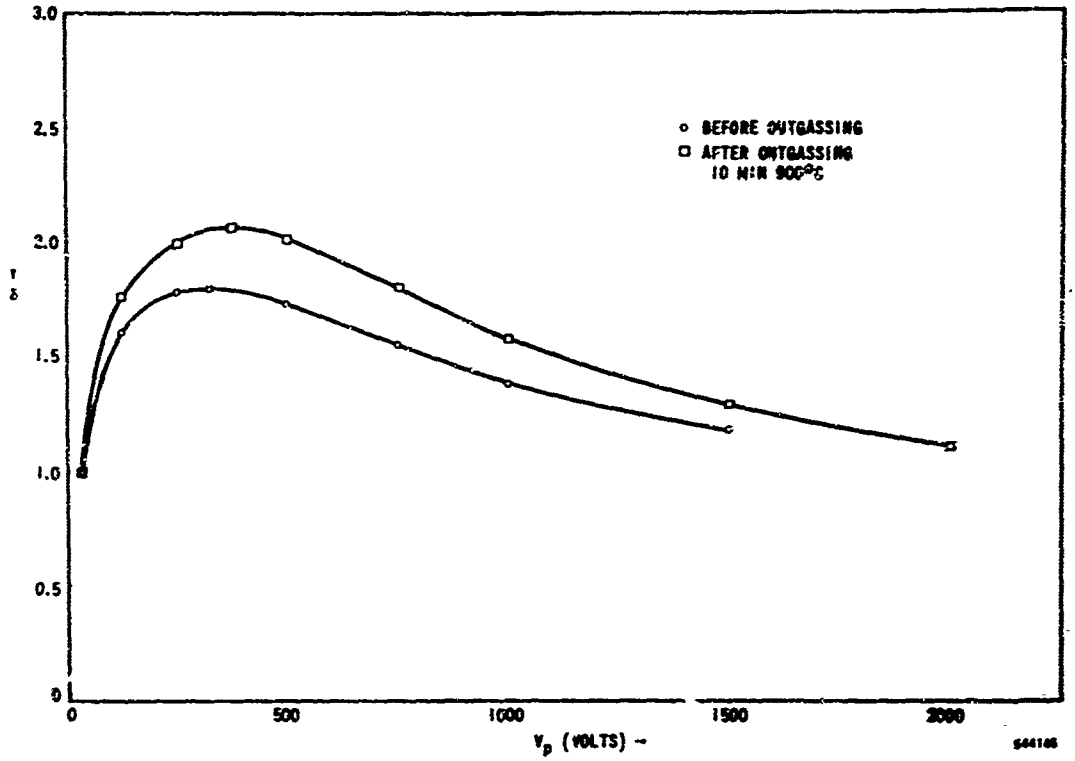

Figure 3-8. Secondary Emission Ratio vs Primary Energy for 1000Å Films of 20% Mo - 80% Al_2O_3 on Pt Substrate

The data of Figure 3-8 also shows the effect of heat treatment for 10 min at 900° C in increasing δ. The usual effect of "outgassing" Pt and also Al_2O_3 on Al samples has been to decrease δ. Perhaps in the present case the increase in δ is not due to outgassing but rather to a change in the nature of the film, for example the agglomeration of Mo. This interpretation is consistent with the observed increase in resistivity due to heat treatment.

Figure 3-9 shows δ vs V_p data for a 30% Mo composite film of 1000Å thickness. The δ and resistance data for 10, 20, and 30% Mo composites were not sufficiently different from each other for the present samples to warrant a discussion of that factor, nor did the resistance measurements always show a monotonic pattern with composition changes. Further work is needed to improve the control of the evaporated film and to obtain a determination of the Mo composition in the film. Nevertheless, the tendency for δ to increase with heating appeared consistently. In addition, δ for the conductive (due to Mo doping) Al_2O_3 samples were not degraded by doping.

In Figure 3-10 the δ vs V_p characteristic for the 1000Å films of various compositions are compared with a constant loss theoretical curve.[13] It can be seen that they are in approximate agreement with the constant loss curve and deviate at large values of V_p/V_{Pmax} in a similar manner to other

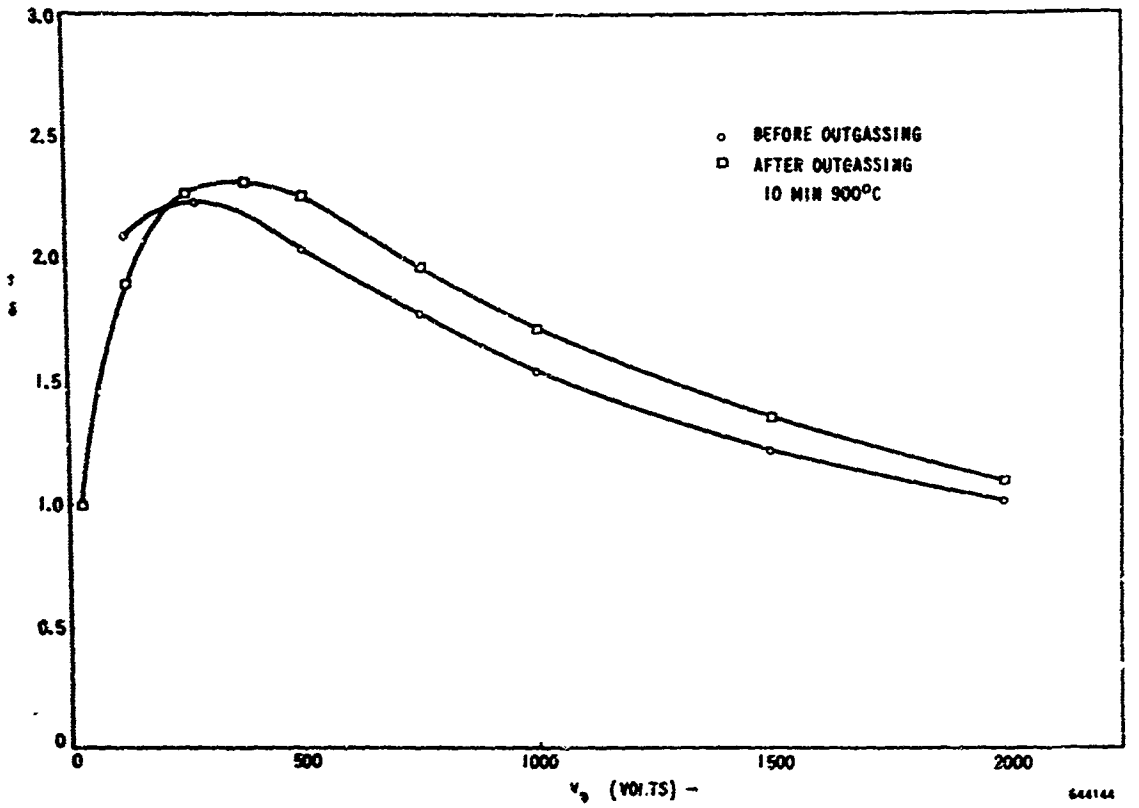

Figure 3-9. Secondary Emission Ratio vs Primary Energy for 1000Å Films of 30% Mo - 70% Al_2O_3 on Pt Substrate

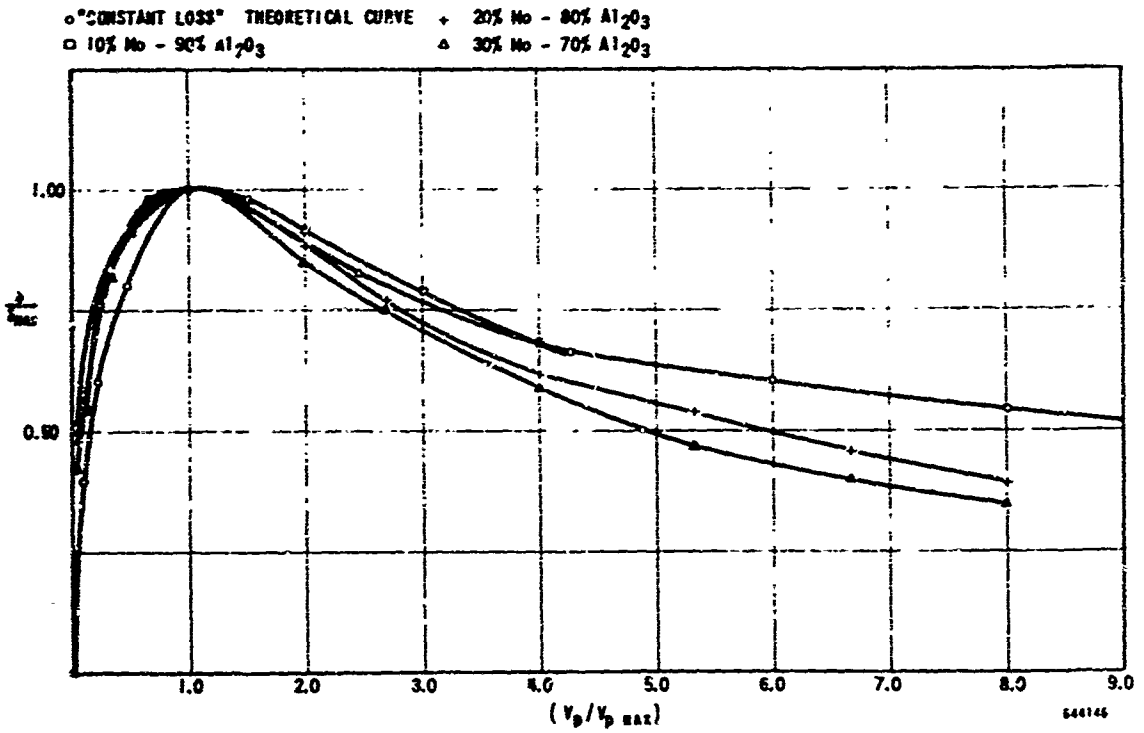

Figure 3-10. Secondary Emission Ratio vs Primary Energy (in Normalized Units) for 1000Å Mo - Al_2O_3 Films on Pt Substrate

materials.[13] The constant loss curve quoted assumes a power law primary range - energy relation with an exponent of 1.35 and takes the scattering of primaries into account so that the energy dissipation (and secondary production) is approximately constant throughout the range.

A typical set of δ vs V_p data is shown in Figure 3-11 for a 100Å film. Several samples of each composition and thickness were measured, and approximate agreement was obtained. It can be seen that the effect of heat treatment persists. A subsequent heat treatment of the 100Å samples at 1100°C (optical pyrometer brightness temperatures are quoted throughout) resulted in a large increase in the pressure. This is interpreted as a vaporization of the film rather than the outgassing of adsorbed gases.

3.1.4 Proportion of molybdenum to alumina. Also accomplished during the program was a second series of experiments which involved molybdenum-alumina films deposited on a hot molybdenum substrate by electron beam evaporation from a pressed powder compact of molybdenum and alumina. Secondary emission data were then obtained as a function of the following three parameters:

a. Proportion of molybdenum to alumina
b. Substrate temperature during deposition
c. Post-deposition heat treatment.

Eight samples were prepared with 2 each having 0%, 10%, 20%, and 30% molybdenum by weight. The molybdenum content refers to the composition of the pressed powder compact. Data were obtained for the dependence of the secondary emission ratio (δ) on the primary energy. The effect of heat treatment on δ was also observed. The data are summarized in Table 3-1.

TABLE 3-1.

Secondary Emission Ratio (δ) of Mo-Al_2O_3 Films for Various Proportions of Mo to Al_2O_3

% Mo in Source	Film Thickness Å	δ_{max} After System Bakeout	δ_{max} After 10 min at < 500°C	δ_{max} After 10 min at 850°C
0	330	4.25	4.23	3.71
		4.36	4.04	3.55
10	1000	3.87	4.38	3.17
		3.93	4.25	3.17
20	1000	3.36	3.85	2.96
		3.87	4.02	2.85
30	1000	4.34	3.75	3.45
		4.39	4.19	3.39

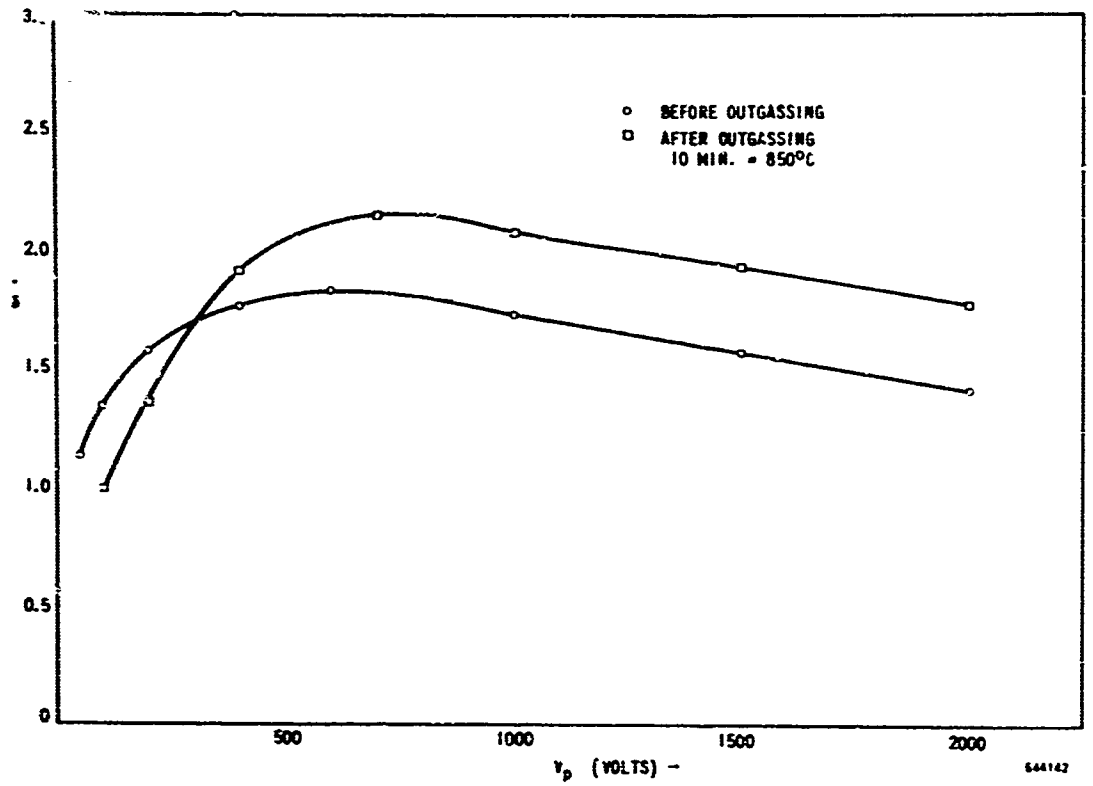

Figure 3-11. Secondary Emission Ratio vs Primary Energy for 100Å Films of 90% Al_2O_3 - 10% Mo on a Pt Substrate

All the samples referred to in Table 3-1 were prepared with a substrate temperature of 600° C during deposition and a post-deposition heat treatment at 1100° C for 5 minutes. The measurements of δ show the relative insensitivity of δ to a source composition of molybdenum of up to 30% by weight. It can also be seen that the δ's of the pure alumina films are high and correspond to crystalline rather than amorphous alumina films. A reduction of δ due to the higher temperature heat treatment is also noted.

3.1.4.1 Substrate temperature during deposition. A series of 1000Å, 30% Mo - 70% Al_2O_3 films were prepared for a series of substrate temperatures during deposition. A range of 600 to 1100° C was covered in 100° C steps. All the films were given a post-deposition heat treatment at 1100° C for 5 minutes.

The measured dependence of maximum secondary emission ratio (δ_{max}) on substrate temperature during deposition is shown in Figure 3-12. A decrease in δ_{max} by approximately a factor of 2 was noted as the temperature was varied from 600° C to 1100° C. The substrate temperature is therefore considered to be a significant parameter. Electron probe and electron diffraction analyses were conducted to determine the differences between the 600° C and 1100° C films. The results of these analyses are described in Section 3.2.2.3 and 3.2.2.4 of this report.

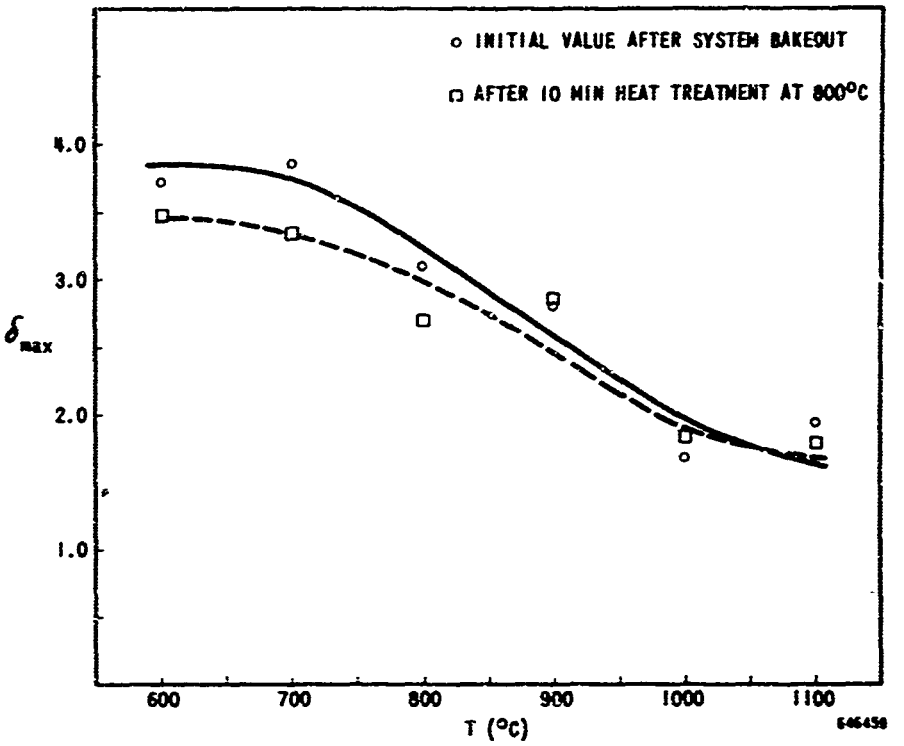

Figure 3-12. Secondary Emission Ratio Maximum (δ_{max}) vs Substrate Temperature at Deposition for 1000Å Moly-Alumina Films on Moly Substrate

3.1.4.2 Post-deposition heat treatment. Six 1000Å, 30% Mo - 70% Al_2O_3 film samples were prepared with a fixed deposition temperature of 600°C and a 5-minute post-deposition heat treatment at a temperature which varied from 600 to 1100°C in 100°C steps. Data were obtained on δ as a function of primary energy. Table 3-2 contains a summary of δ_{max} for the various post-deposition heat treatments.

TABLE 3-2.

Maximum Secondary Emission (δ_{max}) for Various Post-Deposition Heat Treatments

Sample No.	Temperature for 5 min. post-deposition heat treatment (°C)	δ_{max} after system bakeout	δ_{max} after 10 min at 800°C
1	600	3.37	2.65
2	700	3.24	2.47
3	800	3.82	2.57
4	900	4.70	2.92
5	1000	4.02	2.92
6	1100	3.73	2.89

It is concluded that, although somewhat higher δ's were obtained for the higher temperatures, the spread in δ, particularly after an additional heat treatment, was not large.

To obtain some estimate of the uniformity of the molybdenum-alumina film samples, a secondary emission scan was obtained (See Figure 3-13) by locating the secondary emitting target behind a 3/8-inch diameter hole in a metal shield. The primary electron beam, which was focussed to a spot size less than 1/32-inch in diameter, was caused to traverse the target while the primary energy was kept fixed at a value which yielded the maximum δ. The observed variation across the sample is estimated to correspond to a 6% spread in the values of δ.

3.2 Physical testing of molybdenum-alumina films.

3.2.1 Resistance and capacitance measurements of molybdenum-alumina films. In conjunction with our interest in obtaining sufficiently conducting high-δ films, we measured the resistance and capacitance of the molybdenum-alumina films. The following types of measurements were performed.

a. Dc resistance

b. Capacitance and ac resistance at 1 kHz (ac bridge measurement)

c. Frequency dependence of capacitance and ac resistance over frequency range 100 Hz to 1 MHz.

The following techniques were employed:

a. Evaporated gold film counterelectrodes of varying diameters and two thicknesses, 500Å and 1500Å.

b. Bent gold wire contact to either a gold film or directly to the top of molybdenum-alumina film.

The following conclusions have been reached based on the resistance and capacitance measurements made during the program:

a. Dc resistivity equals ac resistivity at 1 kHz.

b. Ac resistivity and dielectric constant are independent of frequency up to 1 MHz.

c. Resistivity values in the range 10^3 to 10^6 ohm-cm have been observed.

d. Values of dielectric constant (real part) in the 10 to 500 range have been observed.

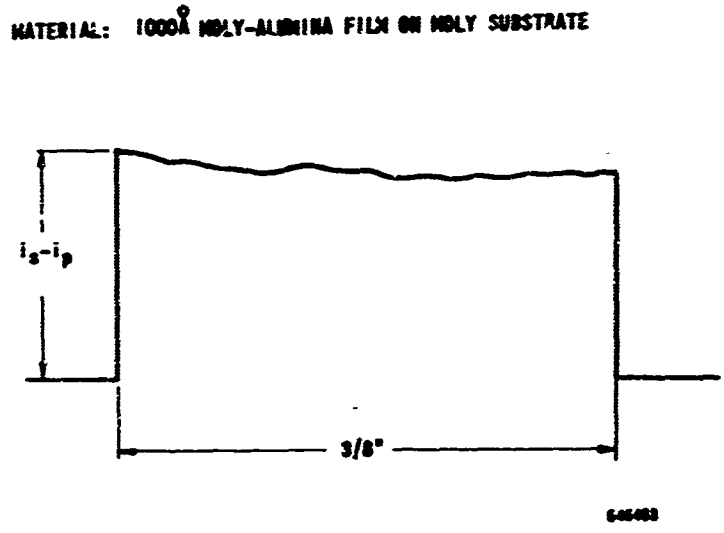

Figure 3-13. Secondary Emission Scan of 3/8 in. Dia Target

The large values of dielectric constant are believed to be valid measurements. Although it is suspected that these may be due to surface space-charge layers, this was not demonstrated experimentally. The values of resistivity observed are in a usable range for the CFA application, with the lower end of the range (10^3 ohm-cm) being preferred.

An improved counterelectrode technique is required to obtain a steady reading, to ascertain more definitely the cross-sectional area involved in the measurement, and to determine that there are no continuous gold threads through the molybdenum-alumina film.

3.2.2 Analysis of Mo-Al_2O_3 thin films. The following information was sought from the Mo-Al_2O_3 thin-film analyses.

a. Semiquantitative analysis of weight factors of Al_2O_3 and Mo in the films and an estimate of the uniformity of the deposits, both by electron microprobe.

b. Chemical and crystallographic state of both Mo and Al_2O_3 in the films by means of electron diffraction techniques.

c. The true thicknesses of the films as compared to intended film thicknesses, using both single-beam and multiple beam interferometry.

3.2.2.1 Mo-Al_2O_3 sample preparation.

Composition:	Al_2O_3 100%, Mo 100%, and Al_2O_3 70% and Mo-30%
Thickness:	500, 1000, and 1500 Å (by quartz crystal monitor)
Substrate:	Nickel
Preparation:	Substrate cleaned in vacuum at 1000° C Substrate temperature during evaporation 600° C
Post Heat Treatment:	1050° C in vacuum for 5 minutes.

3.2.2.2 Thickness measurements. The surfaces of the substrate were initially too rough for measurement of thickness, but by depositing the film on a metallographically polished surface, thickness measurements were obtained.

3.2.2.3 Chemical composition. Samples of 100% Al_2O_3 and 100% Mo were used to calibrate the electron probe machine. With the calibration curves obtained from these samples, the 70% Al_2O_3 - 30% Mo samples were then analysed by the probe, for both composition and homogeneity. The results are shown in Table 3-3.

TABLE 3-3.

Results of Al_2O_3-Mo Sample Analysis

Sample	Film Thickness Å	Wt % Mo
70% Al_2O_3 + 30% Mo	500	33.0
70% Al_2O_3 + 30% Mo	1000	26.0
70% Al_2O_3 + 30% Mo	1500	24.0

All three samples were found to be homogeneous in composition and devoid of island structure.

3.2.2.4 Electron diffraction analysis of molybdenum-alumina films. Secondary emission measurements (See Figure 3-12) showed the importance of the substrate temperature during film deposition. The secondary emission ratio of the 1000Å thick, 30% Mo-70% Al_2O_3 films decreased by a factor of 2 as the Mo substrate deposition temperature was varied from 600 to 1100° C. It was therefore of interest to determine any differences in film structure or composition to correlate with the δ changes.

Electron diffraction patterns were obtained from two 1000Å films of 70% Al_2O_3-30% Mo deposited at 600 and 1100 respectively onto molybdenum substrates.* Diffraction rings representing polycrystalline material were obtained from both specimens, and the following conclusions were drawn from the patterns:

a. Evaporation at 1100°C

1) The diffraction rings were moderately sharp, suggesting sizable crystalline areas, probably containing at least several hundred atoms.[36]

2) Seven of the rings represent d-spacings which are in good agreement with those for elemental molybdenum, as listed in the American Society for Testing Metals file.

3) The remainder of the rings do not, as a group, match any single Al_2O_3 pattern, although individually each approximates a d-spacing for one of the various alumina structures. Nor do they agree with any other single phase pattern in the ASTM file. Since it is thermodynamically unlikely that any reaction products of Mo and Al_2O_3 have formed, it is probably safe to assume that these additional rings were caused by some form of aluminum oxide, possibly a mixture of several allotropes.

b. Evaporation at 600°C

1) The diffraction rings were fewer in number than those for the 1100°C specimen, and more diffuse, indicating a lower degree of crystallinity.

2) No molybdenum rings were present, suggesting a high degree of dispersion of Mo atoms in the film. This also provides evidence that the molybdenum pattern mentioned above is not due to the underlying molybdenum substrate, but arises from the film itself.

3) As above, the rings are not in agreement with any single pattern, but are not inconsistent with the assumption of a mixture of Al_2O_3 phases.

It can be seen from the above analysis that increases in the size of agglomerated molybdenum particles, for sizes up to approximately several hundred atoms, decreased δ to values which more nearly approach δ of the molybdenum phase.

---

* The electron diffraction work reported in this section was performed by W. R. Bekebrede of Raytheon's Research Division.

3.2.3 Nickel cermet and impregnated cathodes. Nickel cermet and impregnated cathodes according to recent Russian literature,[15, 16] showed the possibility of obtaining desirable secondary emitters for cold cathode usage from some commonly used thermionic emitters, namely nickel cermet and barium aluminate impregnated tungsten matrix cathodes. We prepared the following samples for secondary emission measurements.

1. Nickel cermet - Four compositions were studied.

   Lot No. 1 - 7.0 gm Mond Ni Powder
   3.0 gm Baker's RM No. 3 (Double carbonate)

   Lot No. 2 - 7.0 gm Mond Ni Powder
   3.0 gm Baker's RM No. 3
   0.2 gm Zirconium Hydride

   Lot No. 3 - 7.0 gm Mond Ni Powder
   1.2 gm Baker's RM No. 3
   1.8 gm Barium Carbonate

   Lot No. 4 - 7.0 gm Mond Ni Powder
   1.2 gm Baker's RM No. 3
   1.8 gm Barium Carbonate
   0.2 gm Zirconium Hydride

   Each of the four lots was mixed thoroughly and pressed into disc forms about 0.02 inch thick at a pressure of 90 tons/in^2. The discs were sintered in a vacuum at 700°C. They were then mounted in a secondary electron emission test vehicle, evaluated, broken down, activated, and measured.

2. Aluminate impregnated tungsten matrix cathode - Disks about 3/8 inch diameter and 0.03 inch thick were machined out of a copper-impregnated, 20% porosity tungsten matrix. Copper was then removed by evaporation in a vacuum and the tungsten matrix subsequently infiltrated with four different compositions of aluminates. These were then evaluated in our SEE test vehicle.

3.2.3.1 Nickel cermet cathodes. The nickel cermet samples having the four different compositions specified above were prepared, and their secondary emission ratios were measured for various states of activation. Table 3-4 summarizes some of the results. The compositions of the samples and the values of δ_{max} are tabulated. The secondary emission ratio is seen to increase and then subsequently decrease as a result of continued heating in a vacuum. Maximum values of δ_{max} ranged from 3.6 go 6.4 for the samples tested. These δ values are comparable to those reported by Alekseyev and Lepeshinskaya.[15] It is noted that the tendency for δ to increase and then decrease as a result of heating was observed for both the nickel cermet and the barium calcium aluminate impregnated cathodes to be described in the following section.

TABLE 3-4.

δ_{max} for 4 Different Ni Cermet Cathodes at Various Stages of Activation

Sample No.	Composition	δ_{max} Before Bakeout	δ_{max} After System Bakeout	δ_{max} After 30 min at 925°C	δ_{max} After Add'l 15 min at 1000°C	δ_{max} After Add'l 30 min at 850°C	δ_{max} After Add'l 30 min at 850°C	δ_{max} After Add'l 30 min at 850°C
1	70% Ni 30% Radio Mix #3	2.20	2.03	6.42	4.36	2.70	2.94	3.05
2	68% Ni 30% Radio Mix #3 2% ZrH_2	2.27	1.87	5.00		3.10	2.88	2.60
3	70% Ni 12% Radio Mix #3 18% $BaCO_3$	2.36	1.83	2.70	Lost Sample			
4	68% Ni 12% Radio Mix #3 18% $BaCO_3$ 2% ZrH_2	2.84	2.14	2.90	3.40	3.62	3.21	2.97

3.2.3.2 Impregnated tungsten cathodes. Two each of four types of barium calcium aluminate impregnated tungsten cathodes were prepared for secondary emission measurement. Measurements were made of δ as a function of primary energy. The results are summarized in Table 3-5 where values of δ_{max} are tabulated for different states of activation. It is to be noted that δ increased as a result of heating at 1050°C. Samples 7 and 8 activated more rapidly than samples 1 through 6, which agree with the relative ease of activation of these cathodes as monitored by thermionic emission measurements. Sample 8 was heated beyond the 40 minutes of heating given to all the samples; δ_{max} rose to 4.39 after a cumulative total of 70 minutes of heating at 1050°C and then declined to a value of 3.33 after a total of 190 minutes at 1050°C. Thermionic emission of such cathodes did not generally show a decline after continued heating, in contrast with the behavior of δ quoted above for sample 8.

3.2.4 Semiconductors. One approach to the choice of a cold cathode material is the use of refractory semiconductors with a high δ. In this case the electron bombardment dissociation processes would release non-volatile atoms (as contrasted with the oxygen which evolves from oxides). The hope was that electron bombardment would not cause the cathode material to deteriorate.

In line with this objective, several semiconductors were measured.

Table 3-5.

δ_{max} for Various Compositions of Barium Calcium Aluminate Impregnated Tungsten Cathodes

Sample No.	Composition**	δ_{max} After System Bakeout	δ_{max} After 10 min at 1050°C	δ_{max} After 40 min at 1050°C
1	5-3-2	1.84	2.00	2.22
2	5-3-2	1.63	1.97	2.50
3	4-1-1	1.77	1.96	2.38
4	4-1-1	1.66	1.80	2.25
5	3.5-1-1	1.82	1.96	2.32
6	3.5-1-1	1.91	2.25	2.57
7*	4-1-1	2.02	2.21	3.63
8*	4-1-1	1.81	2.64	3.73

* Samples 7 and 8 are processed so as to activate more rapidly than samples 1-6.

** Numbers indicate mole ratios of $BaCO_3$, $CaCO_3$, Al_2O_3

Measurements of the secondary emission ratio as a function of primary energy are shown in Figures 3-14 and 3-15. The semiconductors GaAs, CdS, and CdTe referred to in Figure 3-14 were obtained from the Raytheon Research Division, while the intermetallic compound, $Ti_{14}Ni_{48.5}Si_{37.5}$, was obtained from Professor Beck of the University of Illinois. Of these materials, GaAs appeared the most promising, having a maximum δ of approximately 3.5. It is possible that an excessive amount of As may be evolved on heating GaAs to tube bakeout temperatures, however the GaAs cathode could be cooled if necessary.

The secondary emission ratio of type IIb semiconducting diamond* was measured as a function of primary energy and a δ_{max} of approximately 2.3 was obtained. This would give an increase of the emission current boundary (see Section 2.3) relative to that for platinum of

$$\frac{2.3-1.0}{1.8-1.0} = \frac{1.3}{0.8} = 1.6 \quad .$$

* On loan from Industrial Distributors Ltd, Republic of South Africa.

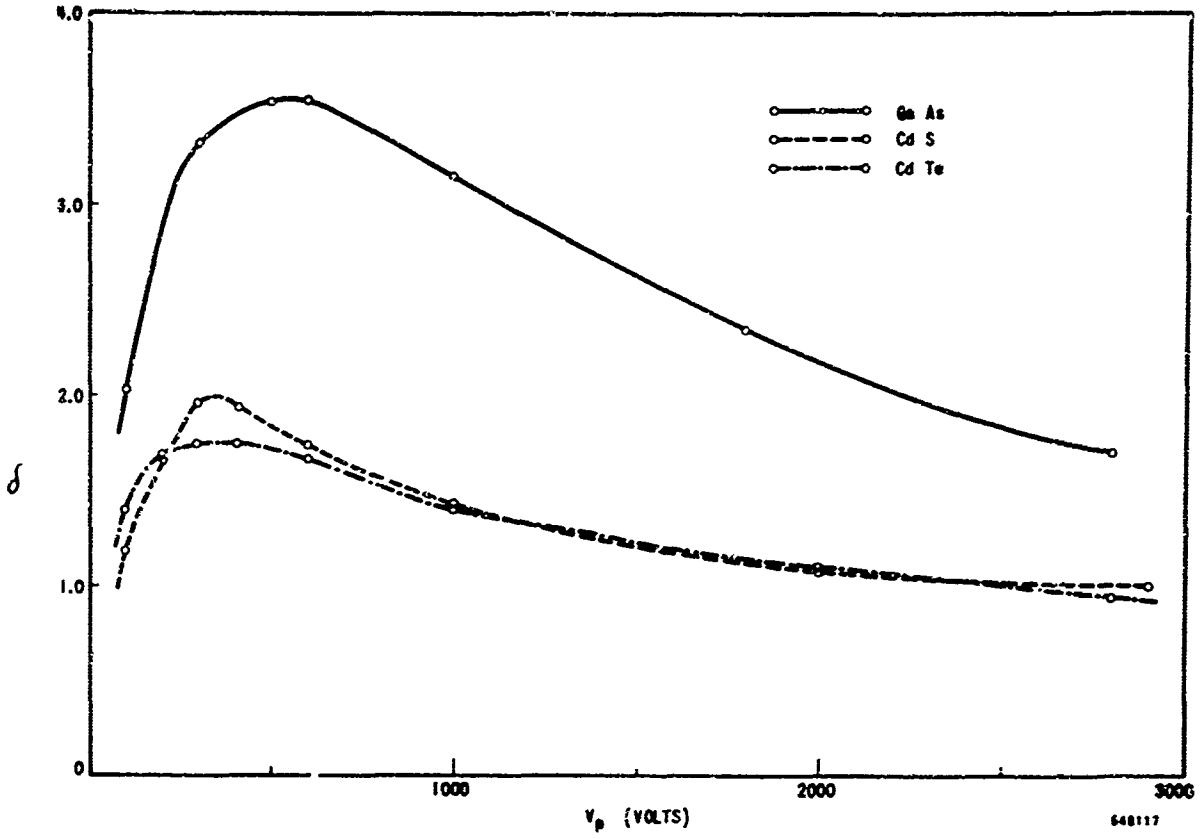

Figure 3-14. Secondary Emission Ratio (δ) vs Primary Energy (V_p) for Several Semiconductors

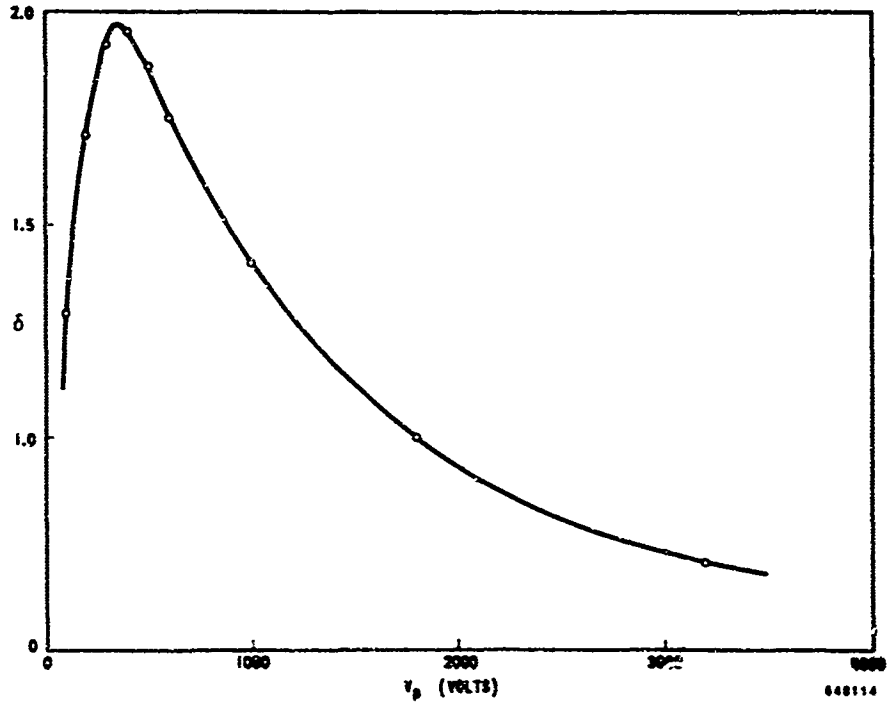

Figure 3-15. Secondary Emission Ratio (δ) vs Primary Energy (V_p) for $Ti_{14}Ni_{48.5}Si_{37.5}$

An increase by a factor of 1.6 in secondary emission limited current would then be available. Diamond, an elemental material, contains only one type of atom (carbon), therefore, it would not be subject to the electron bombardment dissociation as are oxides. In addition, being semiconducting, these diamonds may be able to transmit the tube current without excessive heat dissipation.

3.2.5 Boron nitride. A sample of a 200Å CVD film of boron nitride, prepared under the direction of Dr. W. Feist of the Raytheon Research Division was evaluated in the Secondary Emission Measurement Test Vehicle. Shown below are the results of the measurements.

Treatment	δ_{max}	$V_{p_{max}}$ (Volts)
After system bakeout	4.86	425
15 min at 400° C	5.82	350
Additional 15 min at 400° C	6.44	375
Additional 15 min at 400° C	5.75	400
Additional 15 min at 400° C	4.30	400
Additional 15 min at 400° C	3.83	400
Additional 15 min at 400° C	4.32	400

Figure 3-16 shows the measured dependence of δ on V_p after the last heat treatment. Based on the experience with molybdenum-alumina films, one may suppose that it is possible to dope the BN film to achieve a desirable conductivity without seriously degrading δ.

3.2.6 Silver-magnesium and beryllium-copper alloys. Two alloys, one silver and 7% magnesium and the other copper and 2% beryllium were tested in the secondary emission test vehicle for secondary emission ratios (δ_{max}). These alloys were reported in the literature to have high secondary emission ratios (δ_{max}) after undergoing an optimum oxidation process described briefly below.

3.2.6.1 Optimally oxidized silver-magnesium. Optimum oxidation of the silver-magnesium alloy (7% Mg) was obtained in a two-step process described in a paper by P. Rappaport.[37] The process consists of the following: a) buffing of the sample on clean buffing wheel, (we elected to hand polish to 4/0 emery paper finish); b) cleaning in soapy H_2O, then rinsing in distilled H_2O, rinsing in acetone (we actually cleaned ultrasonically in freon, again ultrasonically in Metalex, rinsing in hot H_2O, again in cold H_2O, then in acetone); c) placing in a vacuum furnace and bubbling air through H_2O into a trap; d) using dry-ice and acetone trap plus diffusion pump, baking the

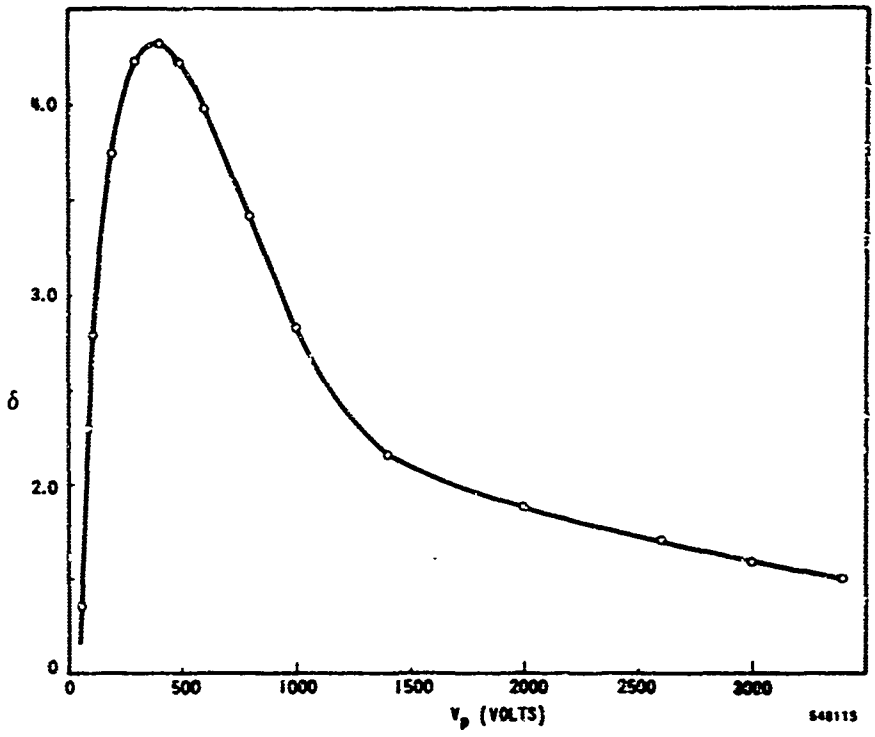

Figure 3-16. Secondary Emission Ratio (δ) vs Primary Energy (V_p) for BN

sample at 550° C for 30 minutes in approximately 10^{-5} torr vacuum. For the second part of the two-step process, the samples were baked in pure dry oxygen (H_2O vapor pressure < 10^{-8} torr) at atmospheric pressure for 30 minutes at 550° C.

3.2.6.2 Optimally oxidized beryllium-copper. This alloy (2% Be) was processed by directions supplied by Bell Telephone Laboratories.[38] The process consists of the following: a) electrolytic polishing; b) rinsing in hot H_2O, alcohol, and acetone; c) firing for 20 minutes at 630° in an O_2-free H_2 stream; d) firing for 20 minutes at 630° in a wet H_2 stream; and e) rapid cooling in the cold zone of the furnace (about room temperature) near the entrance of the H_2 stream for 20 minutes.

3.2.6.3 Secondary emission measurements. A set of silver-magnesium (7% Ag) and beryllium-copper (2% Be) samples consisting of both optimally oxidized and unprocessed specimens were prepared for secondary emission measurements. The set of eight samples included two of each case; however, only one sample of processed AgMg was available. A clean platinum sample was substituted as the eighth sample. The unprocessed samples were prepared in the same manner as the processed ones up to the point of the oxidation step.

The eight samples were installed in the Secondary Emission Test Vehicle (SEE) and baked out overnight (20 hours) at 200° C. A vacuum of less than 10^{-8} torr was reached after bakeout of the system. Secondary-electron emission measurements as a function of primary energy were carried out on the samples as follows: a) after the 20-hour-200° C bakeout, b) after heating the sample for 20 minutes at 200° C by radiant heat as measured by an infrared pyrometer, and c) after heating the sample by radiant heat for 20 minutes at 400° C. Each sample was heated and checked individually. Pressure increases during the sample heatings were observed to be small; the largest of these did not exceed approximately 8×10^{-8} torr.

The δ_{max} values listed in Table 3-6 measured after system bakeout at 200° C (measured by the thermocouple attached to the system) are generally in good agreement with those values obtained by others. The value of δ_{max} for the platinum also is in good agreement with the generally accepted value of 1.8. The optimally oxidized samples are improved by approximately 3-to-1 over the unprocessed samples at this point. After the 20-minute radiant heating at 200° C, the greatest change occurred in the δ_{max} value of the processed AgMg sample, which decreased by about one-half in value, (6.33 to 3.39). No curve was obtained for the processed BeCu sample located in the SEE next to the processed AgMg sample, due to charging phenomena on the sample, and the value of the Pt sample which also was adjacent to the processed AgMg had increased slightly. Considering the large change in the δ_{max} of the processed AgMg sample, it is quite possible that Mg was evaporated during the radiant heating and that deposition of this Mg on the two adjacent samples was the cause for their behavior. This reasoning might also apply to S2 and S6 whose δ_{max} values decreased. Samples S3, S4, and S5 show essentially no change. After the 400° C radiant heating for 20 minutes, the greatest change occurred in the processed BeCu samples. Their values decreased by about 1.0 from the values of δ_{max} after system bakeout. The δ_{max} of the processed AgMg (S8) had increased slightly, from 3.39 to 3.69. The rest of the samples showed no significant change in δ_{max}.

The δ_{max} values obtained from the secondary-emission test are in good agreement with those predicted in the Bell Laboratories letter[38] in the case of BeCu, and from the Rappaport paper[37] in the case of AgMg. The δ_{max} of the Pt sample remained within a reasonable range of the 1.8 standard value for that metal. From the data to date, it would seem that the processed BeCu is less affected by temperature (outgassing) than the processed AgMg, and encounters smaller decreases of δ.

3.2.7 Summary of secondary emission measurements in the SEE Vehicle. The main purpose of performing the measurements of secondary emission in the SEE vehicle was to select the most promising cold cathode materials for evaluation under electron and ion bombardment conditions.

Changes in δ vs V_p have been demonstrated for the methods of material preparation, oxidation, and heating under vacuum conditions.

The study is briefly summarized in the following sections.

TABLE 3-6.

δ_{max} for Plain and Optimally Oxidized BeCu and AgMg

Sample No.		δ_{max} After 20 hr Bakeout at 200° C	δ_{max} After 200° C - 20 min Radiant Heating	δ_{max} After 400° C - 20 min Radiant Heating
S1	Pt	1.86	1.94	1.96
S2	Unprocessed BeCu	1.88	1.53	1.69
S3	Unprocessed BeCu	1.95	2.00	1.89
S4	Unprocessed AgMg	2.19	2.17	1.98
S5	Unprocessed AgMg	2.05	2.04	1.94
S6	Processed BeCu	5.63	5.40	4.45
S7	Processed BeCu	5.86	No curve due to charging	5.00
S8	Processed AgMg	6.33	3.39	3.69

3.2.7.1 Aluminum. Thin oxide layer (~25Å) on surface.

a. δ_{max} in the SEE vehicle was approximately 2, while the effective value in a CFA is typically ~6.

b. δ_{max} measured as a function of angle of incidence (θ) was found to vary from 2.0 to 2.6 for θ variation from 0° to 70°. This is insufficient to account for the discrepancy mentioned under a.

3.2.7.2 Alumina (100Å - 1000Å) films on molybdenum substrate. Electron-beam evaporated Al_2O_3 films on Mo substrate.

a. The use of a Mo substrate allows for heating at a high temperature to achieve a higher degree of crystallinity and thus higher δ (in comparison with Al_2O_3 on Al).

b. $\delta_{max} \sim 5$, independent of film thickness in the range of 100 - 1000 Å.

3.2.7.3 Molybdenum-alumina films on molybdenum substrate. Electron beam evaporated films.

a. The purpose of Mo is to make thick films electrically conductive. Thick films mean long sputtering life.

b. The most significant parameter of film preparation is substrate temperature during deposition.

c. Agglomeration of Mo caused a reduction in δ_{max} from 2.5 (deposition temperature = 600°C) to 1.8 (deposition temperature = 1100°C), whereas composition variation of 10% to 30% of Mo resulted in δ_{max} variation only in the range of 3.5 to 4.0.

3.2.7.4 Molybdenum-alumina films on platinum substrate. Electron beam evaporated films.

a. (same as "a" in 3.2.7.3)

b. δ_{max} for 20% and 30% Mo 100Å and 1000Å films before outgassing was 2.1 to 2.3 and after outgassing was 1.8 and 2.2 respectively.

3.2.7.5 Barium calcium aluminate impregnated tungsten.

a. δ_{max} was 1.6 to 2.0 before activation.

b. δ_{max} rises to a value of 4.4 after continuing activation at 1050°C, then decreases to a value of 3.33, and then levels off.

3.2.7.6 Nickel cermet.

a. δ behavior, due to thermal activation, was similar to that for impregnated tungsten.

b. Maximum value of δ_{max} ~6.

c. δ_{max} leveled off at ~3.

3.2.7.7 Semiconducting diamond (elemental semiconductor).

a. δ_{max} ~2.3.

b. Would evolve only one type of atom during electron bombardment dissociation.

3.2.7.8 Semiconducting compounds (non-oxidic).

a. The electron bombardment dissociation process would release non-volatile atoms (as contrasted with the oxygen which evolves from oxides). Therefore, electron bombardment may not cause the cathode materials to deteriorate.

b. δ_{max} of GaAs was 3.5

c. δ_{max} of CdS was 2.0

d. δ_{max} of CdTe was 1.75.

3.2.7.9 $Ti_{14}Ni_{48.5}Si_{37.5}$ (refractory, intermetallic compound, possibly semiconducting).

a. δ_{max} was 1.95.

3.2.7.10 Boron nitride films on molybdenum substrate. (non-oxidic, large gap material.

a. δ_{max} of one sample (200Å CVD preparation) was 4.3.

b. δ_{max} of 2 additional (similarly prepared) samples were in range 1.7 to 2.0 (measured in EBV which might be ~15% low).

3.2.7.11 Beryllium copper alloy (2% Be).

a. δ_{max} for unprocessed sample was ~ 1.90

b. Heating of unprocessed sample caused no decay of δ_{max}

c. δ_{max} for processed sample was 5.63 and 5.86.

d. Heating of processed sample caused decay of δ_{max} to 4.45 and 5.00.

3.2.7.12 Silver magnesium alloy (7% Ag)

a. δ_{max} for unprocessed sample was ~2.10.

b. δ_{max} was unchanged after heating unprocessed sample.

c. δ_{max} for the processed sample was 6.33.

d. δ_{max} of heated processed sample was 3.69.

3.3 Electron bombardment of cold cathodes. An electron bombardment vehicle (EBV) was used for this study to simulate the back bombardment conditions encountered in a crossed-field amplifier.

The electron bombardment vehicle is depicted in Figure 3-17 and the electrical circuit is schematically presented in Figure 3-18.

The gridded electron gun has a perveance of 1.5×10^{-6} $A/V^{3/2}$ and has enabled the achievement of $1 A/cm^2$ electron bombardment at the target at a voltage of 1.2 KV under dc conditions. This represents a dissipation of 1.2 kW/cm^2 at the target surface in a circular area of 1/16 inch diameter. When the gun current is reduced, the beam converges slightly so that the secondary emission measurement may be made within the area of electron bombardment on the target surface. With the circuit arrangement shown in Figure 3-18 δ could be measured for the range of primary energy from 0 to 800 V.

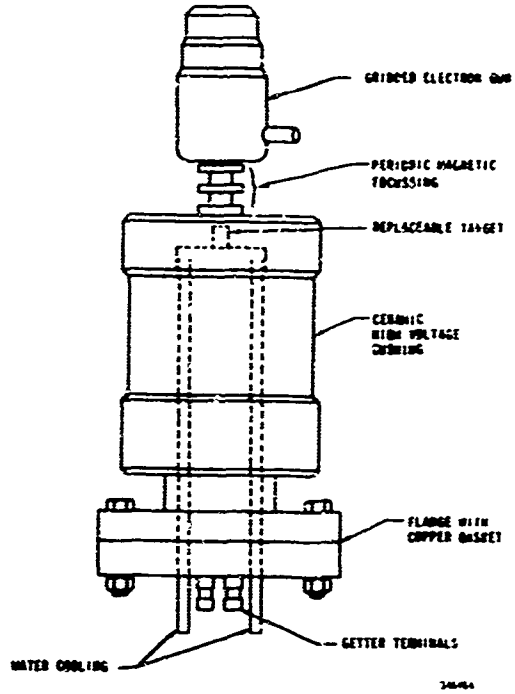

Figure 3-17. Electron Bombardment Vehicle

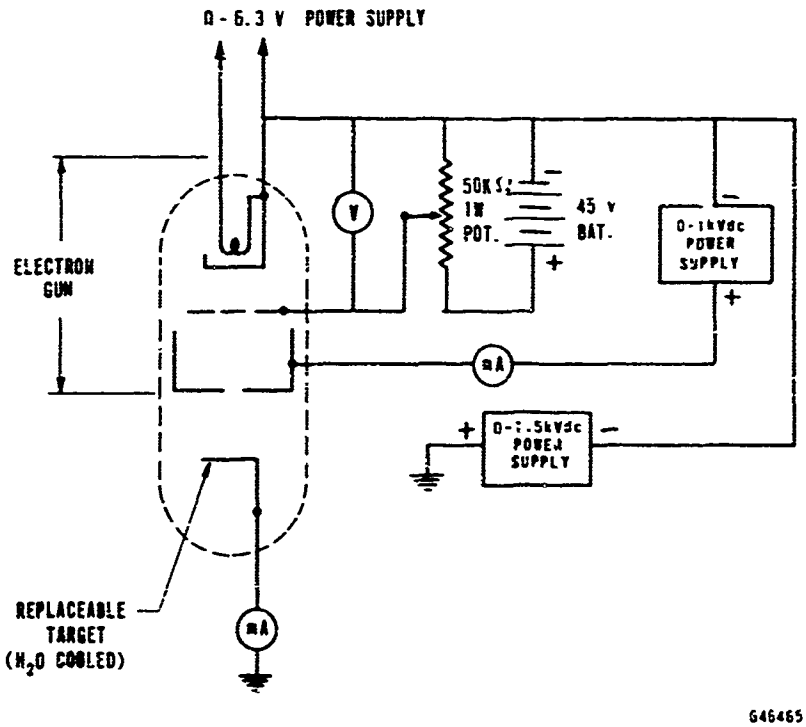

Figure 3-18. Circuit for Electron Bombardment Vehicle

The target assembly which holds the cold cathode sample is shown in Figures 3-19 and 3-20. The target is heated by a radiant tungsten heater or cooled by water flowing through the target base. The tungsten heater, mounted in a molybdenum radiation shield, can heat the target to 1100° C. The results of a calibration plot of temperature vs heater power of the target heater in a vacuum bell jar is shown in Figure 3-21. Typical vacuum in the EBV is between 10^{-8} and 10^{-9} torr. An overall view of the EBV setup is shown in Figure 3-22.

A Pt sample was mounted in the EBV to serve as a reference source in the secondary emission measurement in the EBV and also to investigate the effect of barium evaporation from the impregnated tungsten cathode of the electron bombardment gun. Secondary emission data for the Pt target in the EBV is shown in Figure 3-23. It can be seen that δ_{max} was about 15% lower than the usual value of 1.8, measured repeatedly in this laboratory.

It was also observed that electron bombardment at levels of up to 0.5 Amp/cm^2 at 1200 volts over a period of several hours had no effect on δ of the Pt target. In addition EBV gun cathode temperature changes from approximately 1025° C to 875° C resulted in no change of δ. This temperature change corresponded to a change in Ba evaporation of at least a factor of 10. It is concluded that Ba evaporation from the gun cathode does not play a significant role in the δ measurements reported in the EBV.

3.3.1 Aluminum oxide films on metal substrates. Secondary emission measurements in the SEE vehicle of alumina or molybdenum-alumina film showed high δ_{max} ranging from 3.5 to 5.0.

Several tests were conducted in the EBV to determine the effects of electron bombardment on δ_{max} for various combinations of alumina films on metal substrates.

3.3.1.1 Molybdenum-alumina films. A sample was prepared by electron beam evaporation of a 30% Mo - 70% Al_2O_3 mixture. The film was 1000Å thick and was deposited on a copper substrate. Figure 3-24 shows the variation of δ_{max} with time resulting from electron bombardment of the Mo-Al_2O_3 surface.

After an initial increase of δ_{max} under bombardment at 1/3 A/cm^2, δ_{max} decreased under bombardment at 1 A/cm^2. After approximately 40 hrs of bombardment δ_{max} seemed to level off (at ~1.7). A typical curve of δ vs V_p for this 1000Å film is shown in Figure 3-25. It can be seen that δ_{max} occurs at approximately 400 volts, which is in agreement with observations in our classical secondary emission test vehicle.

A 100Å molybdenum-alumina film was prepared on a molybdenum substrate. It was derived from a 30% molybdenum source and deposited at 600° C substrate temperature. The observed variation of δ_{max} with time under electron bombardment is shown in Figure 3-26. It shows a decrease in δ_{max} from 3.5 to 2.5 in about 2.5 hours. Subsequent to this, the value of δ_{max} remained essentially constant for approximately 5 hours. The possible influence of barium vapor from the gun cathode depositing on the target was ascertained by varying the cathode temperature for the same electron bombardment current density.

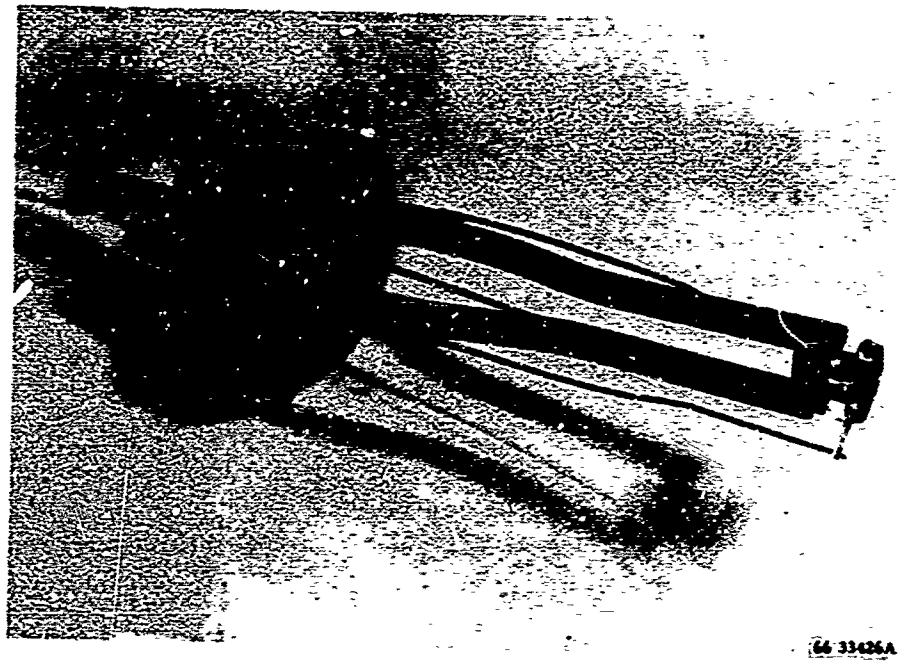

Figure 3-19. Target Mount and Support Flange Hot-Cold EBV

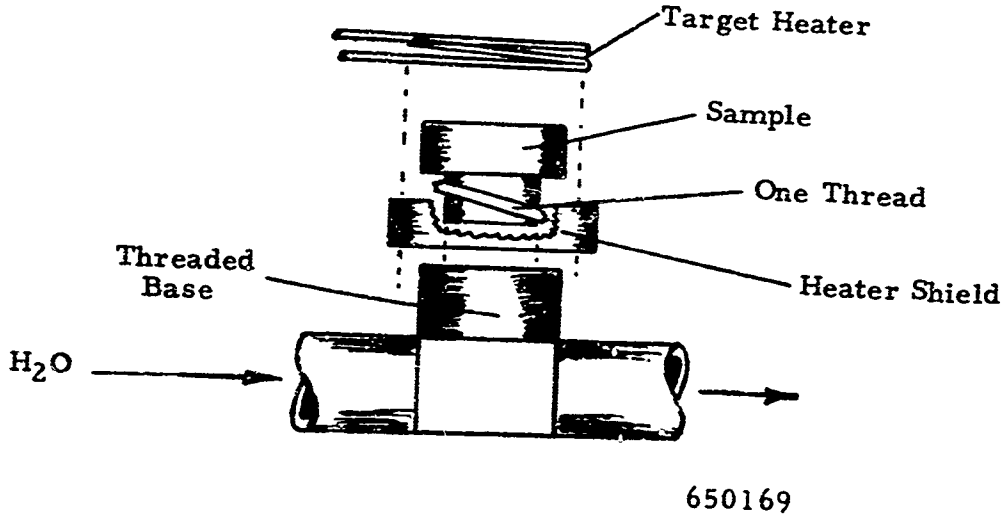

Figure 3-20. Target Mount of Hot-Cold EBV (exploded view)

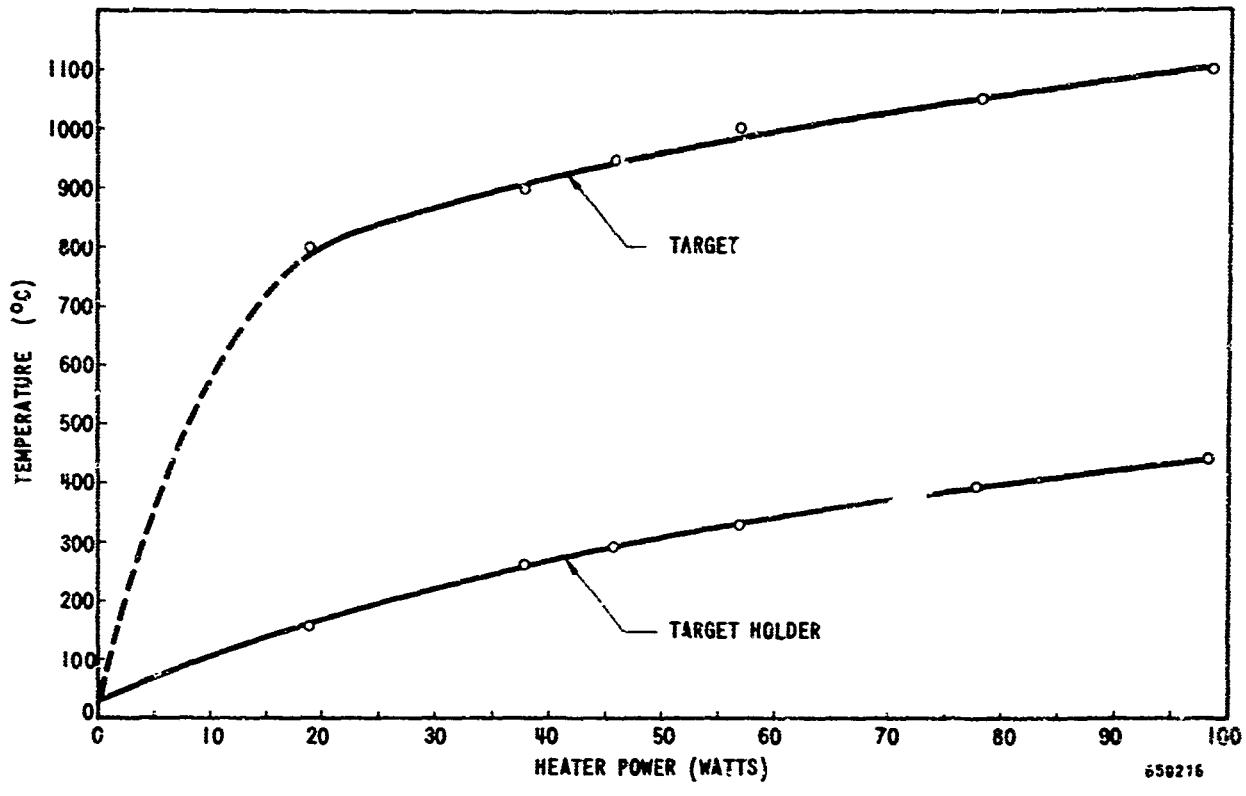

Figure 3-21. Temperature vs Heater Power for Hot-Cold EBV

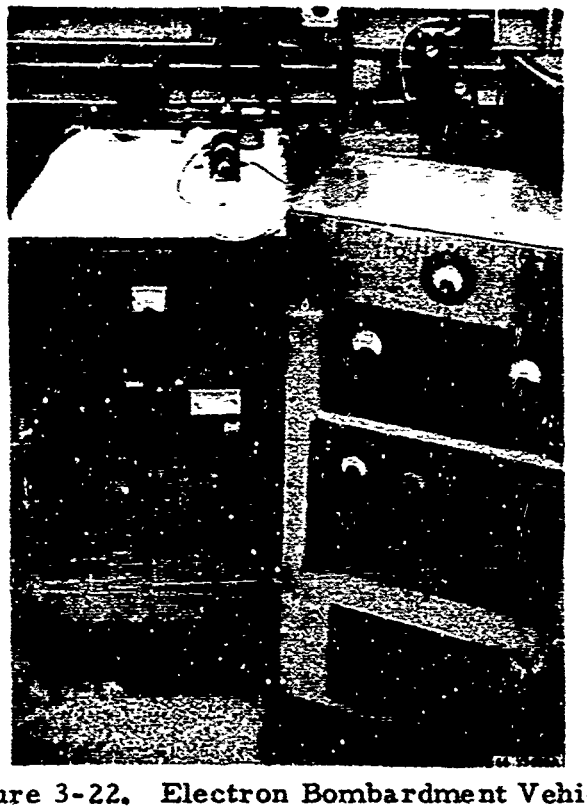

Figure 3-22. Electron Bombardment Vehicle Setup (overall view)

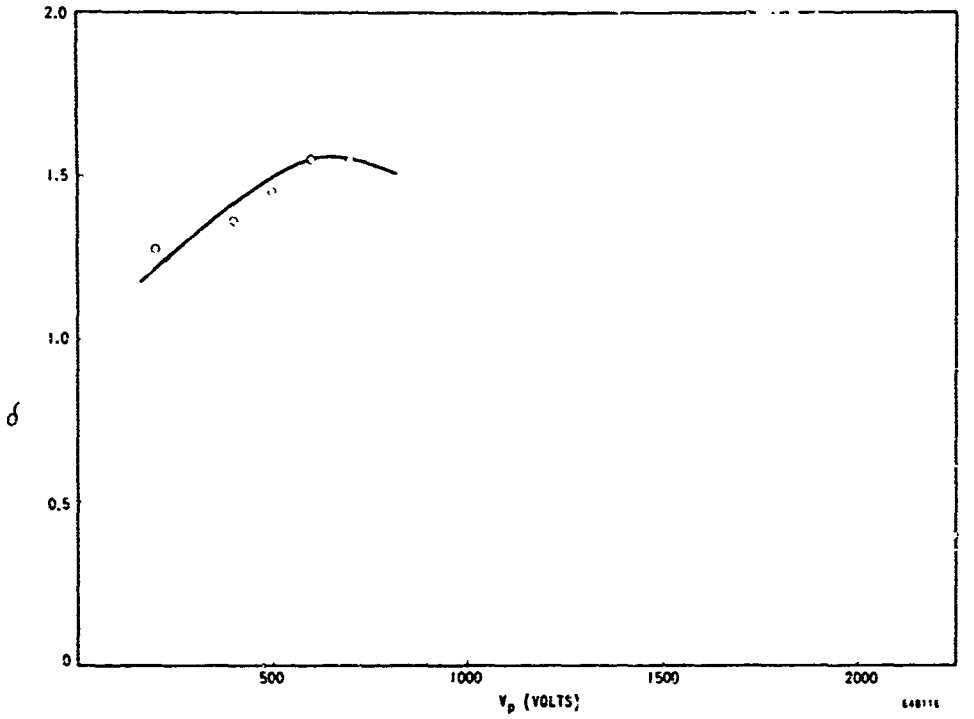

Figure 3-23. Secondary Emission Ratio (δ) vs Primary Energy (V_p) for Pt in EBV

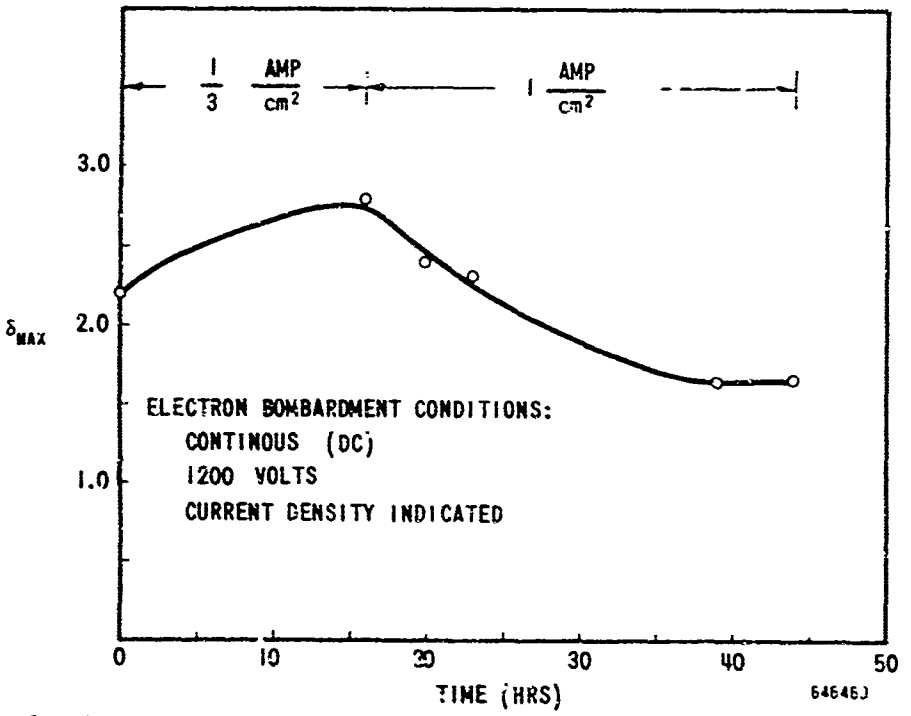

Figure 3-24. Secondary Emission Ratio Maximum (δ_{max}) vs Electron Bombardment Time for 1000Å Moly-Alumina Film on Copper Substrate

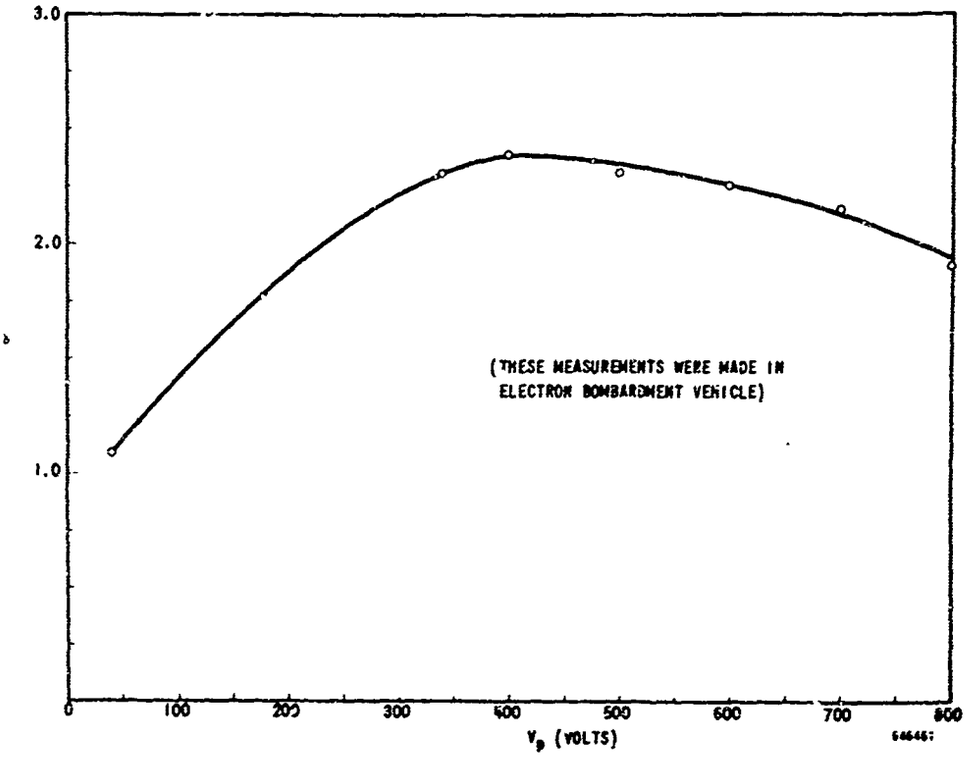

Figure 3-25. Secondary Emission Ratio (δ) vs Primary Energy (V_p) for 1000Å Moly-Alumina Film on Copper Substrate

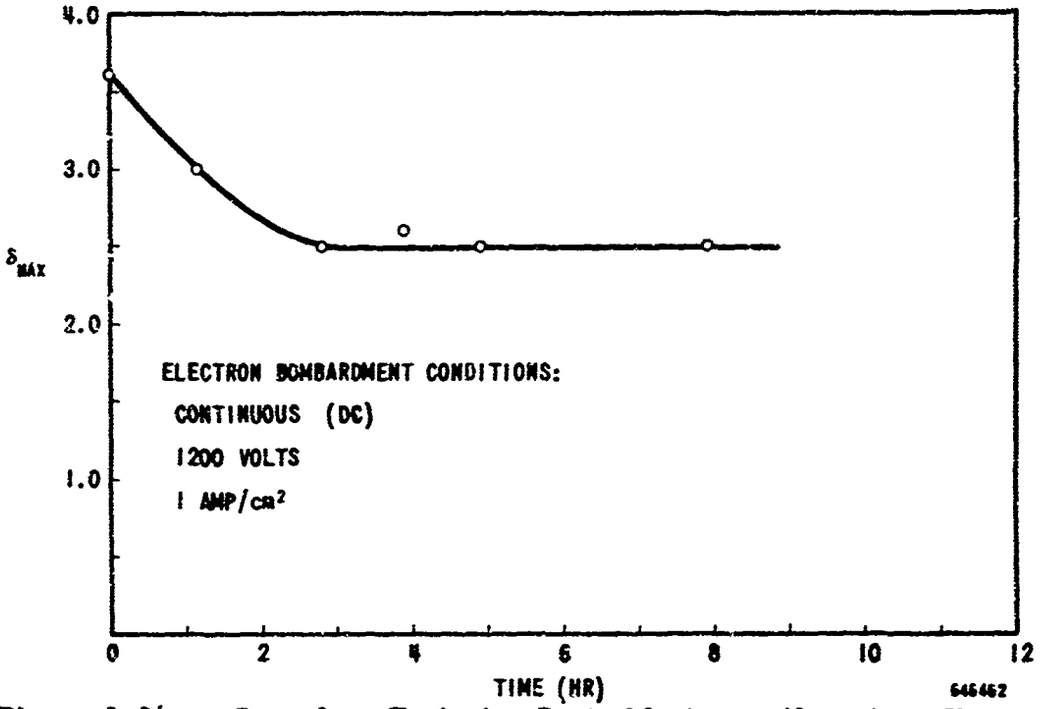

Figure 3-26. Secondary Emission Ratio Maximum (δ_{max}) vs Electron Bombardment Time for 100Å Moly-Alumina Film on Moly Substrate

A 500Å thick 30% Mo-70% Al_2O_3 film on a Mo substrate was studied in the EBV for effects of electron bombardment on the surface of the film. The results are shown in Figure 3-27.

The deactivation of the film (decrease of δ_{max}) was due to continuous electron bombardment at 0.5 A/cm^2 and at 1.0 A/cm^2, both at 1200 volts. Reactivation of the film was accomplished by the use of an auxiliary oxygen source. CuO powder was pressed into the shape of a pellet and trapped at the end of a molybdenum cylinder, inside of which a tungsten heater was mounted. Thus the oxygen partial pressure in the vacuum system could be controlled by adjusting the temperature of the CuO pellet.

The data for the Mo-Al_2O_3 film shown in Figure 3-27 represents a typical segment of the activation-deactivation procedures performed. Electron bombardment at 0.5 A/cm^2 caused a deactivation of δ_{max} from 3.8 to 3.2 in 3 hours. The oxygen source was then turned on to a CuO pellet temperature of 560° C. This corresponds to an oxygen partial pressure of 7×10^{-8} torr.* The secondary emission ratio recovered partially while bombardment of 0.5 A/cm^2 continued (hours 3 to 6 1/2). More complete recovery was achieved at an oxygen pressure of 6×10^{-7} torr (hours 10 1/2 to 14). Recovery of δ was also observed to occur while the equipment was turned off for 64 hours (hour 6 1/2). This is attributed to reoxidation of the surface; the oxygen may come from other tube surfaces or from deeper sites within the cathode. As seen in Figure 3-24, the deactivation of the Mo-Al_2O_3 film was more rapid for electron bombardment at 1.0 A/cm^2, a decrease in δ_{max} from 3.4 to 2.6 occurring in 3 hours (hours 15 1/2 to 18 1/2). Recovery was observed using oxygen at a pressure of 6×10^{-7} torr. The recovery was only partial; presumably a higher oxygen pressure is needed to maintain δ under higher current density electron bombardment conditions.

3.3.1.2 Alumina films. Two samples of 300Å electron-beam-evaporated Al_2O_3 on Mo were prepared for the EBV vehicle. The effect of high current-density electron bombardment (up to 0.75 A/cm^2) on the secondary emission ratio (δ_{max}) was measured as well as the recovery of δ_{max} with oxygen. Also, nitrogen and carbon dioxide were used instead of oxygen.

The first sample showed an initial δ_{max} of 2.0 which subsequently increased to 3.8 with oxygen treatment (primarily under bombardment at 0.15 A/cm^2 in O_2 of 1.5×10^{-5} torr).

---

* A calibration of oxygen pressure as a function of CuO pellet temperature yielded the expected exponential dependence $P = P_o \exp(-Q/kT)$ with an activation energy of 220 kilocalories/mole.

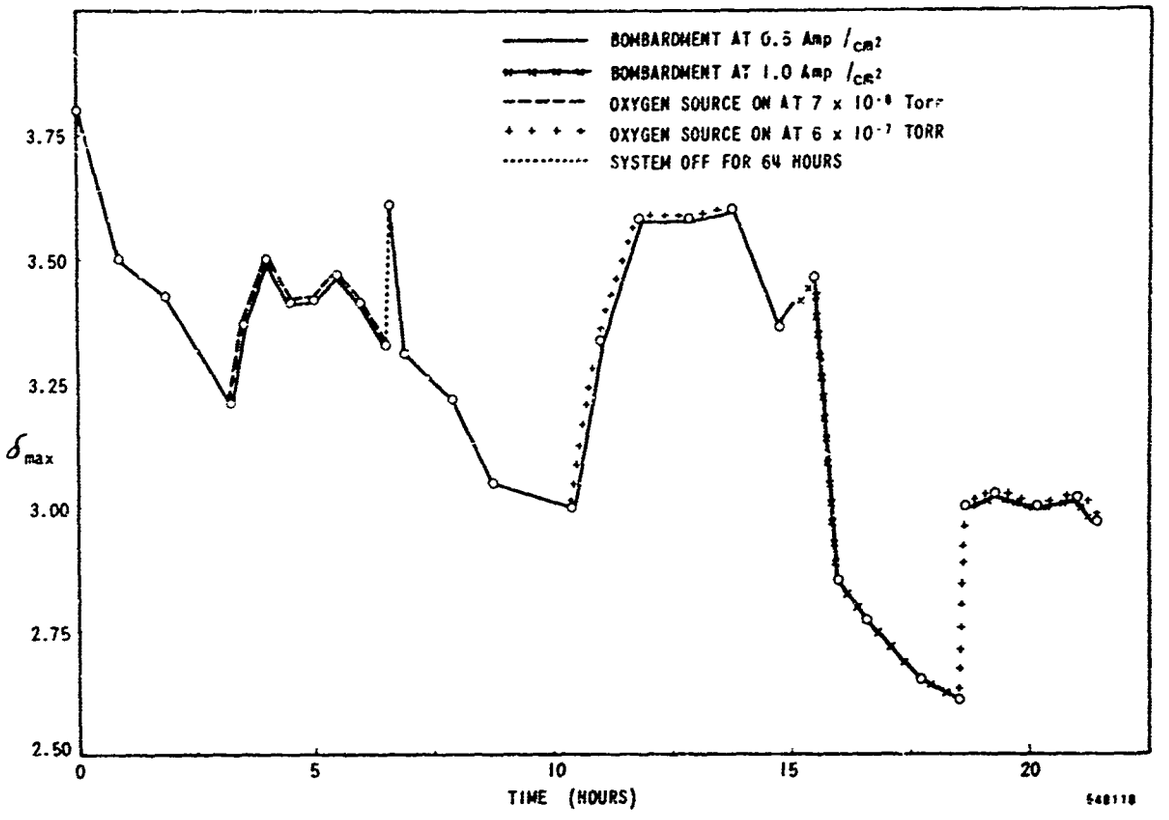

Figure 3-27. Activation of 500Å 30% Molybdenum - 70% Al_2O_3 Film on Molybdenum Substrate using CuO Oxygen Source

The second sample was exposed to O_2, N_2, and CO_2 during a 41-hour period of EBV evaluation. (See Figure 3-28.) The initial effect of O_2 at 6×10^{-6} torr pressure was to increase δ_{max} from 2 to 4.2. Subsequent degradation of δ_{max} to 2.6 due to 0.75 A/cm² electron bombardment was followed by an unsuccessful attempt to increase δ by the use of N_2 at 6×10^{-6} torr. Following this, an O_2 treatment at 6×10^{-6} torr did increase δ_{max} from 2.6 to 3.05. Although this increase was smaller than the initial effect, the N_2 effect was decidedly much smaller than that of O_2.

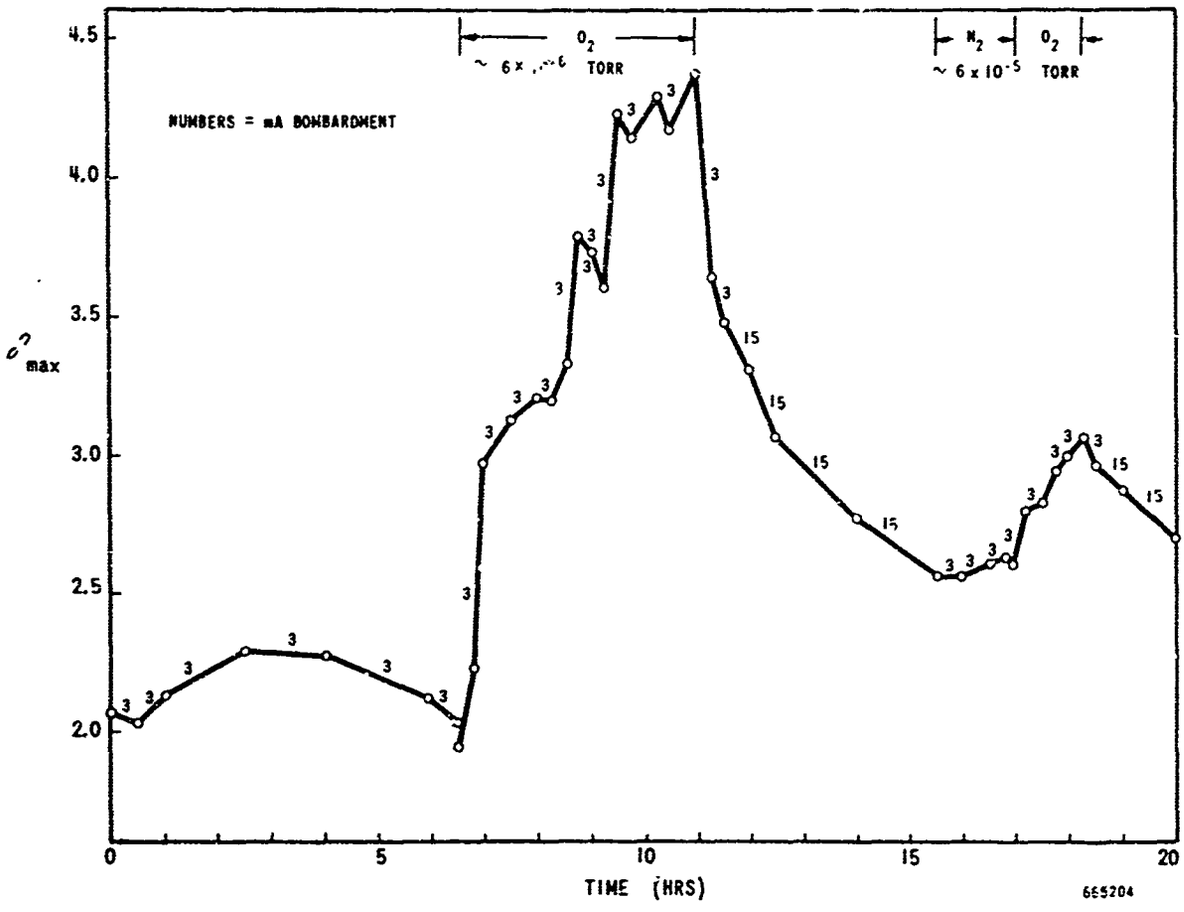

Figure 3-28. Sheet 1. δ_{max} vs EBV Time for 300Å Electron-Beam-Evaporated Al_2O_3 on Molybdenum

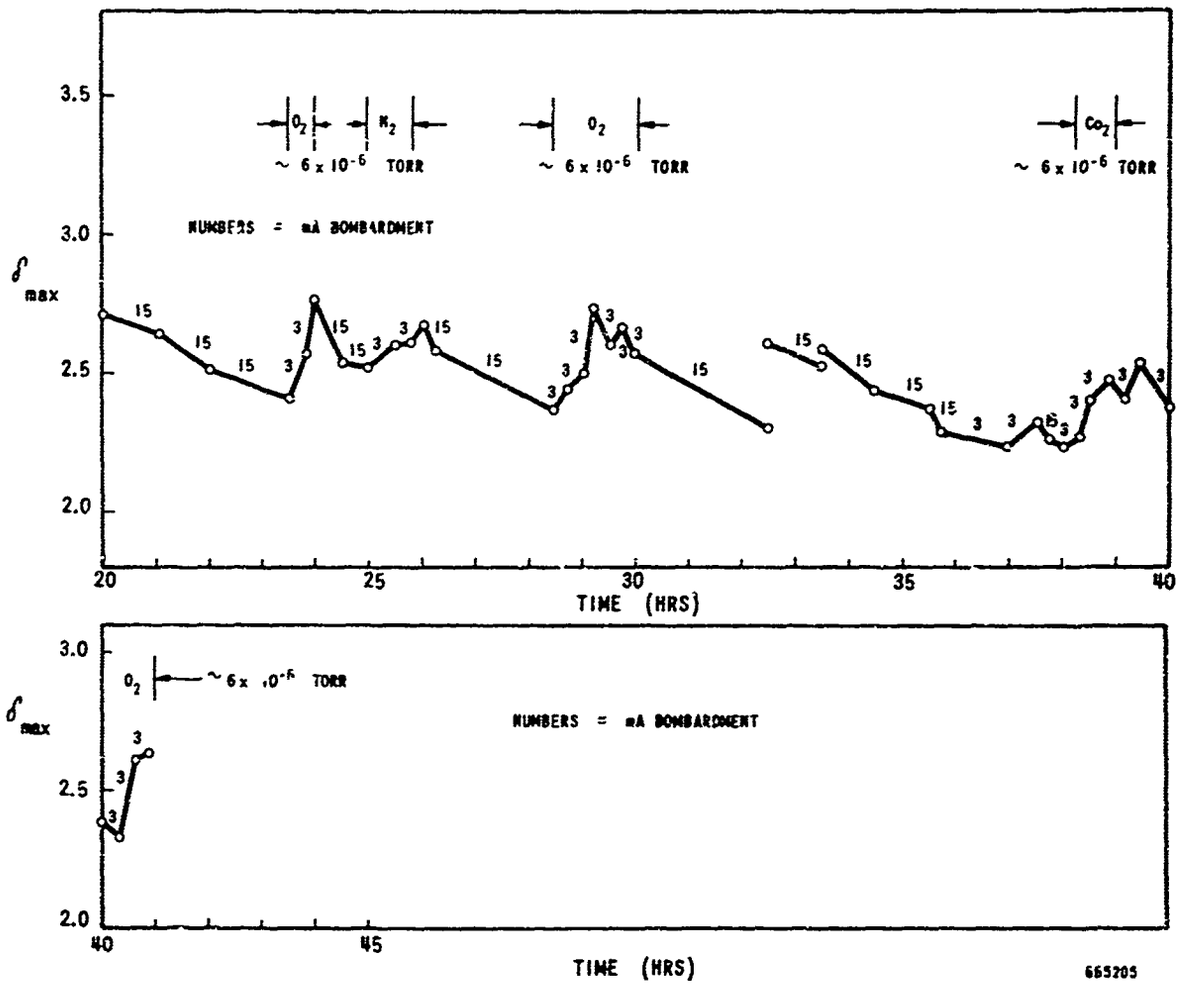

Figure 3-28. Sheet 2. δ_{max} vs EBV Time for 300Å Electron-Beam-Evaporated Al_2O_3 on Molybdenum

Subsequent gas treatments caused only small effects, with δ_{max} varying between 2.3 and 2.75. The results during this latter portion of the EBV evaluation (hours 23 to 42) are deemed inconclusive since the condition of the sample was not "normal" as evidenced by the lack of a strong, positive O_2 response.

3.3.1.3 Oxidized aluminum films. A series of tests was conducted in the EBV vehicle using aluminum metal targets made either by evaporating an aluminum layer on a chemically cleaned, wet-polished OFHC copper substrate or by machining and chemically cleaning an aluminum alloy.

The target samples were either naturally oxidized (25Å layer of oxide) or anodized 300Å oxide layer).

Three samples (E-1, E-2 and E-3), of an evaporated aluminum layer of 9500Å thickness were deposited on a chemically cleaned, wet-polished OFHC copper substrate and tested in the EBV vehicle. The results of 80 hours of evaluation in the EBV for sample E2 are shown in Figure 3-29. Residual vacuum without oxygen addition was approximately 5×10^{-8} torr. Recovery with oxygen at 8×10^{-6} torr is shown during hours 3 to 11. After a small increase of δ_{max} (overnight) while the equipment, including the gun, was off, a large increase to a δ_{max} in excess of 4.0 was observed (hours 11 to 19). During this time, the gun heater and gun cathode were at elevated temperature, but without electron bombardment. The increase may have been due to gases released by the heater-cathode structure of the electron gun. Subsequent to this, electron bombardment at 0.75 A/cm^2 from hours 19 to 35 caused δ_{max} to decrease from 4.0 to 1.4. This sample never again reached the high δ value of 4.0. The sample continued to show the expected response to O_2 and to high-density electron bombardment. The decrease of δ_{max} due to bombardment of 0.75 A/cm^2, which occurred during hours 60-79, was quite slow. δ_{max} decreased from 3.2 to 1.5 in 24 hours. The results from samples E1 and E3 were similar in all respects.

An aluminum target alloy 6061 (97.5% purity) was cleaned and the surface prepared in a manner similar to that required for plating. The aluminum target was then mounted in the EBV and evaluated for 92 hours. The resultant data are summarized in Figure 3-30. The residual gas pressure was approximately 5×10^{-8} torr. Additional oxygen was supplied from an auxiliary, thermally activated, CuO source.

The initial value of δ_{max} was approximately 5 and stands out as an unexpected result. Previous δ measurements on room temperature, air-oxidized, aluminum alloy 6061 showed δ_{max} values of approximately 2. Bulk, crystalline, aluminum oxide displayed δ_{max} values of 5, and similar high δ values were observed for Al_2O_3 films deposited on a Mo substrate by electron beam evaporation techniques. However all previous room temperature, air-oxidized, aluminum samples had δ_{max} values less than 2.5, typically 2.0.

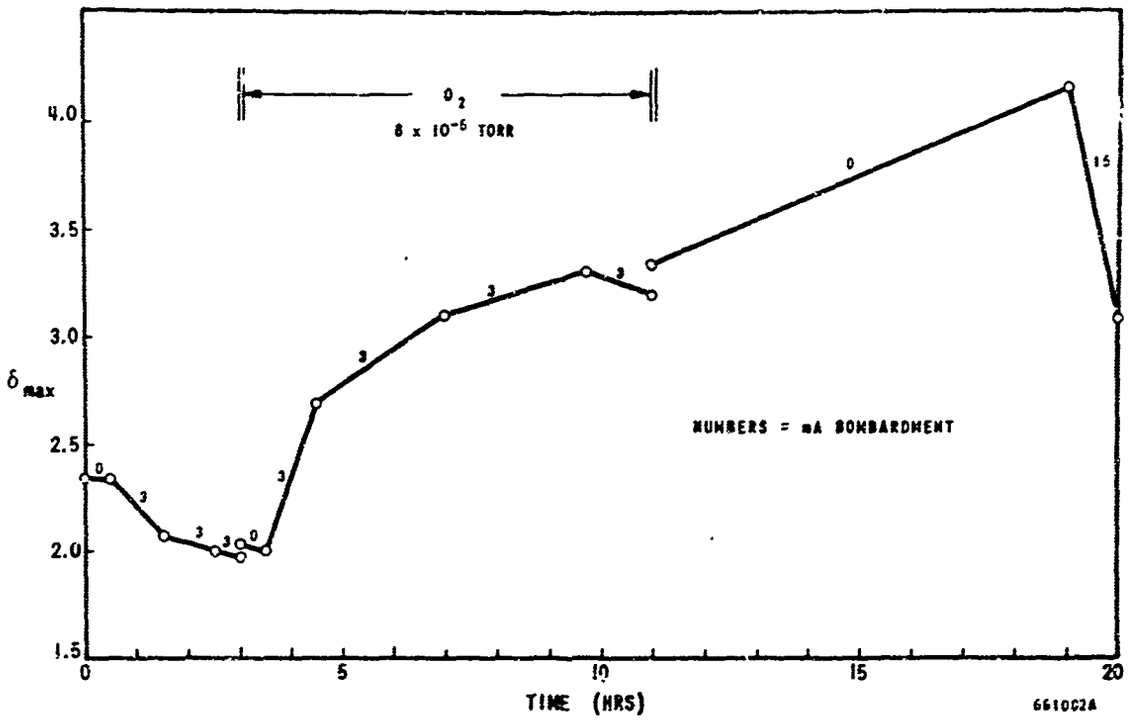

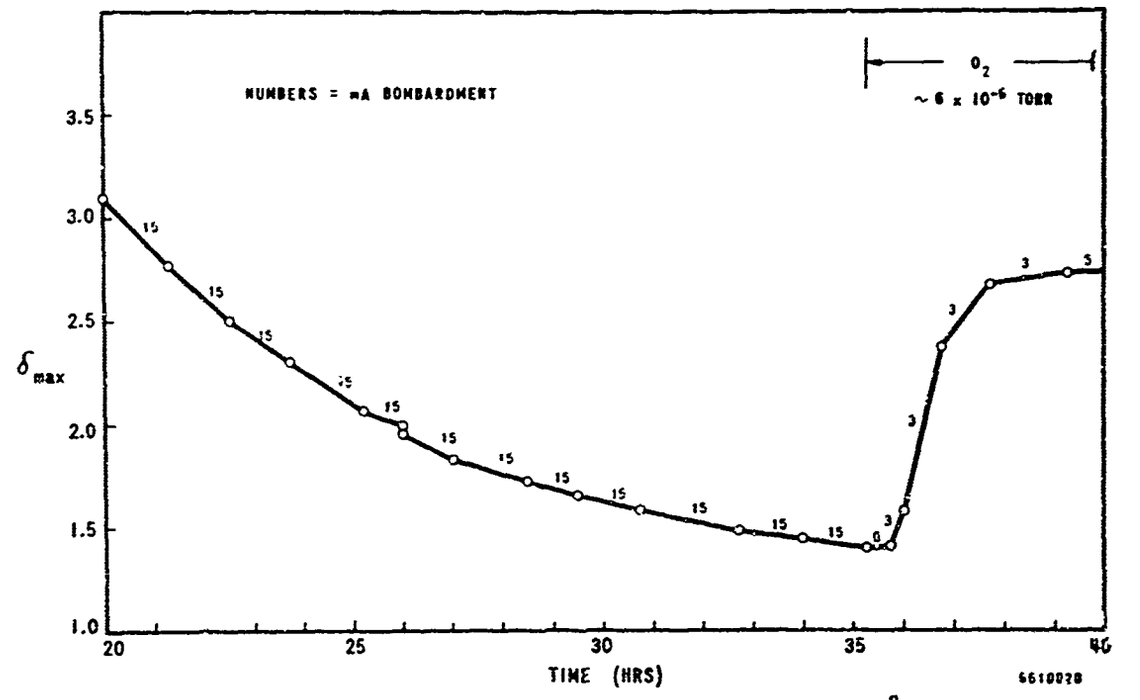

Figure 3-29 Sheet 1. δ_{max} vs EBV Time for 9500Å Aluminum Evaporated on Copper and Naturally Oxidized (Sample E-2)

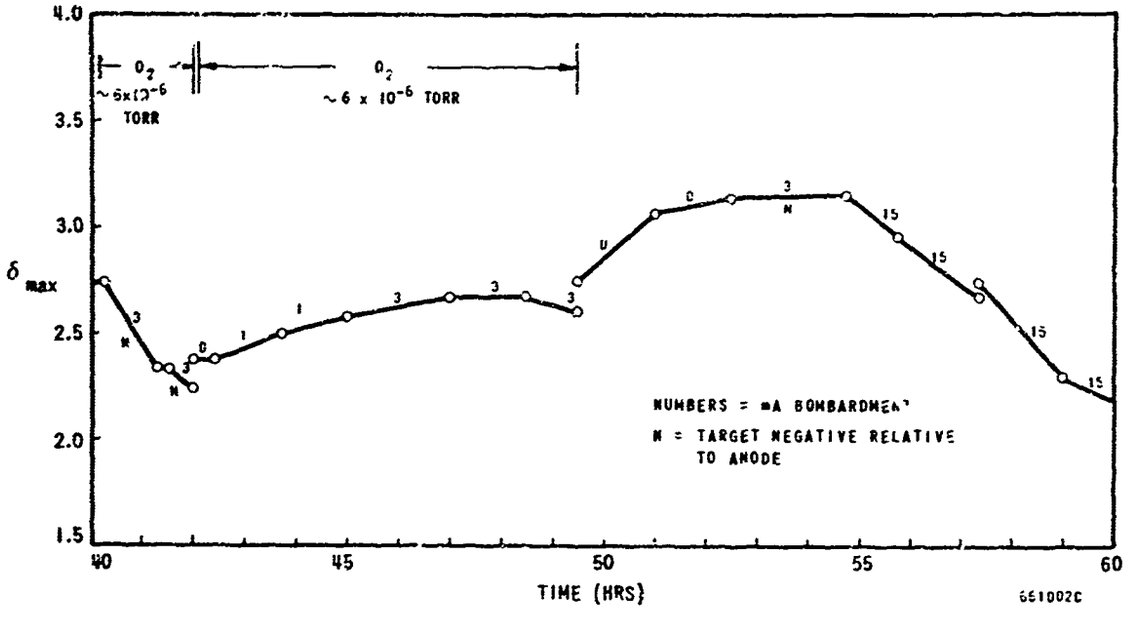

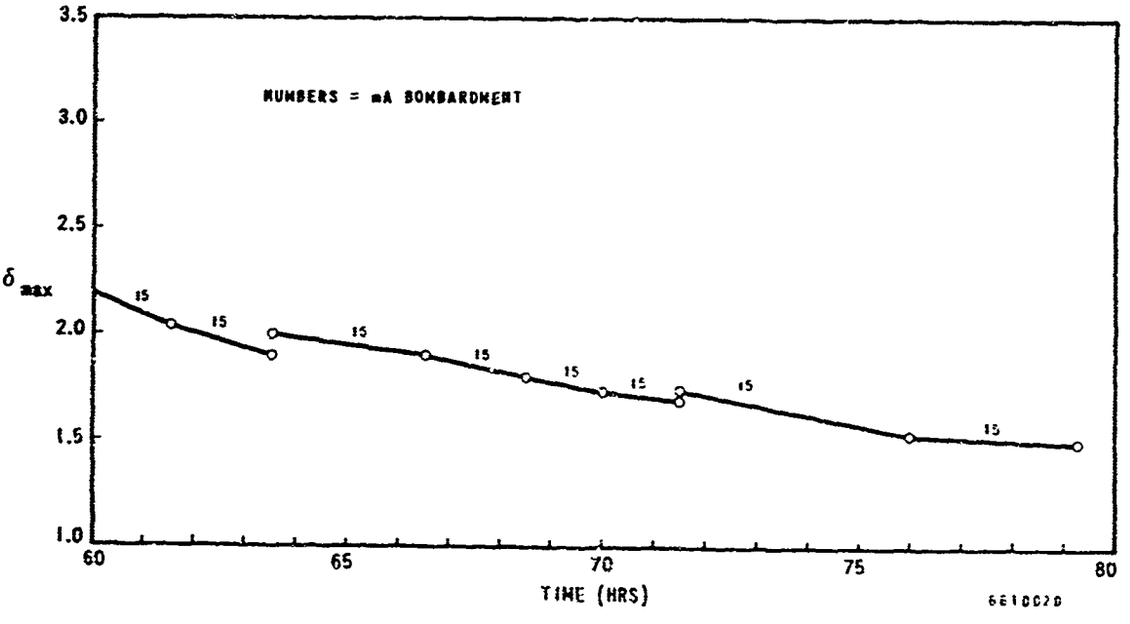

Figure 3-29 Sheet 2. δ_{max} EBV Time for 9500Å Aluminum Evaporated on Copper and Naturally Oxidized (Sample E-2)

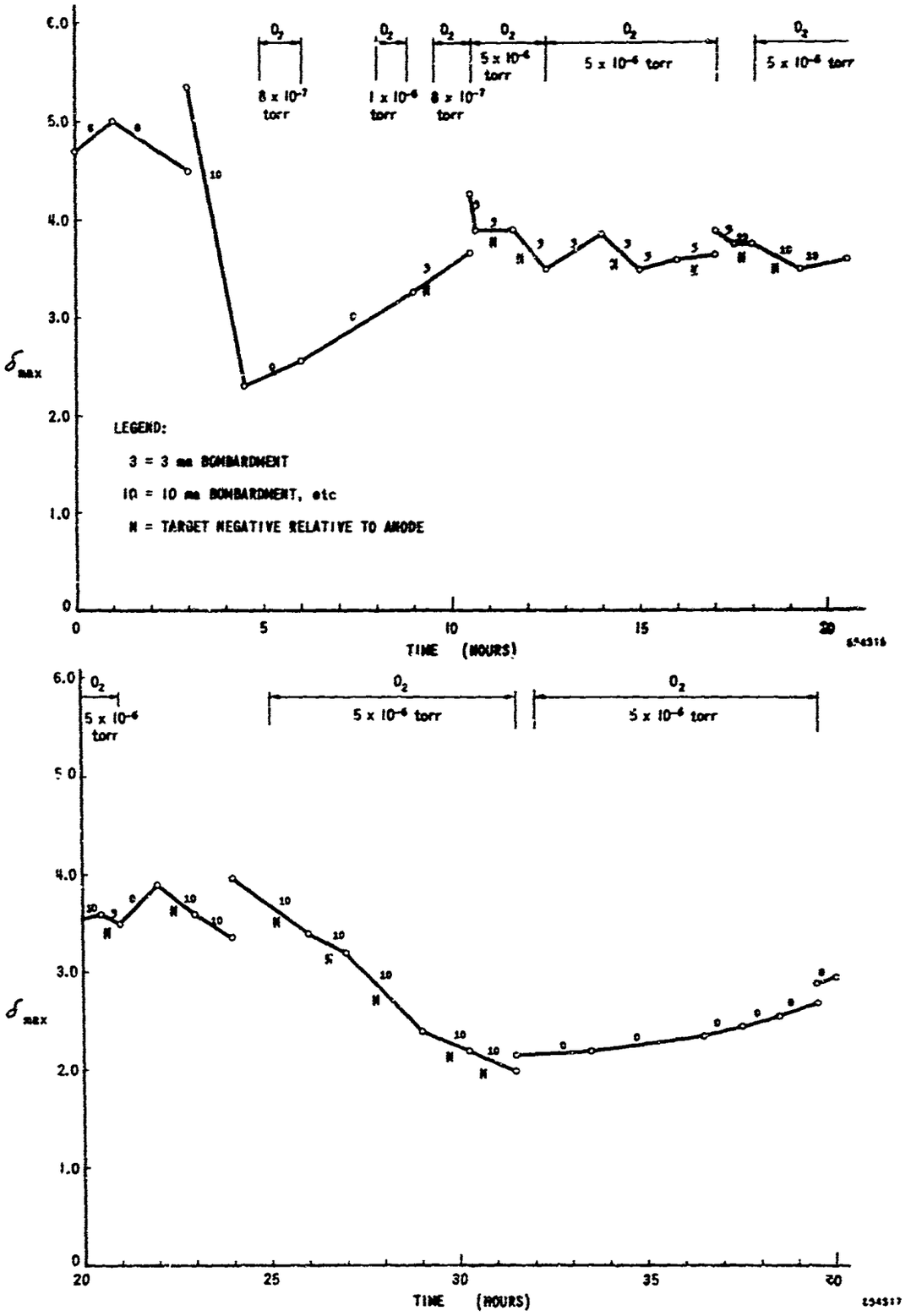

Figure 3-30 Sheet 1. δ_{max} vs Time in Electron Bombardment Vehicle for Aluminum (Alloy 6061) Target (Naturally Oxidized)

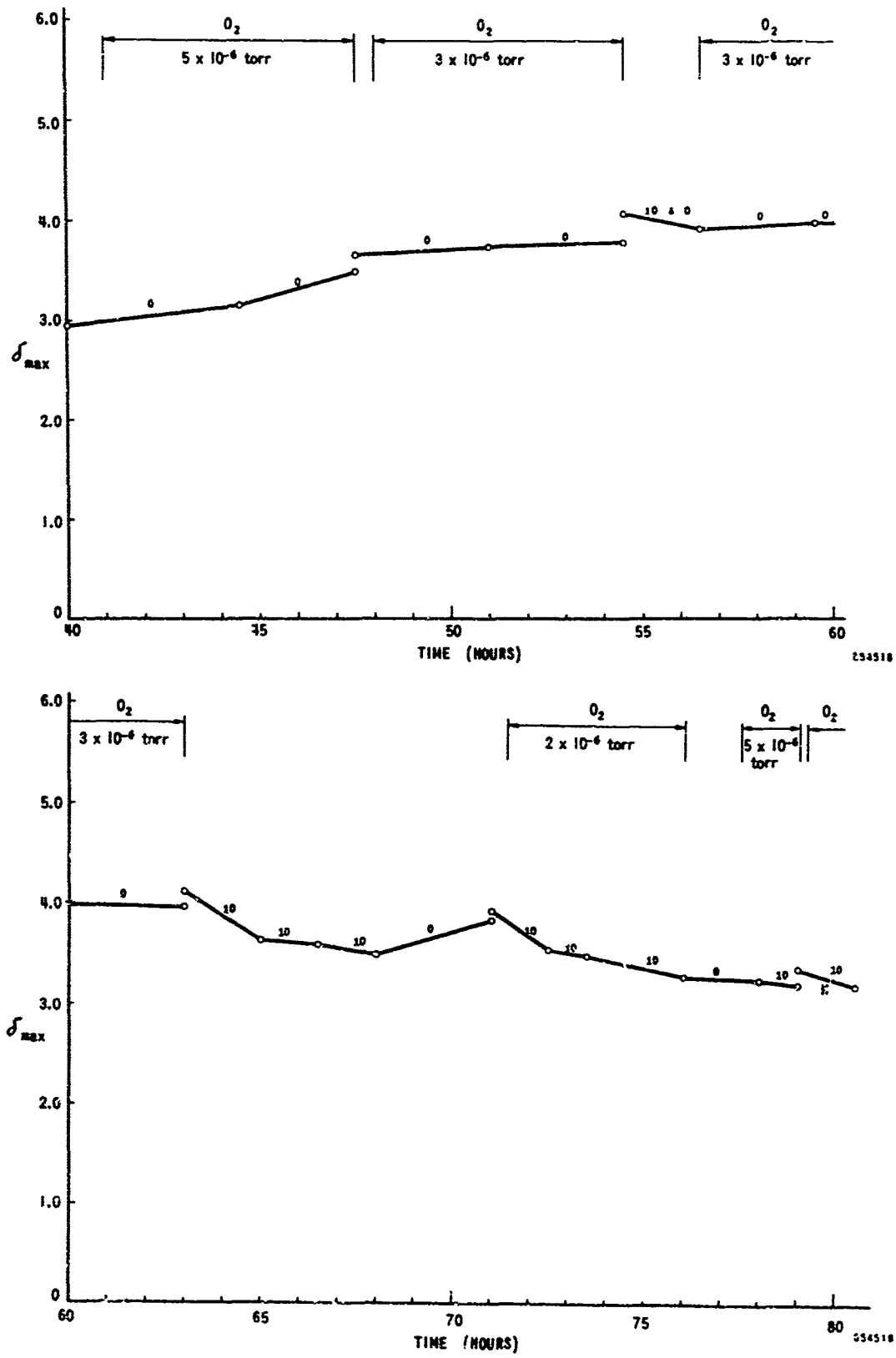

Figure 3-30 Sheet 2. δ_{max} vs Time in Electron Bombardment Vehicle for Aluminum (Alloy 6061) Target (Naturaliy Oxidized)

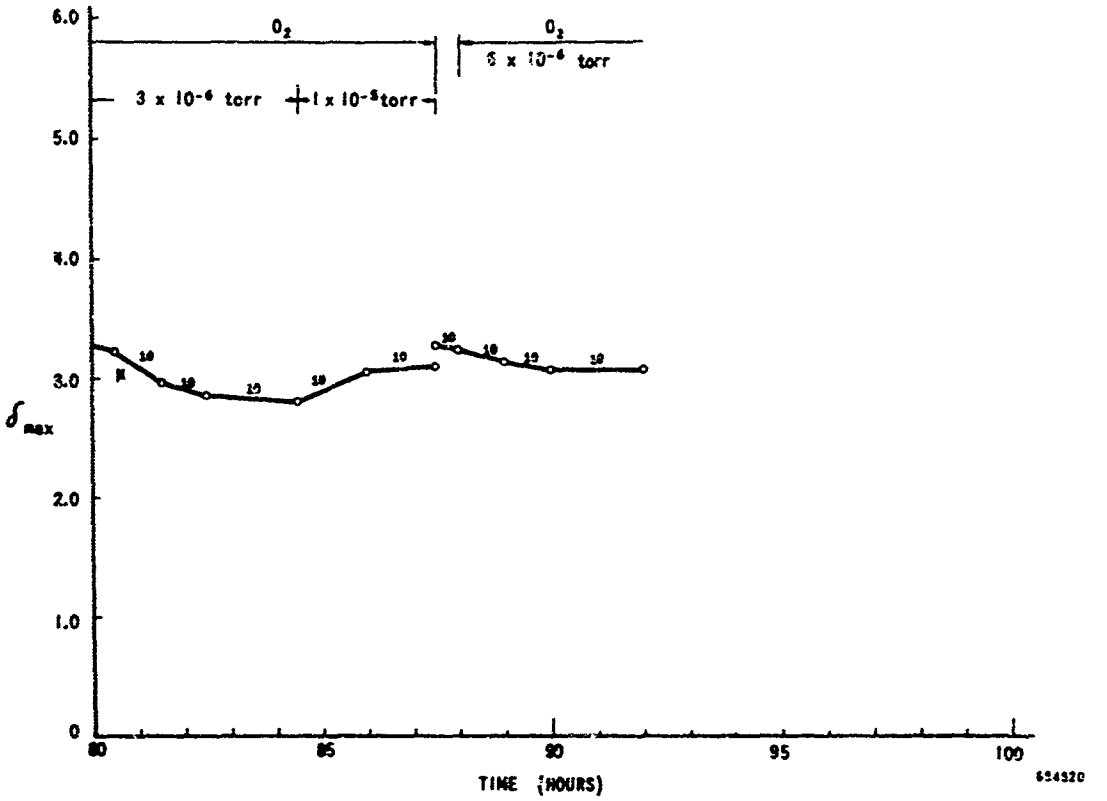

Figure 3-30 Sheet 3. δ_{max} vs Time in Electron Bombardment Vehicle for Aluminum (Alloy 6061) Target (Naturally Oxidized)

Figure 3-30 shows that bombardment at the 10 mA level (i.e. 0.5A/cm^2) results in rapid degradation of δ and some recovery occurs with the beam turned off. As seen in Figure 3-30 (hours 84 1/2 to 87 1/2) an O_2 pressure of 1 x 10^{-5} torr was sufficient to maintain a δ_{max} of about 3 during 0.5 A/cm^2 bombardment. O_2 pressures less than 5x10^{-6} torr allowed degradation at this bombardment level. It appears that, in general, O_2 pressures in the range 10^{-6} - 10^{-5} torr are needed to maintain stable δ's of a naturally oxidized aluminum target at high bombardment levels.

The tests with aluminum targets (alloy 6061) were repeated twice and showed secondary emission ratios (δ_{max}) from 1.5 to 2.5 under various conditions of electron bombardment and oxygen treatment (for details see Quarterly Reports No. 8 and 12). It may be mentioned that in one experiment the presence of hydrogen during bombardment resulted in δ_{max} degradation.

A similar test was conducted with a cleaned target of 1100 aluminum (99.0+% purity) in the EBV for 43 hours. The results showed δ_{max} varying between 1.5 to 2.5 during the bombardment and oxygen treatment (for details see Quarterly Report No. 8).

Samples consisting of aluminum alloys 6061 and 1100 were anodically oxidized to a depth of 300Å in a tartaric acid solution, but before oxidation the sample surfaces were highly polished. This method is known to produce a non-porous oxide film. During a test period of 55 hours the samples responded to the oxygen treatment in the same manner as described for the naturally oxidized aluminum films. δ_{max} varied from 1.5 to 3.0. (for details see Quarterly Reports No. 9 and 10).

3.3.2 Beryllium Oxide Films. Beryllium disc samples 98+% pure were cut from a beryllium sheet by a photoetch process and then diffusion-bonded to a copper surface. These samples were either naturally oxidized or anodized in tartaric acid to a 300Å oxide layer.

Four beryllium samples with naturally oxidized surfaces were tested in the EBV vehicle for periods of time extending from 50 to 100 hours.

Typical test results for a period of 98 hours are shown in Figure 3-31.

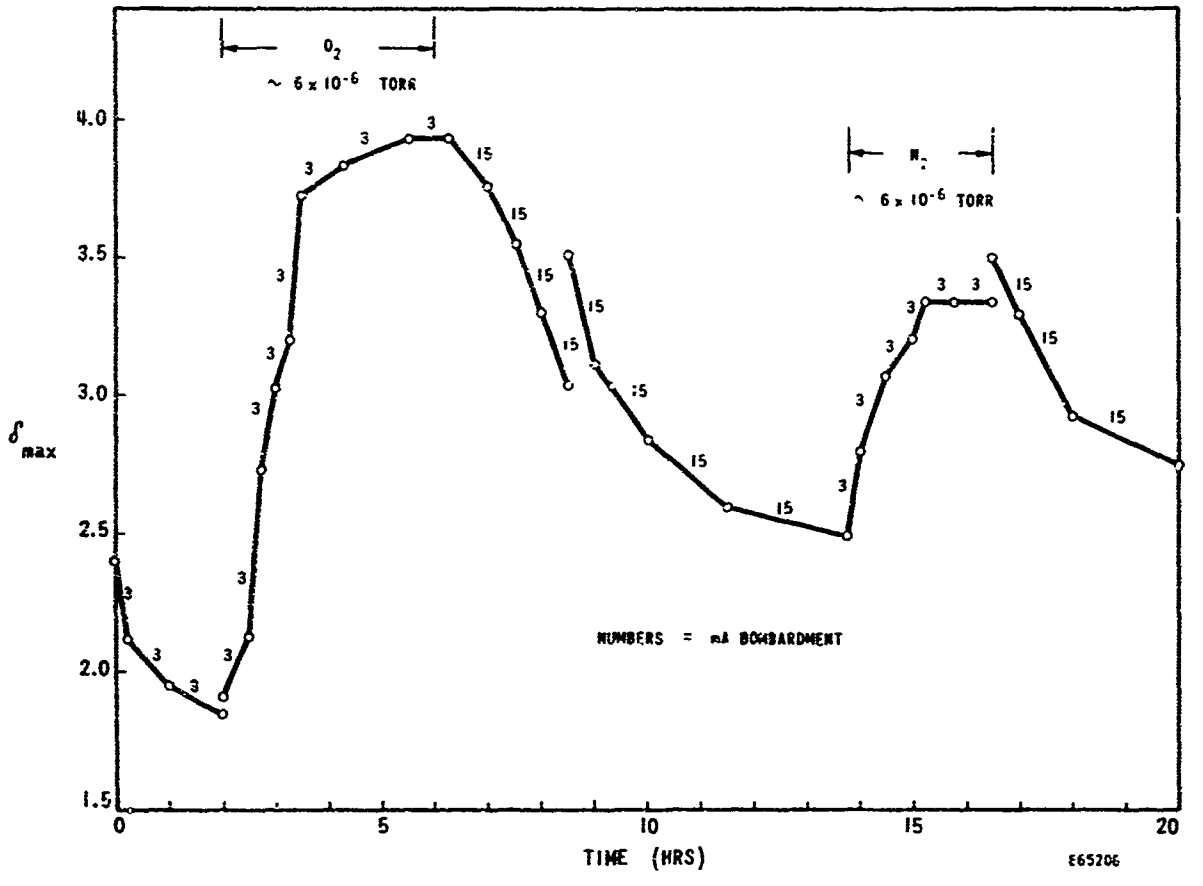

Figure 3-31 Sheet 1. δ_{max} vs EBV Time for Naturally Oxidized Beryllium

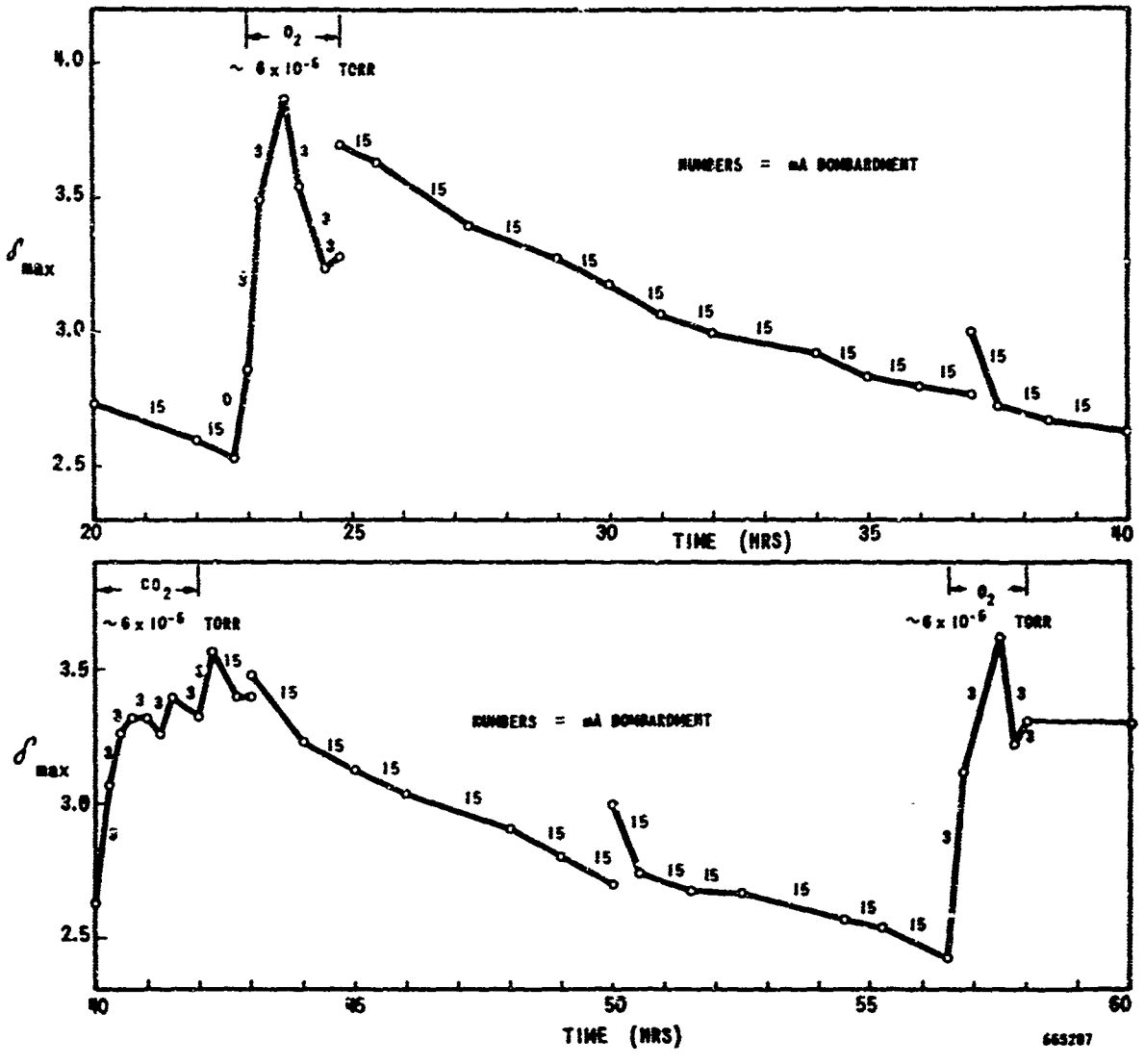

Figure 3-31 Sheet 2. δ_{max} vs EBV Time for Naturally Oxidized Beryllium

Beneficial effects were noted for O_2, N_2 and CO_2, all at the same pressure of 6×10^{-5} Torr. The sequence of gas treatments was O_2, N_2, O_2, CO_2, and O_2. All showed significant effects, but O_2 was perhaps the most effective. Typically, the gas treatment increased δ_{max} from approximately 2.5 to between 3.5 and 4.0 during the first 58 hours of testing. After several gas treatments, the rate of degradation of δ, due to 0.75 A/cm^2 electron bombardment had slowed down. Note in Figure 3-31 hours 25 to 40 and also 43 to 56.

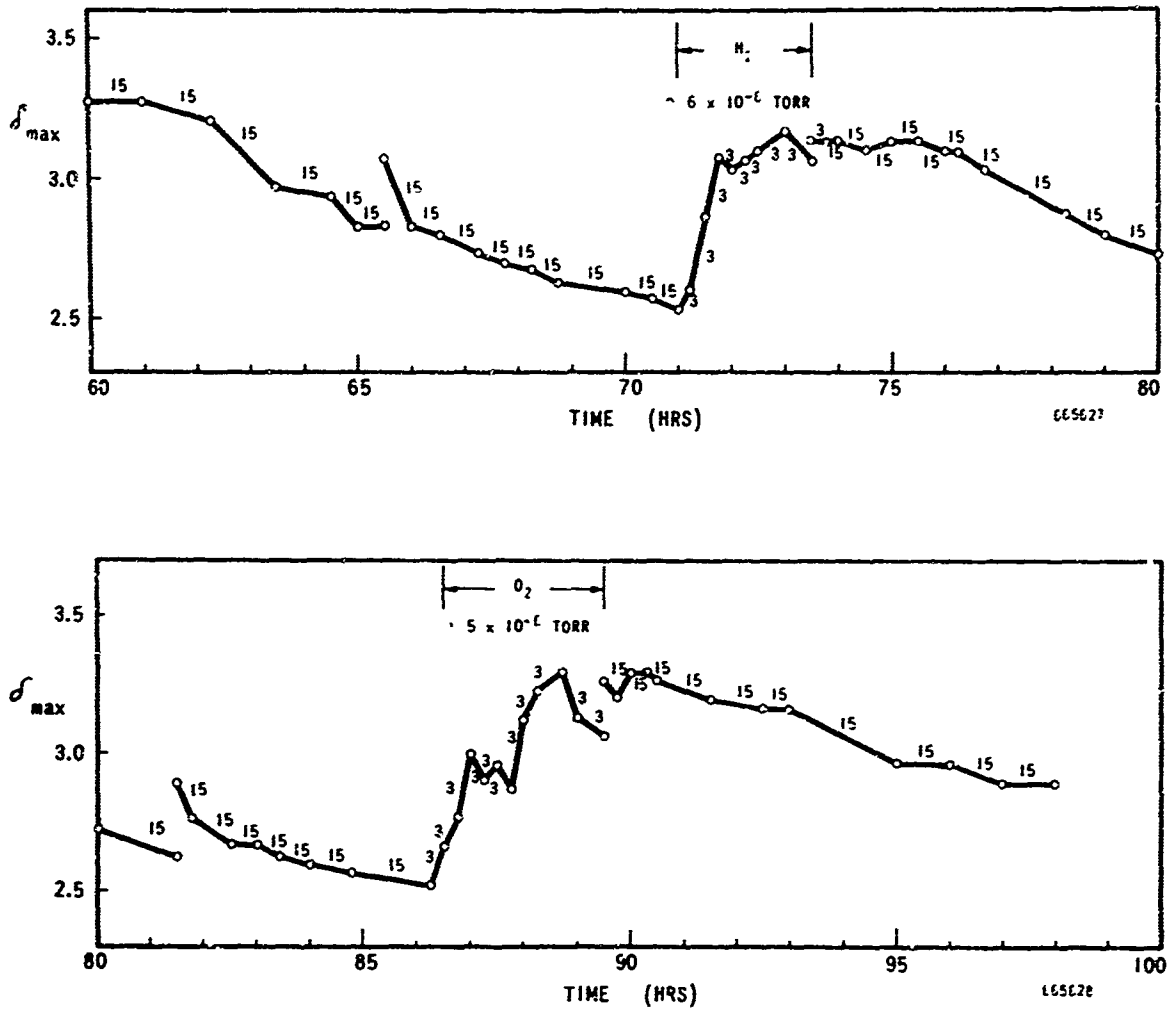

Figure 3-31 Sheet 3. δ_{max} vs EBV Time for Naturally Oxidized Beryllium

During the last 40 hours of evaluation, the sample was exposed to atmospheres of O_2 and H_2 at approximately 6 x 10^{-6} torr residual gas pressure; the background pressure was approximately 1 x 10^{-8} torr at all times and bombardment was carried out at 15 mA (0.75 A/cm^2) and 3 mA (0.15A/cm^2). The value of δ_{max} increased from approximately 2.5 to 3.2 during this time for both O_2 and H_2 treatments. Fluctuations in the value of δ_{max} decreased further with successive gas treatments, and degradation due to the 15 mA (0.75 A/cm^2) electron bombardment became more difficult to achieve. (Figure 3-31, see hours 60 to 71, 73.5 to 86, and 89.5 to 98.)

Two beryllium samples with an anodized oxide layer 300Å thick were tested in the EBV vehicle for periods of time up to 140 hours.

Figure 3-32 shows the results from a typical sample for a period of 140 hours. During this time, the target was exposed to residual atmospheres of O_2 and N_2 at pressures of 5×10^{-6} torr; the background pressure was always approximately 1×10^{-8} torr. Bombardment levels of 0.75 A/cm^2 (15 mA) and 0.15 A/cm^2 (3 mA) were used.

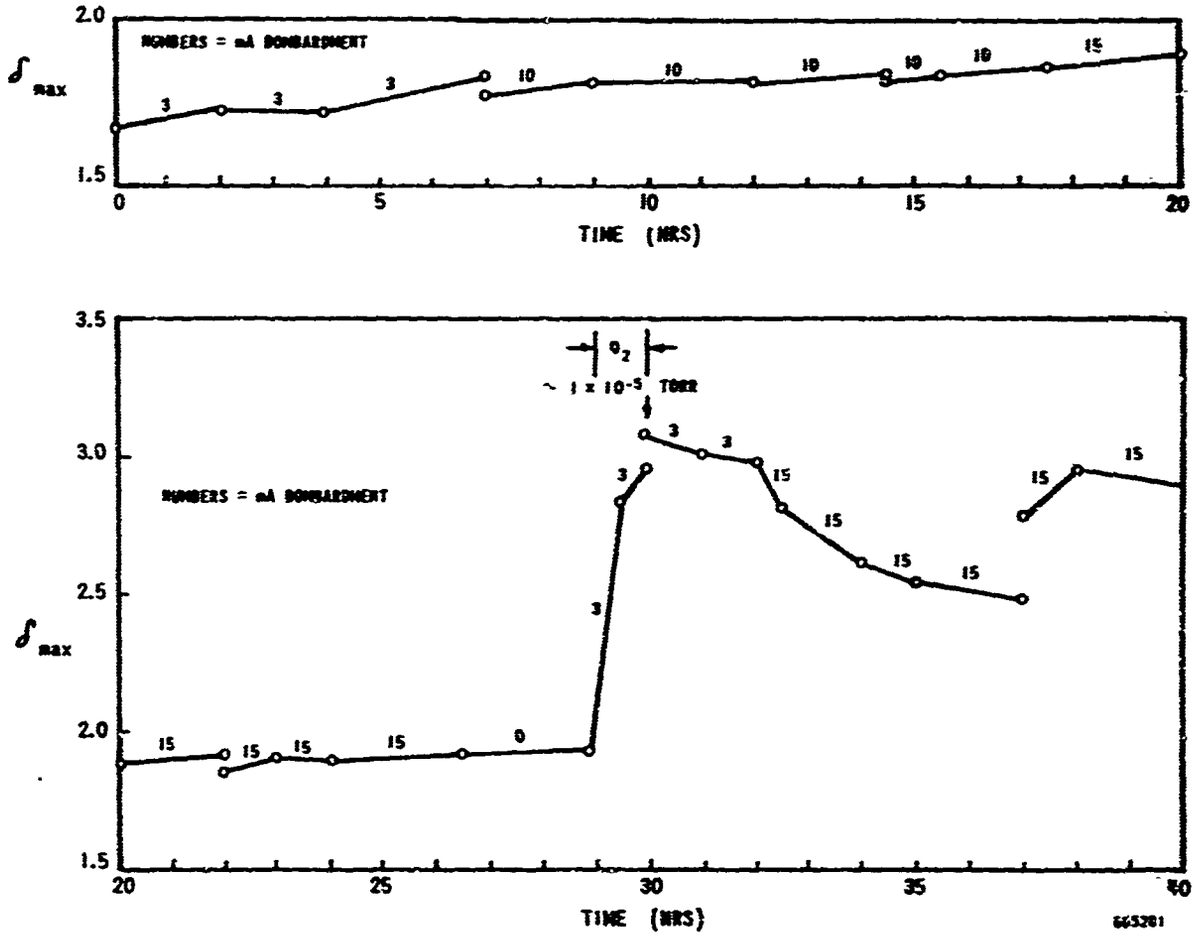

Figure 3-32 Sheet 1. δ_{max} vs EBV Time for 300Å Anodized Beryllium

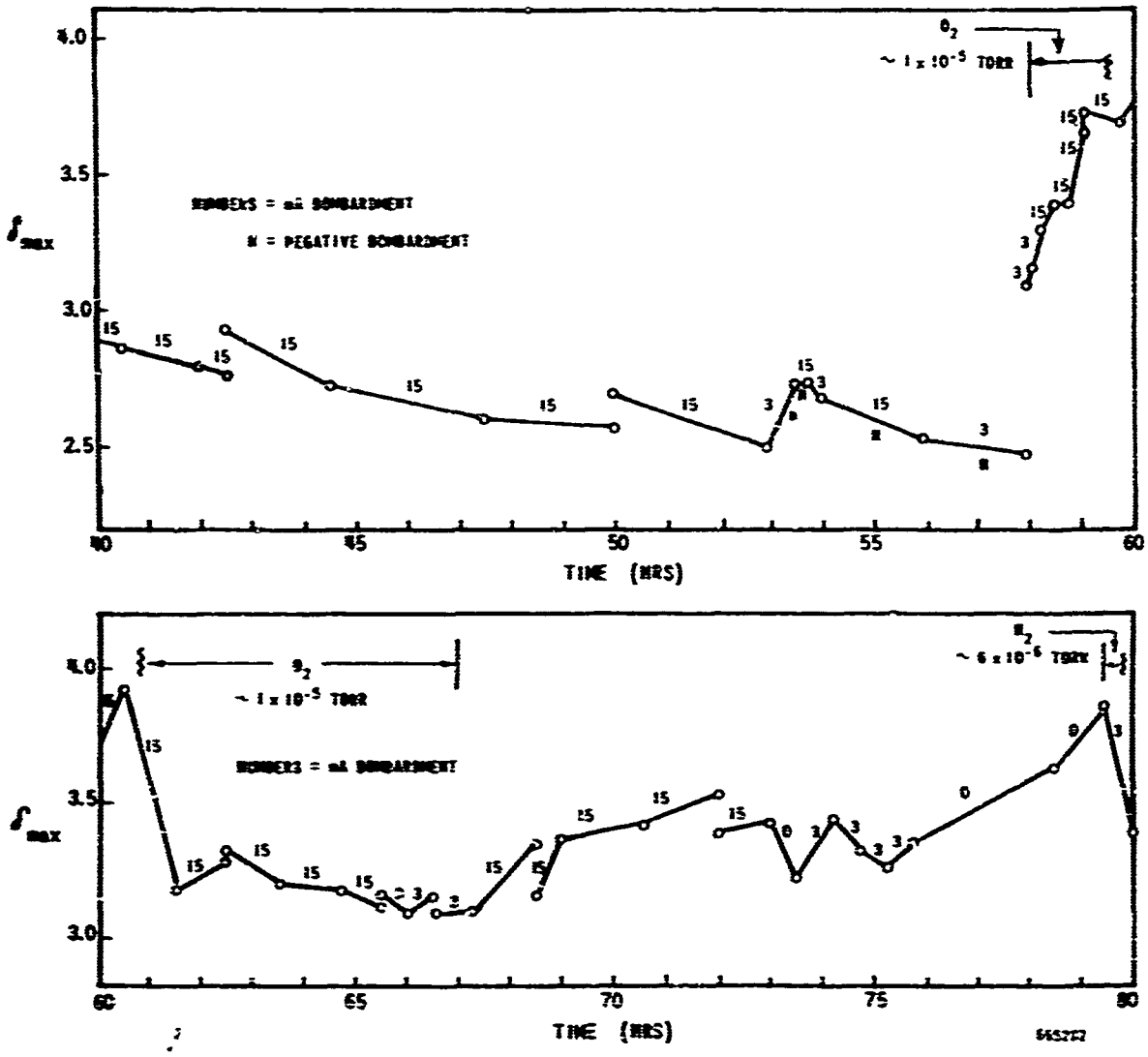

Figure 3-32 Sheet 2. δ_{max} vs EBV Time for 300Å Anodized Beryllium

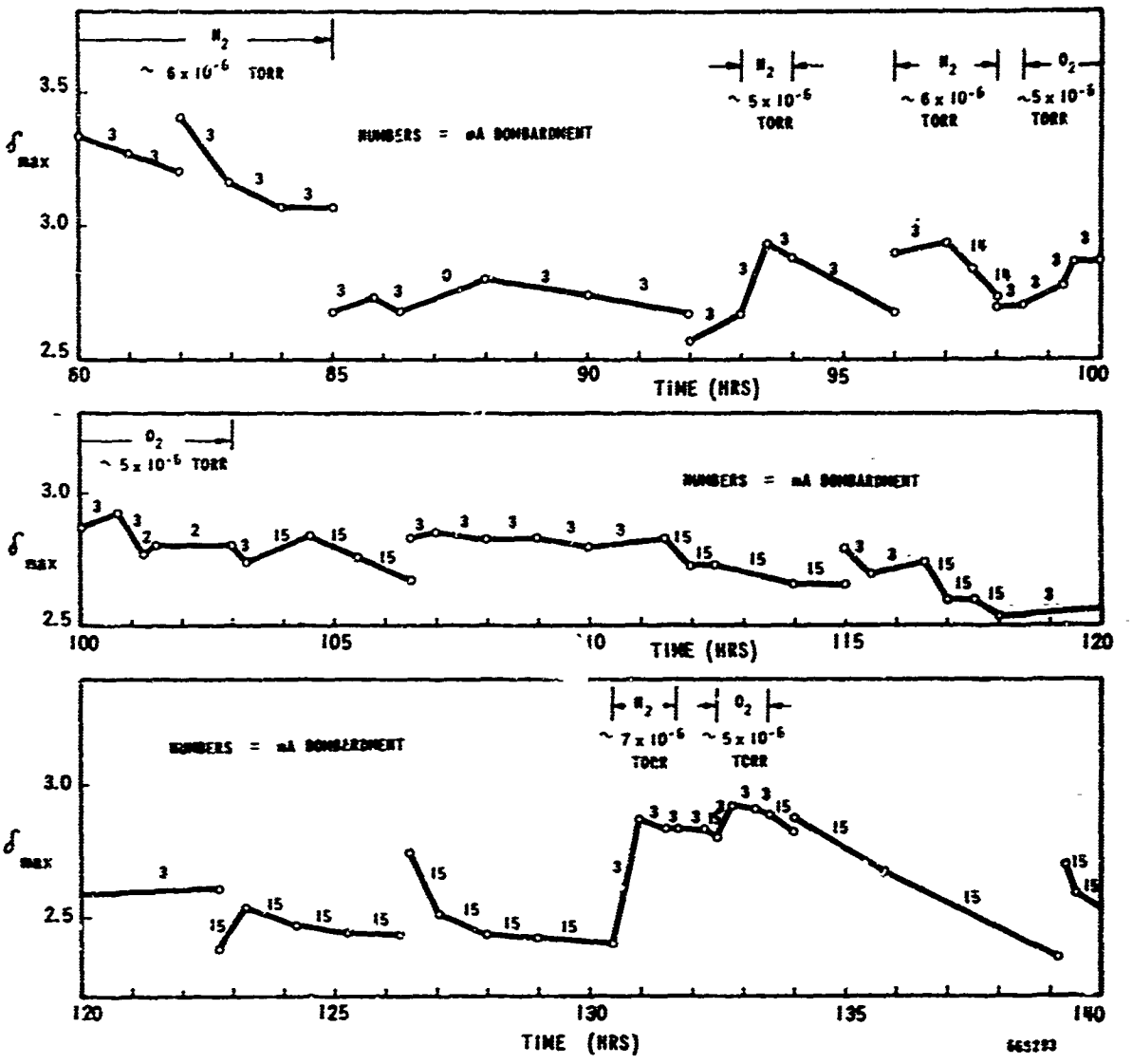

Figure 3-32 Sheet 3. δ_{max} vs EBV Time for 300Å Anodized Beryllium

The data taken during the first 37 hours showed a positive response to O_2 at 1 x 10^{-5} Torr. Further evaluation showed a positive response to O_2 at the same pressure starting at hour 58. Continued bombardment of 0.75 A/cm^2 caused δ_{max} to decrease to 3.2 after reaching a maximum of 3.9. Subsequent efforts to determine the restorative effects of N_2 were inconclusive; δ_{max} remained between 2.8 and 3.0, with at most a small

N_2 effect which was not reproducible. Rechecking the restorative effect of O_2 at hour 99 showed a negligible effect with δ_{max} at ~2.8. This may be interpreted to imply a deteriorated sample. However, a positive response to N_2 at hour 130.5 showed an increase of δ_{max} from 2.4 to 2.85. It seems reasonable to suppose that the "condition" of the sample at that time was such that recovery with N_2 or O_2 would only be evident if δ_{max} fell below 2.8 and that recovery would occur to a maximum value of δ_{max} of 2.8.

3.3.3 Impregnated tungsten and nickel-cermet cathodes. Three impregnated tungsten samples of the standard (4-1-1) impregnant composition and 20% porosity were prepared and tested in the EBV vehicle.

The results for sample no. 2 are shown in Figure 3-33 which shows the effects on δ_{max} caused by heating for purposes of activation and by electron bombardment in the hot/cold EBV.

After disassembly the samples appeared clean, there being no apparent discoloration due to extraneous deposits, nor to the electron bombardment stress, nor to the activation heating.

Prior to the testing of sample no. 1 the target heater had been modified for greater thermal efficiency. Additional shielding of the target had also been provided to prevent the deposition of foreign material on the target surface. These modifications appear to have been successful.

The samples appeared to stabilize to a δ_{max} of 2.2 to 2.3 after periods of electron bombardment. The maximum value of δ_{max} observed was 3.3 in the case of sample no. 1 and 2.6 for sample no. 2. These are lower than a value of 4.4 reported in connection with the work in the SEE vehicle for a similar sample at best activation.

A nickel-cermet sample was run for 38 hours during which time several activation periods at different temperatures ranging from about 800° C to 1100° C were tried, but the sample failed to respond. During the tests δ_{max} ranged from 1.3 to 1.8. The sample appeared clean and the structure showed minimal evaporation upon disassembly.

3.3.4 Beryllium-copper and silver magnesium alloys. The beryllium-copper alloy (2% Be) was processed by directions supplied by Bell Telephone Laboratories.*

The sample was then run for 40 hours of EBV time (Figure 3-34) during which O_2 rejuvenation of δ_{max} was carried out with 3 mA (0.15 A/cm^2) bombardment. After each O_2 treatment, δ_{max} was deteriorated by bombardment with both 3 mA and 15 mA (0.75 A/cm^2) bombardment current.

---

* See Section 3.2.6.2.

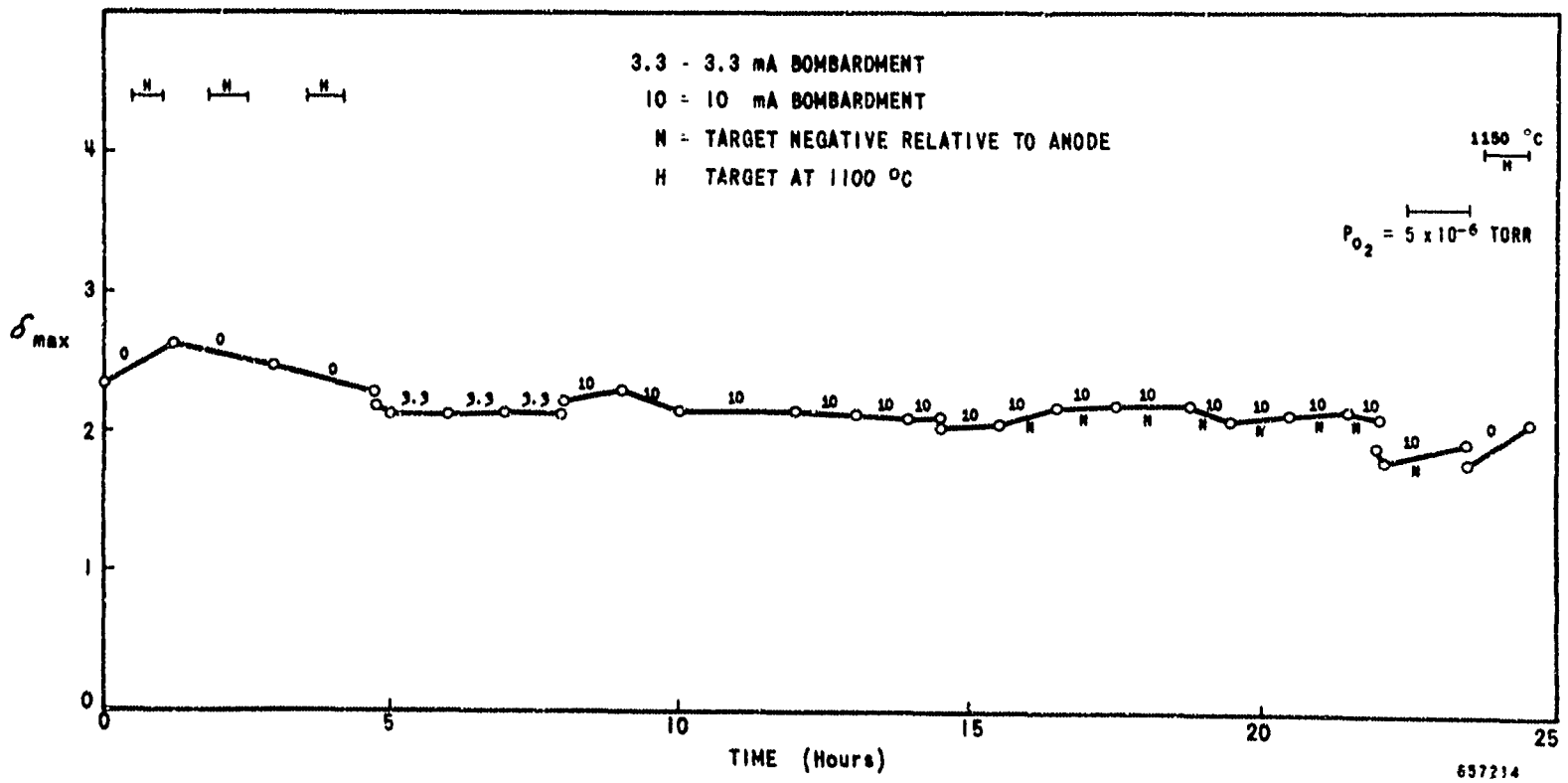

Figure 3-33. δ_{max} vs EBV Time for Impregnated Tungsten Sample No. 2

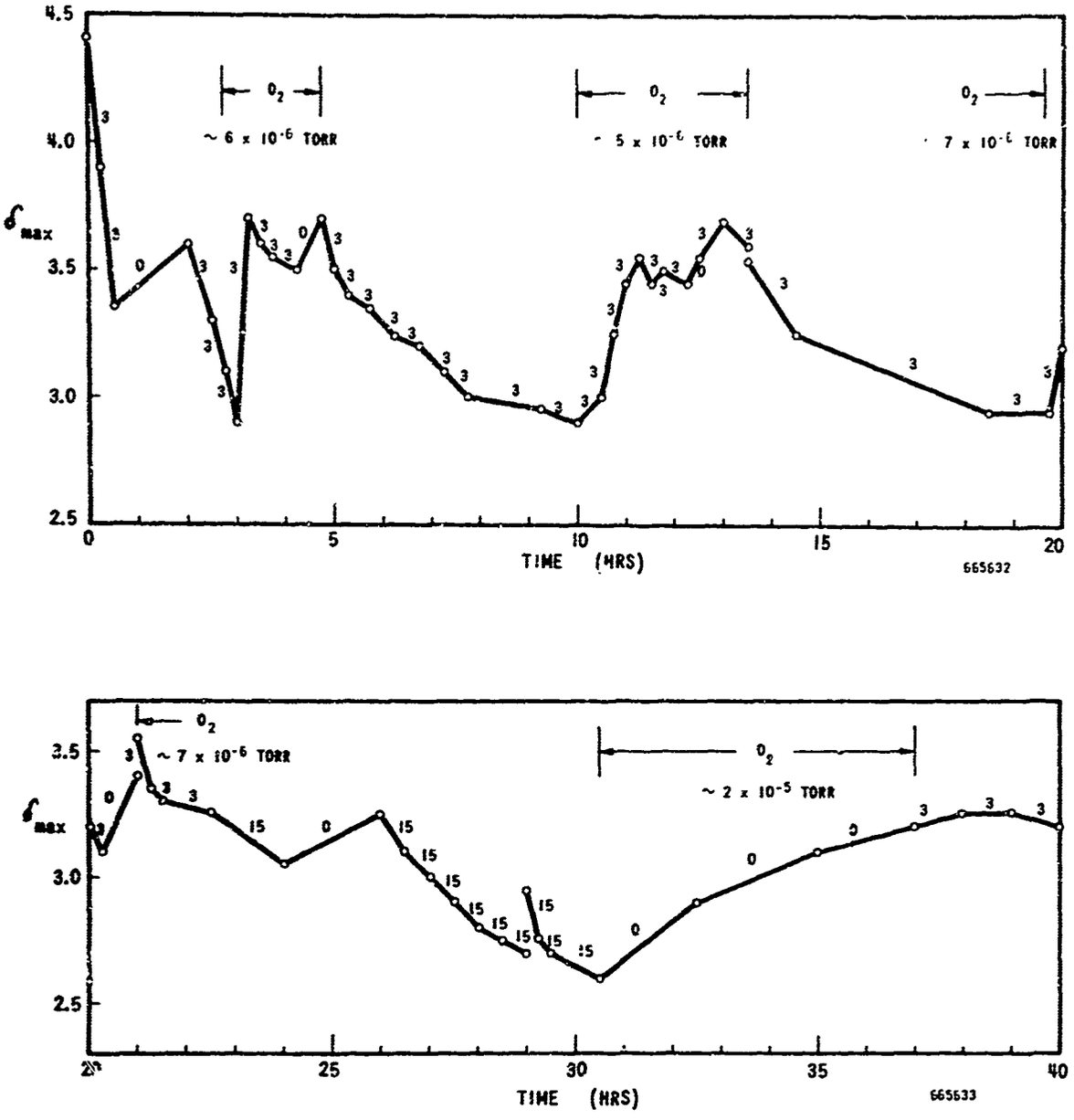

Figure 3-34. δ_{max} vs EBV Time for Optimally Oxidized Beryllium-copper

The background pressure during the tests was always 1×10^{-8} torr or less, and O_2 pressures used for reactivation varied from 5×10^{-6} torr to 2×10^{-5} torr.

The initial value of δ_{max} for this sample was 4.4, but this deteriorated rapidly to 3.35 in 30 minutes under 3 mA (0.15A/cm^2) electron bombardment. This initial value of δ_{max} corresponds well with the values obtained in the secondary emission vehicle for optimally oxidized beryilium-copper. The sample responded favorably in all instances when O_2 reactivation of δ_{max}

was attempted both with and without the 3 mA (0.15 A/cm^2) bombardment. It was also observed that δ_{max} increased typically from 2.9 to 3.7 with bombardment and slightly less without it.

Optimum oxidation of the silver-magnesium alloy (7% Mg) was obtained using a two-step process described in Section 3.2.6.1 of this report.

The appearance of the film on the sample at this point, as reported by Rappaport,[37] should be a shiny yellow. Our samples compared favorably with this description.

The sample which was run for 12.5 hours in the EBV (Figure 3-35) showed a lower δ_{max} than was expected initially. Improvement of δ_{max} which is sometimes observed when the testing is continued, did not occur. The sample was given two O_2 treatments, but did not show any great response so the test was ended. During the tests, δ_{max} varied from approximately 2.3 to 2.7. After examining the sample and considering all possible reasons for the lack of response, it was concluded that the bakeout temperature (400°C) was too high. At that temperature the vapor pressure of the Mg is excessive, probably causing fresh Mg to diffuse through to the surface and, in turn, causing the sample to change characteristics as far as δ is concerned. The work with these samples in the SEE vehicle, using a lower (200°C) bakeout temperature (see Section 3.2.6.3), seems to verify these deductions.

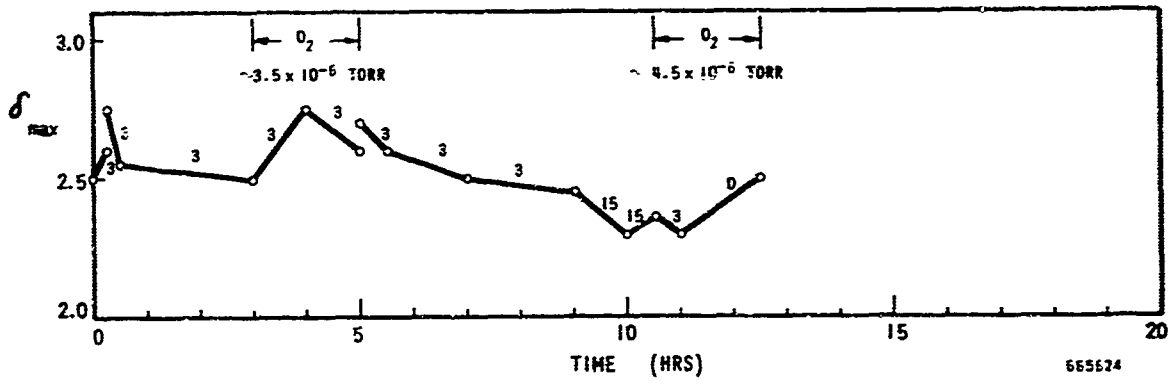

Figure 3-35. δ_{max} vs EBV Time for Optimally Oxidized Silver-magnesium

3.3.5 Boron nitride. Two BN film samples were prepared and evaluated in the Electron Bombardment Test Vehicle (EBV). These films were formed by chemical vapor deposition (CVD) techniques to a thickness of 200Å on Mo substrate.

The results of electron bombardment at 0.5 A/cm^2 and 1.2 kV are shown in Figures 3-36 and 3-37 for BN samples no. 1 and 2 respectively. The secondary emission ratio remained constant for up to 8 hours of bombardment. δ_{max} was between 1.7 and 2.1 and $V_{pm_{ax}}$ was between 350 and 400 volts.

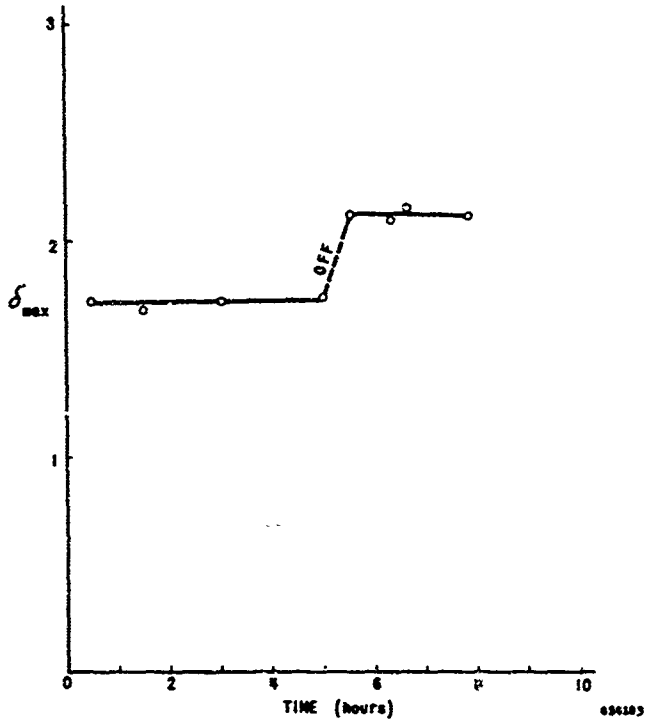

Figure 3-36. δ_{max} vs Electron Bombardment Time in EBV at 0.5 A/cm^2 and 1.2 kV for 200Å CVD BN Film No. 1 on Mo Substrate

The observed values of δ were much lower than the value of δ_{max} of 4.3 measured in the SEE Vehicle on apparently similar BN film (see Section 3.2.5).

A repeat of the test with another BN film sample had similar results as those shown in Figures 3-36 and 3-37. No explanation can be given for the unexpected low δ values. Values of δ in the EBV may be 15% low as indicated by our previous measurements on platinum. The discrepancy is definitely outside of experimental error.

3.3.6 Summary of results in the Electron Bombardment Vehicle. The results of the tests conducted in the EBV are briefly summarized as follows:

1. Platinum

   a. δ_{max} measured in the EBV was 1.54, i.e. 15% lower than the value measured in the Secondary Emission Test Vehicle (SEE).

   b. Electron bombardment at 0.5 A/cm^2 and 1200 V dc for several hours caused no deterioration of δ_{max}.

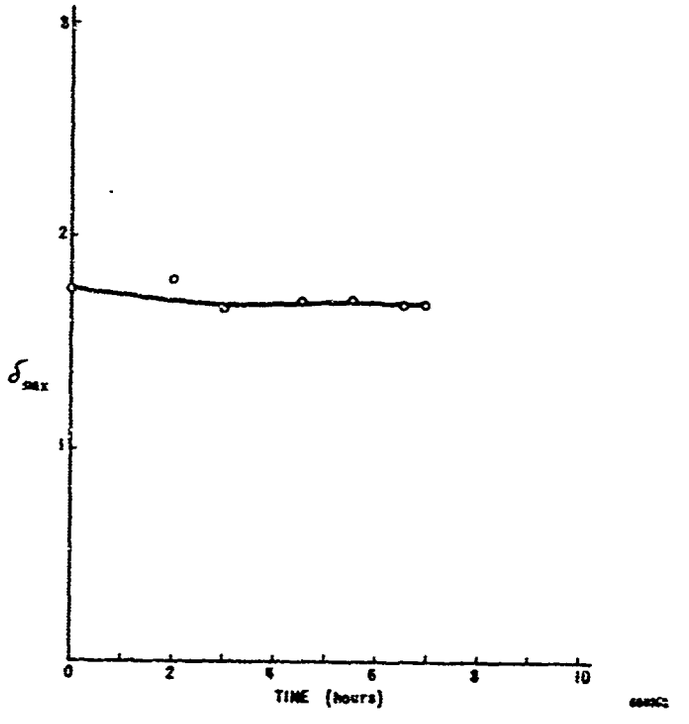

Figure 3-37. δ_{max} vs Electron Bombardment Time in EBV at 0.5 A/cm^2 and 1.2 kV for 200Å CVD BN Film No. 2 on Mo Substrate

2. Molybdenum-alumina films on copper substrate

a. A 1000Å film of 30% Mo - 70% Al_2O_3 showed an increase of δ_{max} from 2.2 to 2.7 after the first 18 hours of electron bombardment in vacuum at 0.3 A/cm^2 and 1200 V.

b. Under electron bombardment in vacuum at 1.0 A/cm^2 and 1200 V, δ_{max} decreased, but appeared to level off at 1.7 after approximately 22 hours of bombardment.

c. δ_{max} measured in the EBV at 0 hour was the same as that found for a similar sample in the SEE.

3. Molybdenum-alumina films on molybdenum substrate

a. The initial δ_{max} of 500Å 30% Mo-70%Al_2O_3 film was 3.8 and decreased to 3.2 within 3 hours of electron bombardment in vacuum at 0.5 A/cm^2 and 1200 V.

b. A δ_{max} of 3.6 could be maintained for a 500Å 30% Mo-70% Al_2O_3 film by an O_2 partial pressure of 6×10^{-7} torr during electron bombardment at 0.5 A/cm^2 and 1200 V.

4. Alumina films

a. Initial δ_{max} values of two 300Å thick electron beam evaporated films on Mo were 2 and 2.4.

b. Presence of O_2 or CO_2 during electron bombardment at 0.15 A/cm^2 had a beneficial effect on δ_{max}. N_2 had a decidely smaller effect, if any. Electron bombardment in vacuum degraded improved δ_{max} values.

c. Optimum values of δ_{max} obtained through the use of O_2 were 3.8 and 4.2.

d. Repeated use of O_2 resulted in a diminishing of the recovery effect.

5. Naturally-grown oxide films on vapor-deposited aluminum

a. Three samples showed initial δ_{max} values ranging from 2.4 to 2.7.

b. Electron bombardment in vacuum at 0.5 or 0.75 A/cm^2 degraded δ_{max} to a fairly stable value of 1.5

c. Presence of O_2 at pressures in the upper 10^{-6} torr range and moderate bombardment improved δ_{max} to values between 2.5 and 3.

6. Naturally oxidized aluminum alloy 6061

   a. Two samples showed δ_{max} values ranging from 1.5 to 2.5 under various conditions of electron bombardment and O_2 treatment.

   b. Hydrogen seemed to have a detrimental effect on δ_{max}.

   c. The initial δ_{max} of a third sample was surprisingly high (about 5), but rapidly deteriorated to about 2 under electron bombardment in vacuum at 0.5 A/cm^2.

   d. Use of O_2 without bombardment gradually increased the δ_{max} of this sample to 4.

   e. O_2 in the pressure range of 10^{-6} to 10^{-5} torr appeared to be capable of maintaining δ_{max} at a level of approximately 3 under electron bombardment at 0.5 A/cm^2.

7. Naturally oxidized aluminum alloy 1100

   a. The sample showed an initial δ_{max} value of 2 to 2.5.

   b. Under electron bombardment at 1 A/cm^2 in vacuum, δ_{max} appeared to become fairly stable at 1.5.

   c. Presence of O_2 improved δ_{max} to about 2.

8. Anodized aluminum alloys 6061 and 1100

   The samples anodized to 300Å thickness showed variation of δ_{max} between 1.5 and 3 under various conditions of electron bombardment and O_2 treatment.

9. Naturally oxidized beryllium

   a. δ_{max} varied between 2 and 4 during 98 hours of electron bombardment under various conditions.

   b. δ_{max} decreased under bombardment in vacuum at 0.75 A/cm^2 and significantly increased under bombardment at 0.15A/cm^2 in atmospheres of O_2, N_2, CO_2, and H_2.

   c. The fluctuations in the value of δ_{max} decreased with increasing number of gas treatments and the degradation of δ_{max} due to electron bombardment at 0.75 A/cm^2 in vacuum was delayed.

10. Anodized beryllium

a. δ_{max} varied between 1.7 and 3.8 during 140 hours of electron bombardment under various conditions.

b. δ_{max} showed the usual deterioration during bombardment in vacuum at 0.75 A/cm^2 and increased under bombardment in O_2 at 0.15 A/cm^2.

c. A beneficial effect of N_2 on δ_{max} was not as clearly indicated as in the case of O_2.

d. The phenomena observed toward the end of the test period suggested that the sample was in such a condition that improvement of δ_{max} beyond a certain value (at that time 2.8) was impossible. Consequently, recovery by O_2 or N_2 treatment was only evident when δ_{max} fell below this value.

11. Impregnated tungsten cathodes

a. δ_{max} remained fairly stable at 2.2 during electron bombardment at 0.5 A/cm^2 in vacuum for 15 hours.

b. O_2 treatment had no significant effect on δ_{max}.

12. Nickel-cermet cathode

δ_{max} ranged from 1.3 to 1.8 in spite of an extensive effort to improve δ_{max} by suitable activation methods.

13. Beryllium-copper alloy (2% Be)

a. The initial value of δ_{max} was 4.4.

b. δ_{max} rapidly deteriorated under electron bombardment in vacuum even at moderate bombardment levels (0.15A/cm^2).

c. δ_{max} responded favorably to O_2 reactivation.

d. Typical increases of δ_{max} in the presence of O_2 were from 2.9 to 3.7 under electron bombardment at 0.15 A/cm^2. (They were somewhat smaller without bombardment.)

14. Silver-magnesium alloy (7% Mg)

a. The initial δ_{max} value of an optionally oxidized sample was 2.5.

b. Electron bombardment in O_2 had little effect on δ_{max}.

15. Boron nitride

a. The initial value of δ_{max} was approximately 1.7.

b. This value was much lower than the value of 4.3 measured for an apparently similar sample in the SEE.

c. δ_{max} remained constant under bombardment in vacuum at 0.5 A/cm^2 for at least 8 hours.

3.4 Ion bombardment of cold cathodes. The Ion Bombardment Vehicle (IBV) is a demountable inexpensive test vehicle used for the evaluation of sputtering erosion of cold cathode materials. A simplified schematic of this device, including circuitry, is shown in Figure 3-38.

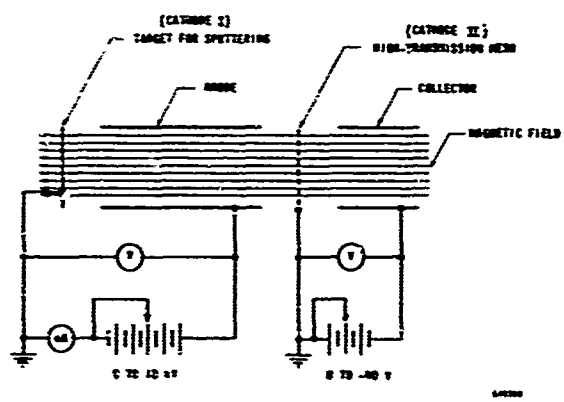

Figure 3-38. Schematic of the Ion Bombardment Vehicle Sputtering Apparatus.

The method used for producing the incident ions constitutes a low pressure gas discharge in a magnetic field. It overcomes some of the undesirable effects of the glow discharge method, such as multiple collisions of gas particles and back-diffusion of sputtered target atoms to the target. The use of a low pressure results in a longer electron mean free path and reduced ionization of the gas. The applied parallel magnetic field (300 gauss) tends to overcome this limitation so that ion current densities of about 4 ma/cm^2 at several kV energy are achievable. Sputtering erosion is confined to an area of approximately 1/8 inch in diameter on the target surface.

Other methods, such as the supplemented low-pressure arc [39] or the use of well defined ion beams, were deemed either not feasible or too complicated for the program.

The IBV was operated with nitrogen at approximately 10^{-3} torr. Under these conditions ion bombardment current densities of 1 and 2 mA/cm^2 were used to sputter the following target materials: Pt, 30% Mo - 70% Al_2O_3 film on Mo substrate, electron-beam evaporated Al_2O_3 films on Mo substate, impregnated tungsten, and nickel cermet.

3.4.1 Material samples.

3.4.1.1 Pt. A Pt target was sputtered at a current density of $1 mA/cm^2$ and a voltage of 2 kV for 1 hour. Under the design conditions of the IBV only a 3/16 in. diameter central portion of the 3/8 in. diameter target was sputtered. The sputtered region had a dull, etched appearance as compared to the shiny unsputtered region. Under microscopic examination (400X magnification) it was observed that the sputtered region was highly decorated with many edge and screw dislocations, evidently due to selective sputtering at the surface.

3.4.1.2 30% Mo - 70% Al_2O_3 films on Mo substrate. A 200Å film was sputtered at 1 mA/cm^2 and 800 volts for 20 minutes. After 10 minutes the central sputtered region was only partially removed, but after 20 minutes the film was completely sputtered away. Following this a series of six 1000Å films were sputtered at 1 mA/cm^2 and 650 volts for various times up to a maximum of 90 minutes. The central sputtered region showed progressive color changes indicating the reduction in film thickness, with complete erosion occurring after 90 minutes. A simplified sketch of the film after 90 minutes of sputtering is shown in Figure 3-39. A central portion shows the Mo substrate where the film has been completely eroded away. Surrounding this region are successive colored rings which are similar to those films which had been sputtered for shorter time periods. The colored rings in Figure 3-39 are enlarged out of proportion for purposes of clarity.

Another set of six 1000Å films were sputtered at 2 mA/cm^2 and 1100 volts, the results being quite similar to the previous set except that it took about half as much time to sputter through to the substrate material.

An estimate was made of the sputtering yield of Al_2O_3 from the above data. By neglecting the Mo component, one obtains a yield of 0.007 molecules/ion at 650 volts for nitrogen. This is in reasonable agreement with a value of yield, S = 0.016 molecules/ion, deduced from the data of Wehner et al [31] for the Hg sputtering of Al_2O_3 at 650 volts when we apply a correction factor of 0.47* to adjust the value to N_2 sputtering of Al_2O_3. The mean free path of N_2 at 25°C and $p = 10^{-3}$ Torr is approximately 5 cm. Therefore the error due to the backscattering of sputtered neutrals is not expected to be large.

Based on a depletion time of 90 minutes for a 1000Å film subjected to an ion bombardment current density of 1 mA/cm^2 at 650 volts, one can project a film life of 50 hours at 0.03 duty cycle operation. However, the average ion bombardment current density in the CFA is estimated to be only ~10 $\mu A/cm^2$. Based on this assumption, the sputtering life of the 1000Å film in the QKS1319 CFA test vehicle, operating at a duty cycle of 0.03, would be approximately 5000 hours.

3.4.1.3 Alumina films on a molybdenum substrate. Two electron-beam evaporated Al_2O_3 films were deposited on a Mo substrate and then sputtered to cause complete erosion of the films. Due to a slight coloration in the films, it was possible to determine when the film was completely removed; the Mo substrate was then directly visible. The sputtering was performed in N_2 at 10^{-3} torr and at an ion bombardment current density of 1.2 mA/cm^2 for both films.

* This factor is obtained from data for sputtering copper with N_2 and Hg.

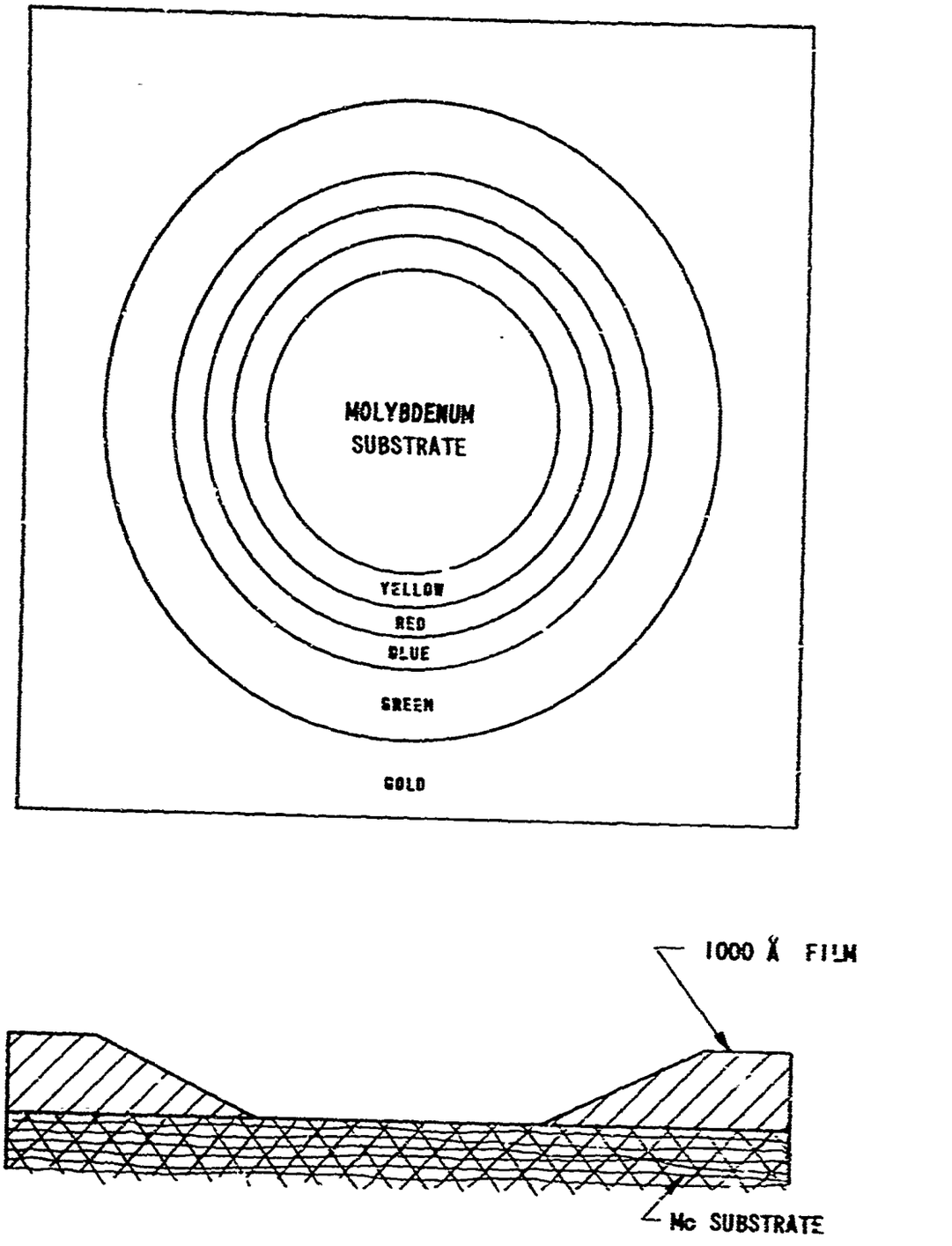

Figure 3-39. Sputtered 1000Å Film of 30% Mo - 70% Al_2O_3 on an Mo Substrate

The 500 Å film was bombarded at 1.2 kV ion energy and was completely eroded in 15 minutes, corresponding to a sputtering yield of 0.017 molecules ion. The 1000 Å film was bombarded at 0.8 kV ion energy and was completely eroded in 35 minutes, corresponding to a yield of 0.015 molecules/ion.

3.4.1.4 Impregnated tungsten. Two impregnated tungsten samples were sputtered at 2 mA/cm^2 and 1.8 kV. These samples were similar to some of those previously reported and had the following compositions:

sample no. 1 - 4 $BaCO_3$: 1 $CaCO_3$: 1 Al_2O_3
faster activating type

sample no. 2 - 3.5 $BaCO_3$: 1 $CaCO_3$: 1 Al_2O_3
slightly slower activating type.

Sample no. 1 was sputtered under the above conditions for 2 hours, while sample no. 2 was sputtered for only 1 hour. The results were qualitatively similar with sample no. 1 showing a more pronounced effect. In each case only a central region of approximately 3/16 in. in diameter was sputtered so that each sample contained both sputtered and unsputtered regions. Figures 3-40 and 3-41 show a comparison of a sputtered and an unsputtered portion of sample no. 1 at a magnification of 210X. In each photograph, the white areas are interpreted as representing reflecting metallic tungsten areas. The dark areas probably represent depressions in the surface, whose bottoms may be filled either with impregnant or with tungsten. The samples had been polished initially to a final polish using 4/0 emery paper. Typically, this type of polishing results in the removal of impregnant, leaving depressions in the surface. An analysis of the photograph of the unsputtered region showed the dark area to cover 15% of the surface. This is in reasonable agreement with the usual 20% porosity of the tungsten matrix. A similar analysis of the sputtered region revealed a 47% dark area coverage of the surface. It is supposed that the sputtering of the surface loosened additional tungsten particles* revealing more depressed areas.

3.4.1.5 Nickel cermet. Two nickel cermet samples were sputtered at a current density of 2 mA/cm^2 and a voltage of 2 kV for one hour. Each had the same composition, namely 70% Ni and 30% Radio Mix No. 3.** One of the samples was polished using 4/0 emery paper; the other was left unpolished. Both samples showed a darkening of the center of the sputtered region. The polished sample was subjected to microscopic examination and as Figure 3-42 shows, at a magnification of 80X there exists a strong contrast between the erosion of the sputtered and unsputtered regions. It is supposed that the initial polishing caused the soft nickel to smear over the areas containing Radio Mix No. 3 and that the sputtering eroded away the smeared-over Ni film. It was also possible to detect many pits in the light areas (metal) of the sputtered region; these were not presented in the unsputtered regions.

Secondary emission measurements were then made of the sputtered samples of Pt, the impregnated tungsten samples, and both the polished and unpolished Ni cermet samples. The results are described in Section 3.4.2.

* Some metallic dust was found at the bottom of the IBV.

** Radio Mix No. 3 contains 60% $Ba\,CO_3$ and 40% $Sr\,CO_3$ by weight and has an average particle size of 5 to 6 microns.

Figure 3-40. Impregnated Tungsten Sample No. 1 Sputtered at 2 mA/cm^2 and 1.8 kV (210X Magnification)

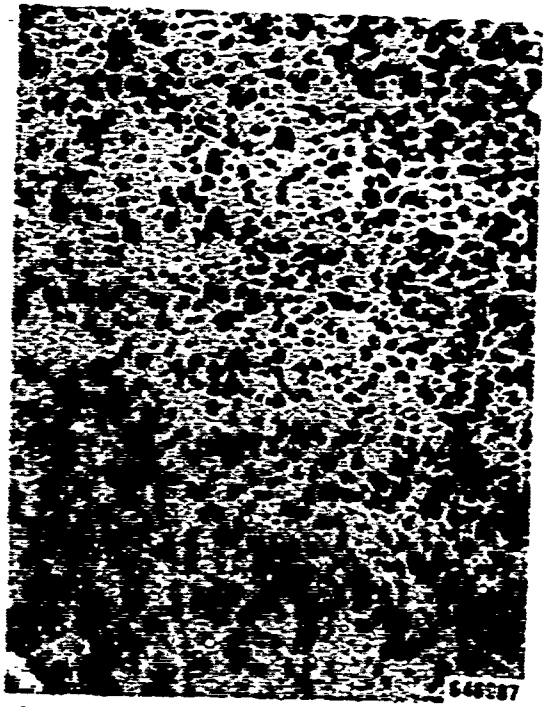

Figure 3-41. Impregnated Tungsten Sample No. 1 Unsputtered (210X Magnification)

Figure 3-42. Polished Cermet Sample Sputtered at 2 mA/cm^2 (80X Mag., sputtered region above diagonal, unsputtered region below).

3.4.2 Secondary emission measurements.

3.4.2.1 Sputtered Samples. After being sputtered in the IBV, the Pt, impregnated tungsten, and nickel cermet samples were installed in the secondary emission (SEE) test vehicle for measurement. The secondary emission measurements are summarized in Table 3-7. There is some indication from these data that the polished samples have a somewhat higher δ than the unpolished samples.

An indication of the effect of sputtering on δ was obtained by scanning across the target surface, thus passing through sputtered and unsputtered regions on the same sample. The indications from these experiments are that sputtering tends to lower δ by up to 10% for the nickel cermet and impregnated tungsten samples. It was observed that sputtering had no discernible effect on δ of the Pt sample.

Some observations of fluorescence were also made in the case of the nickel cermet samples; the other samples did not show any fluorescence. There were differences between sputtered and unsputtered regions as well as between polished and unpolished samples of Ni cermet. These observations are summarized in Table 3-8. The white spots observed in the unsputtered region of the polished Ni cermet samples were regions which had a high δ, and showed charging effects. It is supposed that the white spots contain BaO.

Table 3-7.

Secondary Emission Ratio (δ_{max}) for Various Sputtered Samples

Sample	δmax, after system bakeout	δmax, after 1st heat treatment	δmax, after 2nd heat treatment
1. Pt, sputtered	1.64	1.95 (1000°C-10 min)	----------
2. Impregnated Tungsten (4-1-1), sputtered	2.30**	5.52** (1050°C-15 min)	3.24** (1050°C-15 min)
3. Impregnated Tungsten (3.5-1-1), sputtered	1.76	2.66 (1050°C-15 min)	2.66 (1050°C-15 min)
4. Ni cermet,* unpolished, sputtered	1.50	1.84 (850°C-10 min)	2.06 (900°C-10 min)
5. Ni cermet,* polished, sputtered	1.91	3.00 (850°C-10 min)	2.84 (1000°C-20 min)
6. Ni cermet,* polished, unsputtered	1.84	3.00 (850°C-10 min)	2.96 (1000°C-10 min)
7. Ni cermet,* unpolished, unsputtered	1.39	2.57 (850°C-10 min)	2.58 (1000°C-10 min)

* All four Ni cermets had the same composition (70% Ni, 30% Radio Mix No. 3), and were processed identically.

** This measurement refers to sputtered region only.

Table 3-8

Fluorescence of Ni Cermet Samples

	Unsputtered Region	Slightly Sputtered Region	Highly Sputtered Region
Polished Sample	greyish white background, with white spots	no white spots, hardly any fluorescence	no fluorescence
Unpolished Sample	blue, no white spots	greyish white	no fluorescence

3.4.3 Summary of results in ion bombardment vehicle.

3.4.3.1 Alumina films on molybdenum. Electron-beam-evaporated films.

a. Sputtering of 500Å and 1000Å films with N_2 resulted in yields of 0.015 molecules/ion at 0.8 kV and 0.017 molecules/ion at 1.2 kV. (Ion bombardment density 1.2 ma/cm^2 in both cases.)

b. These films, when half eroded by sputtering, had δ_{max} (in SEE vehicle) of ~1.4 in the sputtered region and δ_{max} of ~2.3 in the unsputtered region of same sample.

3.4.3.2 30% Mo - 70% Al_2O_3 films on Mo substrate. Electron-beam-evaporated films.

a. Sputtering of 1000 Å films with N_2 resulted in a yield of 0.007 molecules/ion at 0.65 kV in N_2. (Ion bombardment density of 1 mA/cm^2.)

3.4.3.3 Impregnated tungsten cathodes.

a. Sputtering with N_2 for 2 hours at 2 ma/cm^2 and 1.8 KV caused a significant amount of falling-out of tungsten particles.

b. These sputtered samples showed a reduction in δ of approximately 10% by comparison of sputtered and unsputtered regions of same sample.

3.4.3.4 Ni cermet cathodes.

a. Some darkening of the sputtered area was observed.

b. Unsputtered areas showed fluorescence; sputtered areas did not.

c. The sputtered samples showed a reduction in δ of approximately 10% by comparison of sputtered and unsputtered regions of same sample.

3.4.3.5 Platinum.

a. Sputtered sample showed no change in δ_{max}.

4. DISCUSSION OF THE RESULTS OF PHASE A AND RECOMMENDATIONS

The materials investigation of the program has indicated a number of prospective cathode materials for use in crossed-field aplifiers (CFA's). Thin films of the refractory metal oxides, such as Al_2O_3 and BeO, and impregnated tungsten were considered as the most promising candidates, and much of the effort was therefore spent on the investigation of these materials. Al_2O_3 and BeO films were attractive because of the relatively high values of δ obtainable under certain conditions. A shortcoming of these materials is the dissociation under electron bombardment. As has been shown, however, this problem can be overcome by providing a suitable gaseous environment. In particular, a low-pressure atmosphere of O_2 was found to stabilize Al_2O_3 and BeO films under electron bombardment so that acceptable values of δ can be maintained over extended periods of time. The feasibility of this approach was confirmed by operating such oxide films as cathodes in CFA test vehicles as will be described in detail in the "Phase B" section of this report.

Although the feasibility of the method has been demonstrated, and numerous experiments have been conducted with different types of Al_2O_3 and BeO films under various conditions, the investigation must still be considered as being far from complete because of the many variables which have to be taken into account. No definite conclusions can therefore be drawn from the present results, and only speculations and guidelines for future work can be offered.

It is reasonable to assume that the electron bombardment causes bond-breaking in the oxide films and release of both metal and oxygen atoms, but predominantly of oxygen atoms (see Section 1.4.3). The loss of O_2 renders the oxide more metallic and this, in turn, tends to decrease δ. Improvement of δ by administering O_2 may then be explained by oxidation of the excess metal, i.e., regeneration of the oxide. However, this simple explanation is acceptable only under the condition that no electron bombardment takes place simultaneously with the O_2 treatment. The processes occuring in the presence of O_2 and electron bombardment are certainly more complicated.

Our observations made in the EBV indicated a tendency of δ to settle down at a value intermediate between the maximum and minimum value found as a result of repeated electron bombardment dissociation and O_2-assisted regeneration of the surface oxides. This may be tentatively explained by assuming that, after much surface manipulation, a metal-rich film of only 2 - 3 atom layers has formed at the surface and now protects the δ enhancing oxide layer underneath from further dissociation.

The observed effects of typical tube gases other than O_2 and δ are also of interest inasmuch as they point to other factors which may have to be taken into consideration when attempting to explain the observations. It is recalled that the presence of H_2, CO_2, and N_2 caused significant recovery of δ in the case of Be. (The improvement of δ was not so dramatic with Al.) This effect on the δ of Be reminds one of the behavior of many metals which show a higher δ prior to degassing, i.e. when absorbed gases are still present at their surface. It may be speculated that work function lowering due to absorbed surface layers is responsible for these effects. In this connection it may be mentioned that, with regard to O_2, there is indeed some indication based on work function measurements reported in the literature, that O_2 absorbed on a previously cleaned Be surface causes a lowering of the work function from approximately 5 to 4 ev. The beneficial effect of O_2 on the δ of Be may therefore result from two sources, i.e. oxide regeneration and work function reduction.

The impregnated tungsten cathode has not been investigated in the program as extensively as the Al_2O_3 and BeO surface layers. The impregnant used in the experiments was exclusively barium-calcium-aluminate. Only the ratio of the components was varied. The result of the investigation indicated the importance of a suitable activation schedule for obtaining favorable δ values. The tendency of δ to increase and then to decrease as a result of the heating during activation was particularly interesting, since thermionic emission from impregnated tungsten cathodes does not generally show a decline after continued heating. It appears therefore that an activation schedule resulting in a good thermionic emitter does not necessarily produce a useful cold cathode. However, certain processes involved in the activation may be equally beneficial in making a good thermionic emitter as well as a practical cold cathode. This seems to be indicated by the observation that the impregnated tungsten samples which were activated such as to exhibit thermionic emission more rapidly showed increased values of δ. The fact that the common activation of impregnated tungsten cathodes for use as thermionic emitters can be drastically changed, and yet a practical cold cathode can be obtained, was most convincingly demonstrated by the successful operation of an impregnated tungsten cathode in a CFA vehicle without prior performance of the usual heat treatment. This will be discussed in detail in the "Phase B" section of this report.

The data on the effects of electron bombardment on the δ of impregnated tungsten cathodes were too few in number to be conclusive. The comparatively high stability of δ under electron bombardment was encouraging and is possibly explained by taking into account that, in contrast to the oxide film cathodes, the impregnated tungsten cathode is not a simple compound, but

a mixture of reactive components. While the oxide film cathodes are simply decomposed by electron bombardment and, hence, δ is degraded, electron bombardment of the impregnated tungsten cathode perhaps promotes a chemical reaction among the components.

The δ of the impregnated tungsten cathode is thought to depend on the Ba activation of the tungsten surface. This can be achieved by electron and/or ion bombardment since these factors can produce Ba from the oxide impregnants and also activate surface diffusion to cover the tungsten surface with Ba.

This process is similar to the continuous activation taking place in a thermionic impregnated tungsten cathode during life as a consequence of the external heating.

In conclusion, it may be stated that the present study has demonstrated the feasibility of arriving at oxide film and impregnated tungsten type of cathodes which deliver sufficient secondary emission and are stable enough to serve as cold cathodes with satisfactory life expectancies in CFA's. The results of the study have indicated a strong need for a deeper insight into the physical and chemical effects which are produced at the surface of these materials by electron bombardment and which depend on the initial state of the materials and the bombarding and environmental conditions. A better understanding of the mechanisms involved will greatly aid in optimizing the performance of the cold cathodes.

Emphasis of future work should therefore be placed on the investigation of the bombardment-induced surface phenomena. Low-energy electron diffraction and Auger analysis are considered as a valuable tool in this study. X-ray diffraction and X-ray fluorescence analysis should be used as additional analytical techniques.

In the study of oxide film cathodes, the nature of the films as a function of the preparation method should be determined prior to electron bombardment and, in addition, the surface changes produced by various bombarding and environmental conditions should be investigated and related to the secondary emission behavior.

In future work on the impregnated cathode, the activation of the cathode by electron bombardment alone should be explored in detail in the EBV. Both activation and operation of the activated cathode should be monitored by a mass spectrometer to identify gaseous by-products. As an additional item of interest, the effect of the degree of the porosity of the tungsten on the secondary emission properties should be included in the study.

PHASE B

EVALUATION AND LIFE TESTING OF SELECTED COLD CATHODE MATERIALS IN OPERATING CROSSED-FIELD AMPLIFIERS

5.0 INTRODUCTION - PHASE B

In a crossed-field amplifier (CFA), part of the emission current is out of phase with the rf fields. This current extracts energy from the rf field, bombards the cathode, and causes the secondary emission needed for operation.

As explained in Section 2.3, crossed-field amplifiers exhibit an emission current boundary which is the locus of emission-limited maximum current termini of operating lines (each operating line is obtained at a constant magnetic field) in the V-I plane. The slope of the emission current boundary is proportional to δ-1.

Platinum with a δ of 1.8 is adequate for many high-voltage CFA tubes. However, larger values of δ are needed for lower voltage tubes and for higher power levels.

In Phase B of this program, the emission current boundary data were evaluated for several secondary emitting cathode materials in operating crossed-field amplifiers. The materials were platinum, beryllium, aluminum, (both solid and thin film), molybdenum-doped alumina, and barium calcium aluminate impregnated tungsten. In addition, the enhancement of emission due to the introduction of oxygen into the tube environment was investigated for the beryllium and aluminum cathodes.

Extended life testing was conducted on the beryllium, aluminum, and impregnated cathodes.

Pertinent life test data are reported on platinum and beryllium cold cathodes that were run on other programs.

6.0 CFA TESTING

6.1 QKS1319. The QKW1319 (illustrated in Figures 6-1 through 6-4) is an L-band forward-wave CFA which provides 100 kW of peak power at 13.5 dB gain over a 100 MHz frequency band. It operates from a dc power supply at 10 kV, and its cold cathode is pulsed on with rf drive and off with a low energy control pulse.

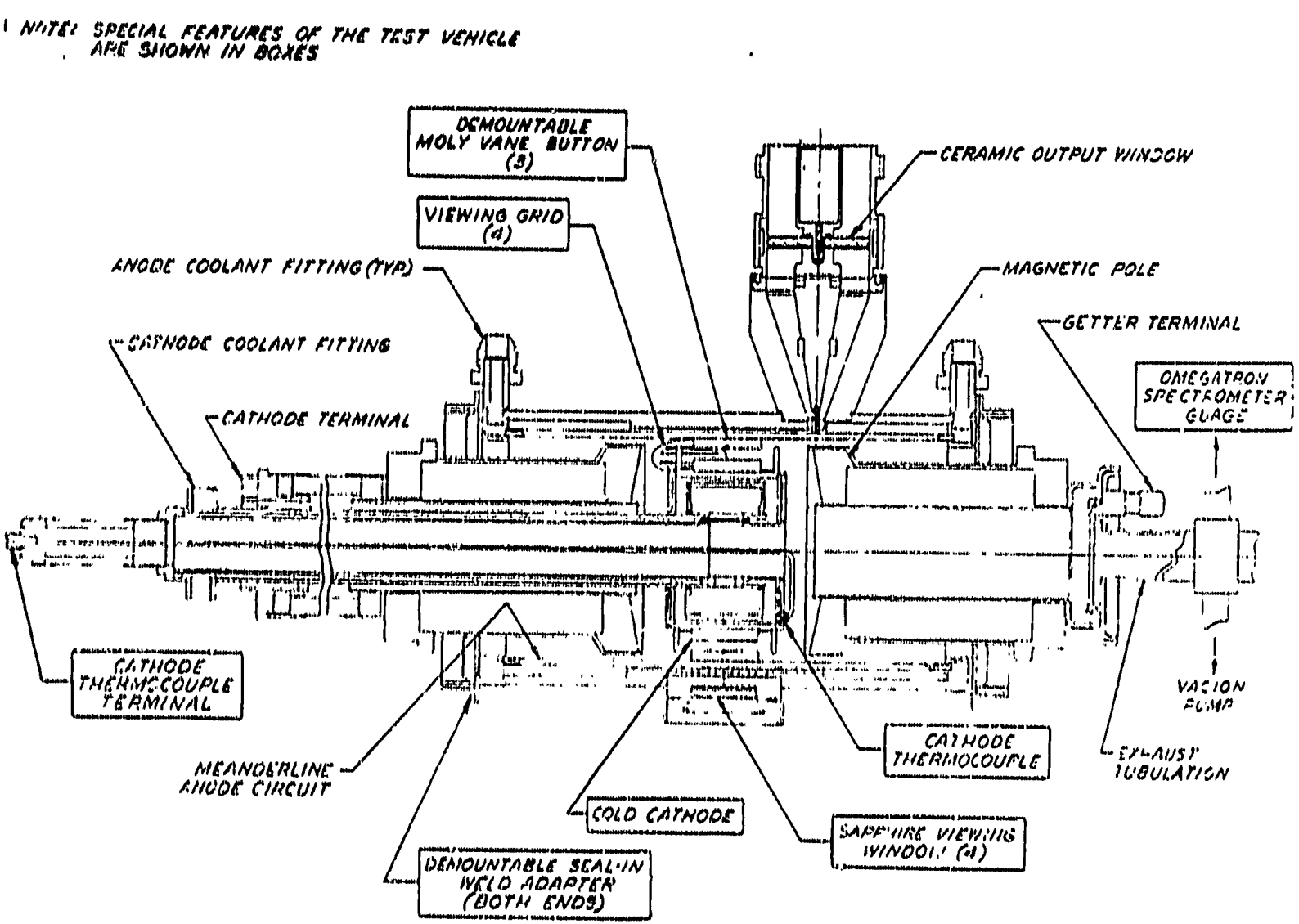

Figure 6-1 QKS1319 CFA Test Vehicle - Layout Drawing

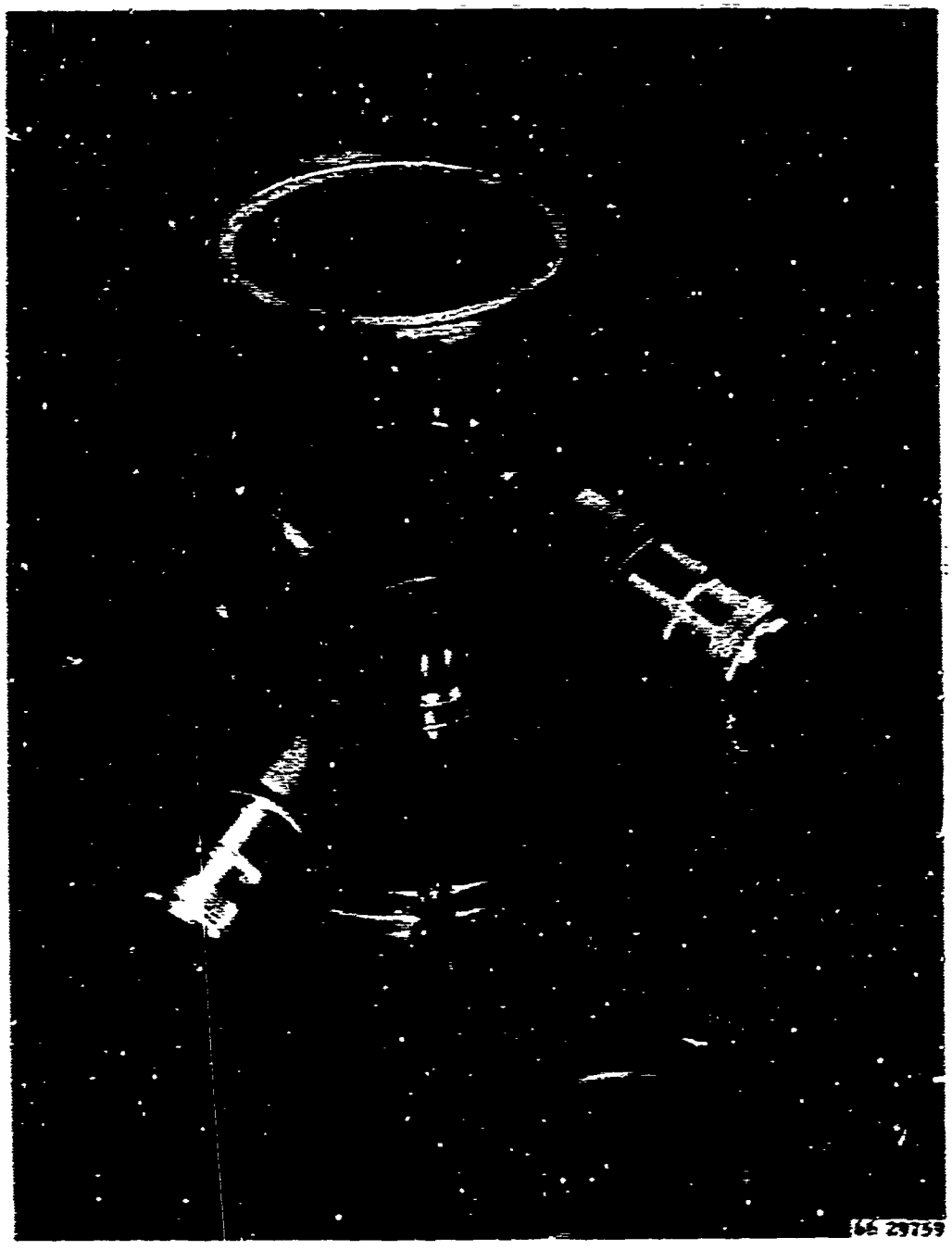

Figure 6-2 QKS1319 CFA Test Vehicle - Anode Assembly

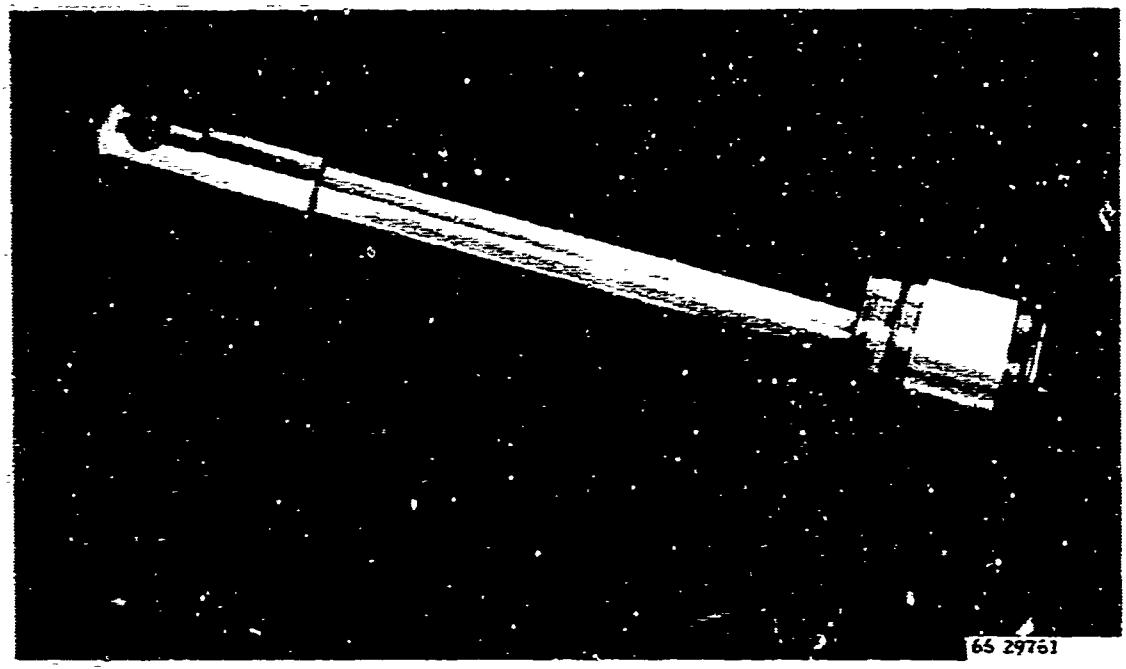

Figure 6-3 QKS1319 CFA Test Vehicle - Cathode Support Assembly

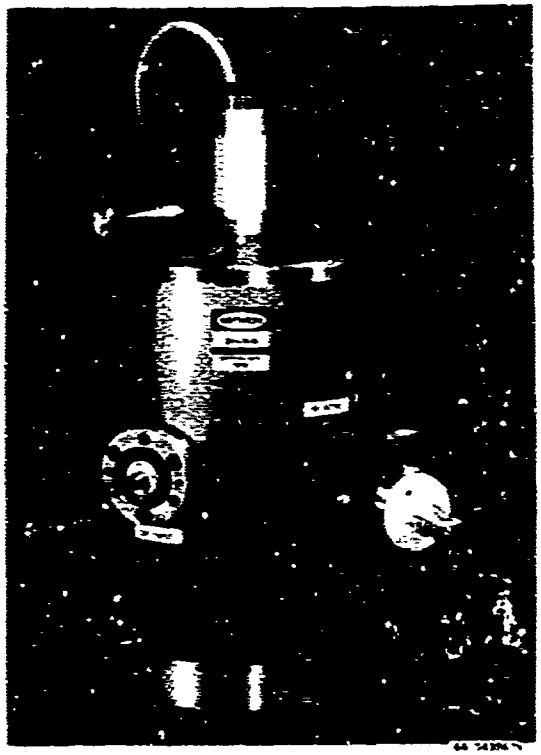

Figure 6-4 QKS1319 CFA Test Vehicle - Packaged Tube

The QKS1319 was under development during the first 12 months of the cold cathode study project. Low and high average power versions of this tube, including the QKS1383, were used for several of the Phase B secondary emitter evaluation tests reported here. The use of an oxygen source in a CFA for prolonging secondary emitter life was first evaluated in a QKS1319 test vehicle.

The principal operating characteristics are given below in Table 6-1.

Table 6-1

QKS1319/1383 Operating Characteristics

Frequency Band	1250 - 1350 MHz
Peak RF Power Output	100 kW
Average RF Power Output	3000 W
Pulse Width	250 μs
Duty Factor	.03
Gain	13.5 dB
Operating Voltage	10 kV dc
Operating Current (nominal)	22 A

6.1.1 Evaluation of the Polished Pt emitter - Test Vehicle (TV) No. 1A. The first cathode tested in the QKS1319 was a pure platinum cathode for a reference. The emitter surface was polished to a mirror finish using a fine aluminum oxide paper (Aloxite 600) and distilled water as a lubricant. The assembly was sealed in, designated TV No. 1A, and was subjected to a normal bakeout at a temperature of 450°C for 20 hours.

Emission current boundary (ecb) data are plotted in Figure 6-5. The cathode produced a peak current of approximately 3.6 peak A and, as a consequence of the low emission yield, no CFA amplification was obtained. Hot insertion loss data revealed low anode circuit losses, indicating that sufficient emission would have produced CFA amplification.

The exhaust cover pole assembly was removed, and no exceptional visual effects were detected. Mechanical inspection of the cathode centering showed no important change. The cathode pole assembly was then removed, and a visual inspection of the cathode emitter surface, cathode pole, end shields, and anode circuit gave no evidence of any exceptional phenomena.

6.1.2 Evaluation of the roughened surface platinum emitter - TV No. 1B The platinum cathode emitter previously evaluated was grit-blasted with fine alumina particles at a nozzle-to-emitter distance of 6 inches and an air pressure of 40 pounds gauge. The nozzle was held normal to the axis of the cathode cylinder. The surface finish, as measured by the profilometer in mechanical inspection read 22 microinches. The cathode was sealed in and the tube was designated TV No. 1B.

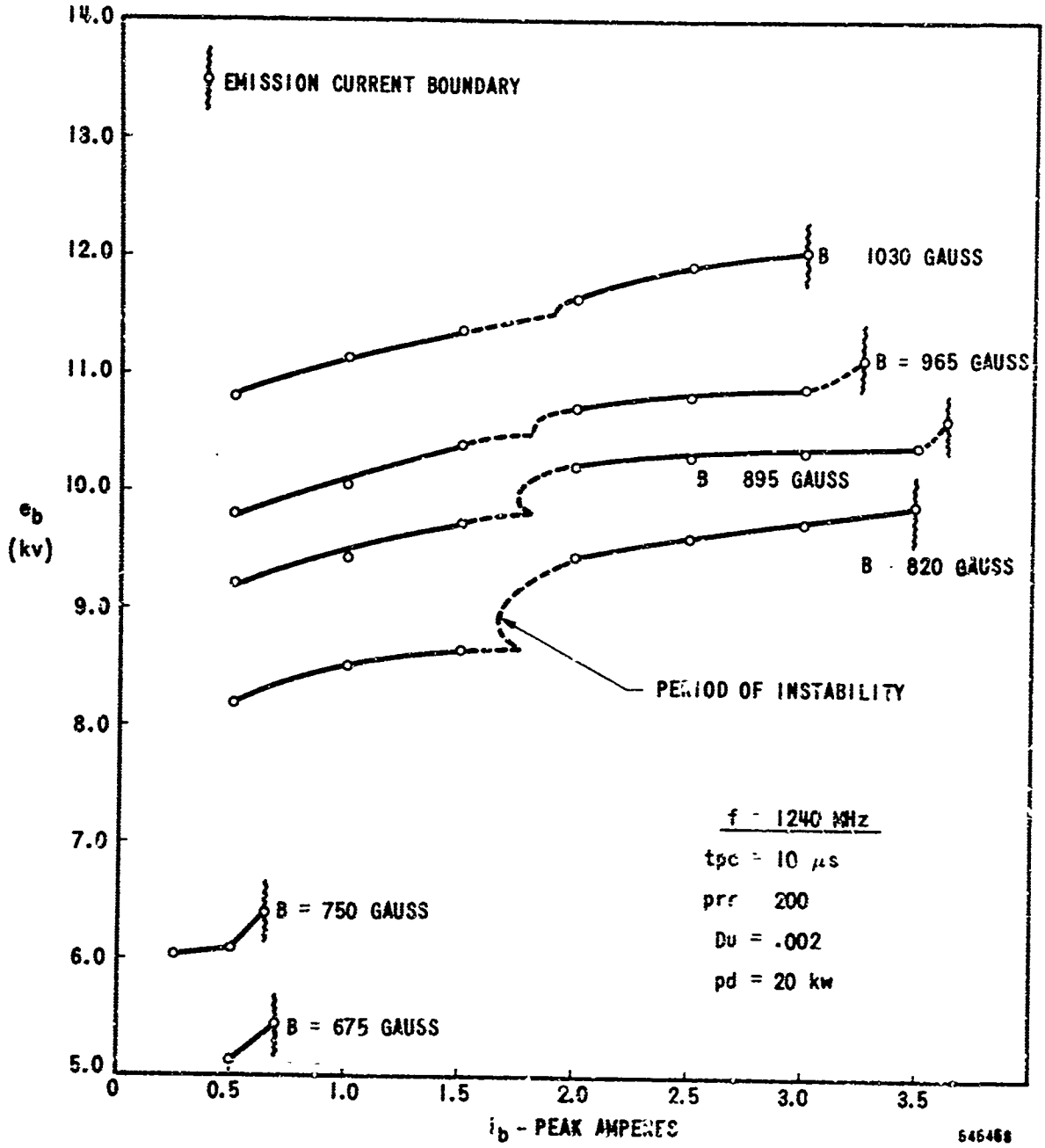

Figure 6-5. Emission Current Boundary Data - Cold Cathode Study - TV No. 1A (Highly Polished Platinum Emitter)

After bakeout, a power output of 120 kW was achieved, with an overall efficiency of over 50%. The emission current boundary data were creditable and yielded a current of approximately 25 peak A.

The current mode boundary dropped rapidly during the test so that in 10 hours the tube was no longer operable. See Figure 6-6.

The rapid decay in emission suggested that the cathode surface was changing with time, probably because particles of alumina were embedded in the platinum during the grit-blasting operation, either came out physically or were reduced to aluminum and oxygen by the electron bombardment.

One experiment produced a very interesting result. A platinum cathode sample was grit-blasted and ultrasonically cleaned in liquid Freon. Chemical analysis proved that aluminum oxide particles remained embedded in the material; therefore, it is probable that the secondary current is enhanced by the presence of aluminum oxide in a grit-blasted or Aloxite-treated platinum surface, and that the performance of the roughened surface platinum emitter is not entirely due to angle of incidence or to increased surface area.

6.1.3 Evaluation of the 1000 Å molybdenum-doped Al_2O_3 emitter TV No. 1C. A molybdenum-doped Al_2O_3 film showed very good secondary emission yield in Phase A of this program. A molybdenum cathode was therefore coated with a 1000 Å molybdenum-doped Al_2O_3 film, sealed into the test vehicle, and designated TV No. 1C.

Initially the low field ecb data were similar to those of the roughened platinum emitter, and efficient CFA operation was obtained. The emission current boundary decreased fairly rapidly. Subsequent investigation placed the emphasis upon the deteriorating effects of electron bombardment dissociation (EBD), sputtering, and arcing conditions. Plots of initial and final low-field ecb data are shown in Figure 6-7.

Sputtering, EBD, and arcing, produced by various combinations of current, magnetic field, and high voltage, were observed through the four viewing ports. Sputtering was believed to occur in the presence of a "blue glow" which was seen to occupy the entire interaction space volume and was always present when the CFA was in its proper amplification mode. Arcs appeared as small bright spots which occured more frequently and increased in intensity at higher voltage levels. To separate the effects which cause emitter deterioration, the CFA was run well below the arc boundary for a specified length of time, with continuous visual monitoring of the viewing ports. If an arc was observed during a test, the data was not considered representative of the effects of sputtering and EBD alone. Controlled arcing runs were produced by raising the high voltage and allowing the tube to arc for specified intervals of time (limited to approximately 2 minutes because of possible damage to the test vehicle anode). In this short period of time, it was possible to note a slight change in the emission current

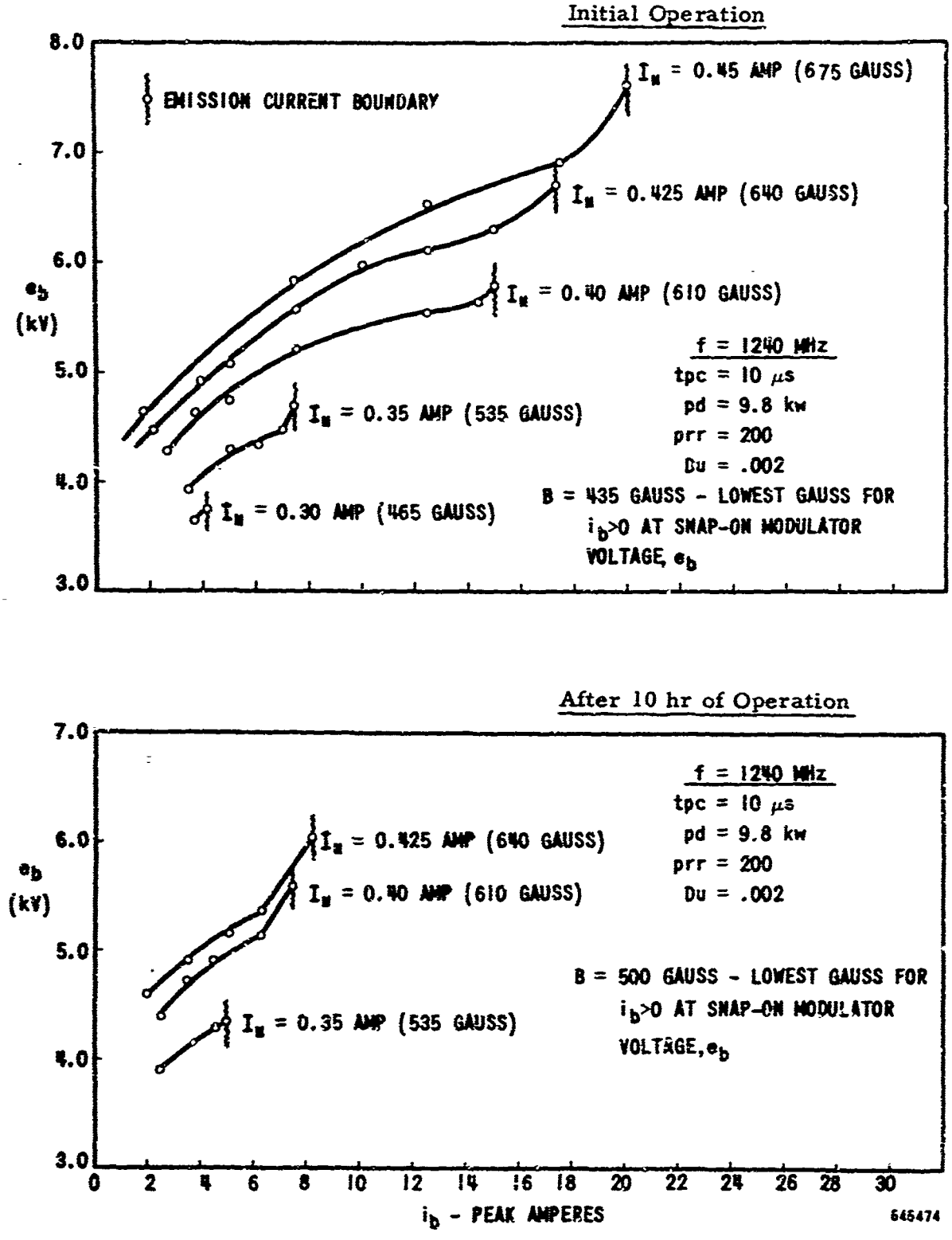

Figure 6-6 Emission Current Boundary Data vs Time - Cold Cathode Study - TV No. 1B (Roughened Platinum Emitter)

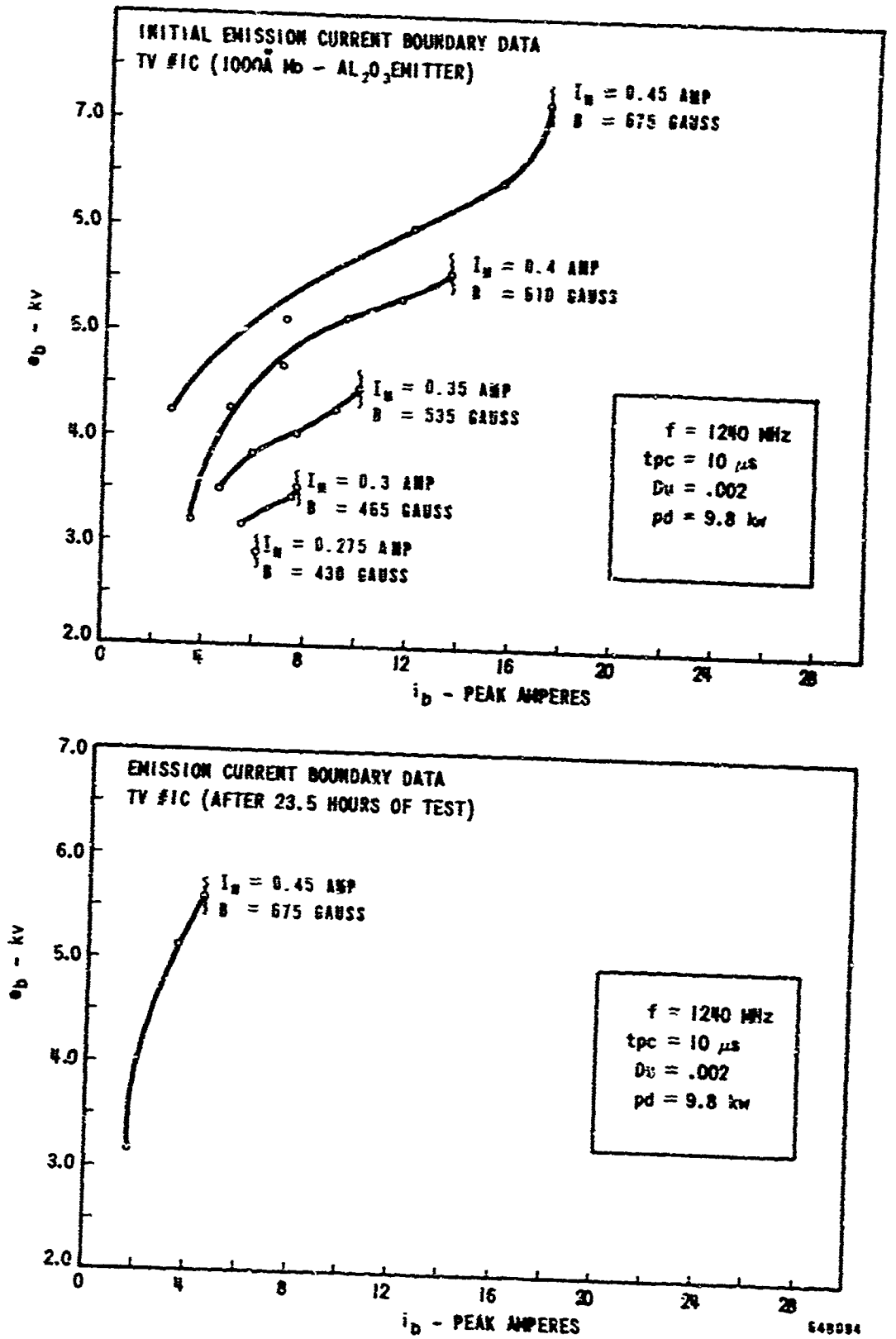

Figure 6-7 Emission Current Boundary vs Time - Cold Cathode Study TV No. 1C

boundary data; however, 20 to 30 minutes of continuous operation was required to detect emission depletion in the presence of EBD and sputtering alone. After several test runs of various time intervals with increasingly severe arcing and sputtering conditions, the data yielded conclusive evidence that a faster rate of emitter depletion occurs in an arcing environment.

Both sputtering and electron bombardment decomposition may contribute to the degradation of δ, as evidenced by the shift in emission current boundary. EBD would cause the surface to be enriched in aluminum content due to oxygen evolution. It was suspected that the EBD mechanism was more significant than sputtering in the observed loss of δ. In order to confirm this suposition, it was decided to break open the exhaust tubulation, expose the emitter surface to air and then to rebake the tube in an effort to restore the original current boundary conditions. The initial emission current boundary data for this test vehicle, designated TV No. 1D is shown in Figure 6-8. The device demonstrated increased emission current almost to the initial values obtained for the original 1000Å Mo-alumina emitter.

Since the natural oxide layer on aluminum is only approximately 25 Å thick, the almost complete recovery of δ due to air exposure is interpreted to mean that EBD depletion in the first 25 Å of the surface is the most important depth in degrading δ. This is consistent with previous measurements in this laboratory which showed a lack of dependence of δ on the thickness of the oxide layer on aluminum for the 25 Å to 1000 Å range. The 25 Å layer had very short life; the ecb dropped gradually as the tube was being run up to the normal operating gauss level.

6.1.4 Evaluation of beryllium emitter - TV No. 2. Another QKS1319 test vehicle, designated TV No. 2, was equipped with a beryllium emitter and subjected to a series of evaluation tests. The initial ecb data compared favorably with the Mo-doped Al_2O_3 emitter. The effect of continuous CFA high-voltage operation on emitter depletion is shown in Figure 6-9.

After 37 hours of high average power operation the emission level was very low. The tube was exposed to air and baked out in the same manner as the 1000 Å Mo-doped Al_2O_3 emitter. Low-field emission current boundary data revealed that almost 100% of the original current value was restored, supporting similar data for the Mo-doped Al_2O_3 cathode.

6.1.5 Investigation of oxygen source for longer life. It was appropriate to provide a continuous source of oxygen during CFA operation to obtain conclusive information on the observed natural oxide emitter depletion.

A method for providing a continuous source of oxygen during CFA operation was devised, and the design and construction of the associated hardware was completed. The oxygen source consisted of a disc of pressed and sintered cupric oxide placed in a container with a heater. An experimental test was performed to determine partial pressures of oxygen as a function of heater power.

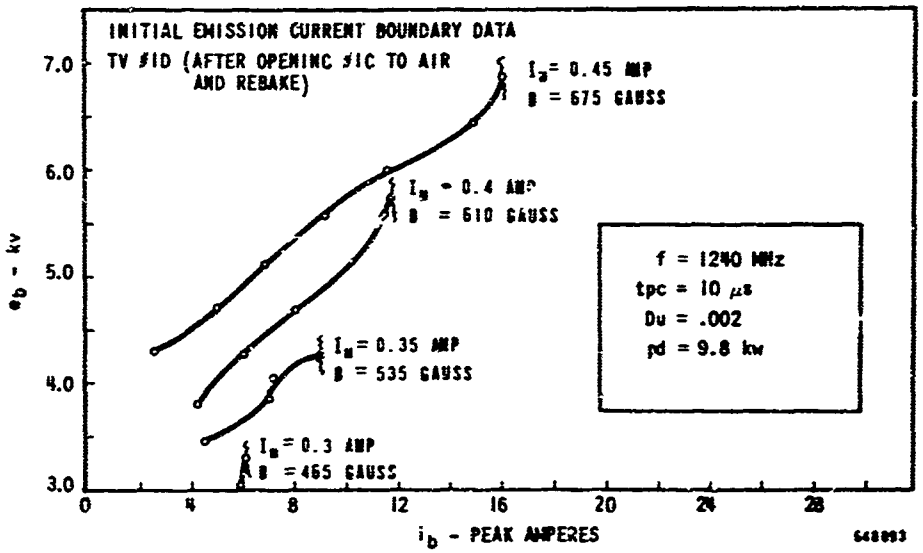

Figure 6-8 Initial Emission Current Boundaries - Cold Cathode Study TV No. 1D

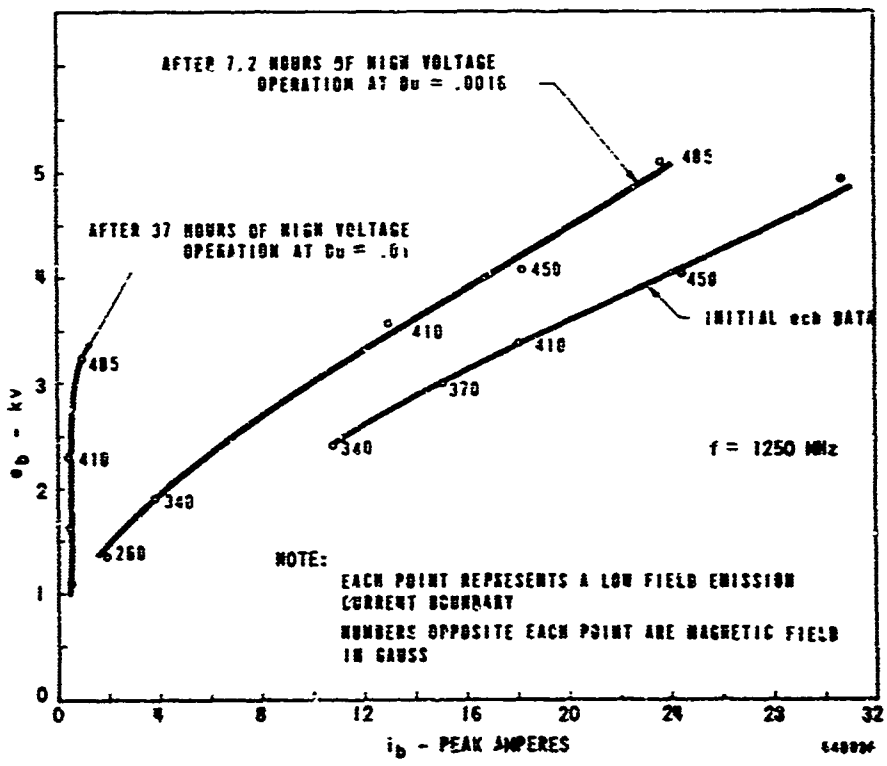

Figure 6-9 Low-Field Emission Current Boundaries vs Time - TV No. 2 (Beryllium Emitter)

6.2 QKS1397 Model No. 8. A QKS1397 test vehicle was constructed. The tube is illustrated in Figure 6-10, and its operating characteristics shown in Table 6-2. It utilized a stub-supported meanderline as the slow-wave circuit, which consisted of 0.070 in. OD tubings spaced 0.040 in. from a backwall ridge. The device also had an "oversize" aluminum (AA1100-F) cathode emitter of 1.702 in. OD. An oxygen source was incorporated for life test evaluation of cathode emission.

Bakeout processing was conducted at a temperature of 400°C for 12 hours. Further processing was conducted at the test station with the use of a Vac-Ion appendage pump during initial test evaluation.

Test evaluation of the tube was conducted with the use of a conventional pulse modulator. Strong pi-mode oscillation prevented proper tube operation at the normal drive power level of 25 to 50 kW peak. A drive power of 200 kW peak was required to "lock out" the pi-mode oscillation at a sufficiently low current level to give a reasonable dynamic operation range for the tube. At a duty factor of .001, the maximum peak current was 106 A for a cathode stress level of 5.7 A/cm^2. The peak rf power output was 1.3 MW. Curve No. 8 of Figure 6-11 shows the emission current boundary for various magnetic fields.

The pi-mode oscillation reappeared for higher duty factor operation (du > .0015) and prevented normal tube operation. Evaluation of the tube was terminated because the severe pi-mode oscillation was considered to be due to the large diameter cathode.

6.2.1 QKS1397 Model No. 8A. The test vehicle was rebuilt as model No. 8A with a smaller diameter (1.690 in.) aluminum cathode. Bakeout and initial test processing remained as before.

A drive power of 125 kW peak was now required to suppress pi-mode oscillation for a reasonable dynamic operating range. A peak current of 98 A was reached at a .001 duty factor, representing a cathode stress level of 5.3 A/cm^2. Curve No. 8A of Figure 6-11 shows the emission current boundary for various magnetic fields.

Cathode emitter life test was initiated at a peak current of 72.5 A at a .001 duty factor, with the oxygen source heater power off. Operation at this duty factor continued for 8 hours; at which time the peak current had decreased to 66.7 A. The solid curve of Figure 6-12 shows the peak tube current as a function of time during this phase of the life test. The average power added by the CFA at the initial current level was 2970 watts, at an efficiency of 46.5%, with the cathode back-bombardment power measured as 370 watts.

The oxygen source was then outgassed and the cathode emission replenished to a peak current level of 83 A (du = .001). The dashed curve of Figure 6-12 shows the oxygen source heater power as a function of time. From this curve it may be observed that to operate the tube at .001 duty factor, and with the oxygen source heater power off, or at a reduced power

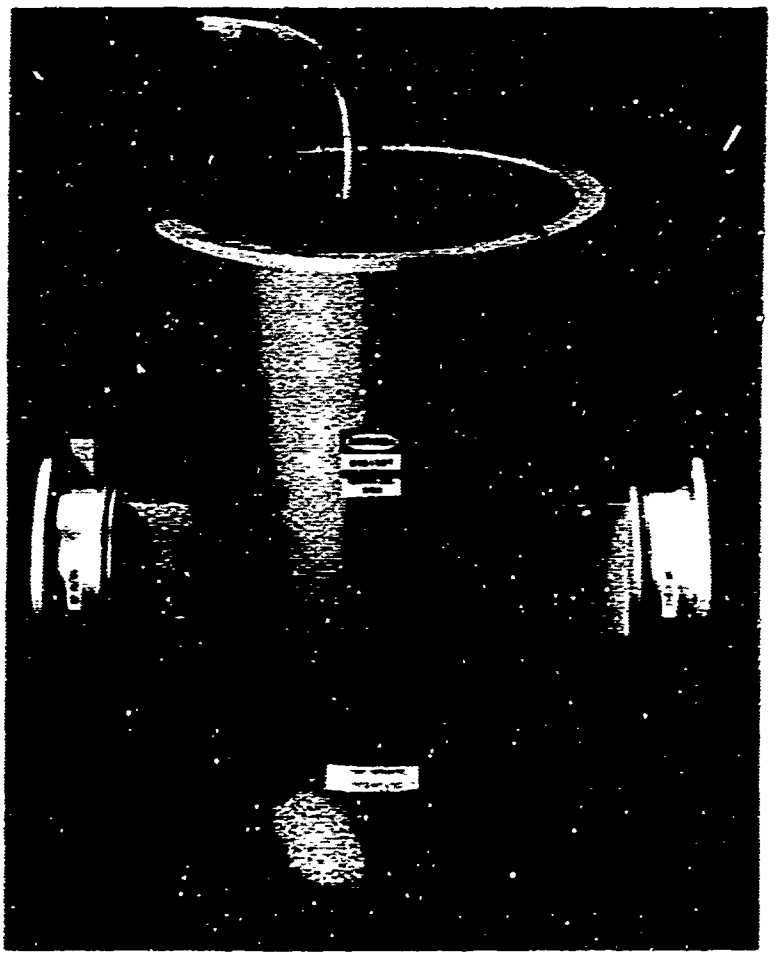

57 38341A

Figure 6-10 QKS1397 CFA Test Vehicle
S-band Forward-wave CFA

Table 6-2 QKS1397 - Operating Characteristics (Preliminary)

Characteristic	Symbol	Quantity	Units
Frequency (Instantaneous Bandwidth)	f	3135-3465	MHz
Peak Power Output (minimum)	P_o	1000	kw
Average Power Output (minimum)	P_o	4000*	W
Pulse Width	t_p	15	μs
Gain (minimum)	A	16	db
Operating Voltage	E_b	28	kV
Operating Current (nominal)	i_b	80	a

* Limited by present power supply

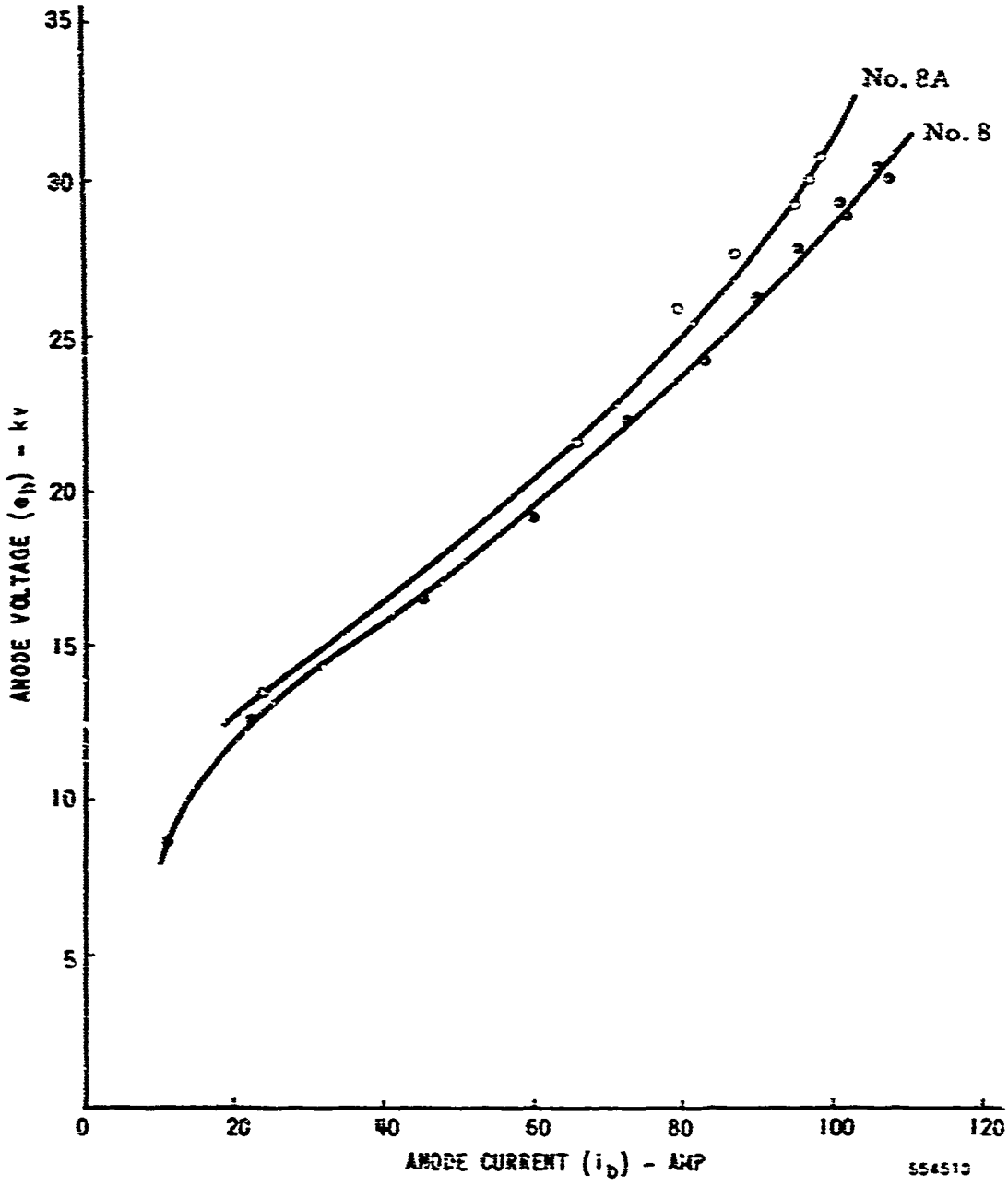

Figure 6-11 QKS1397 Emission Current Boundary (Various Magnetic Fields) - Solid Aluminum Cathode

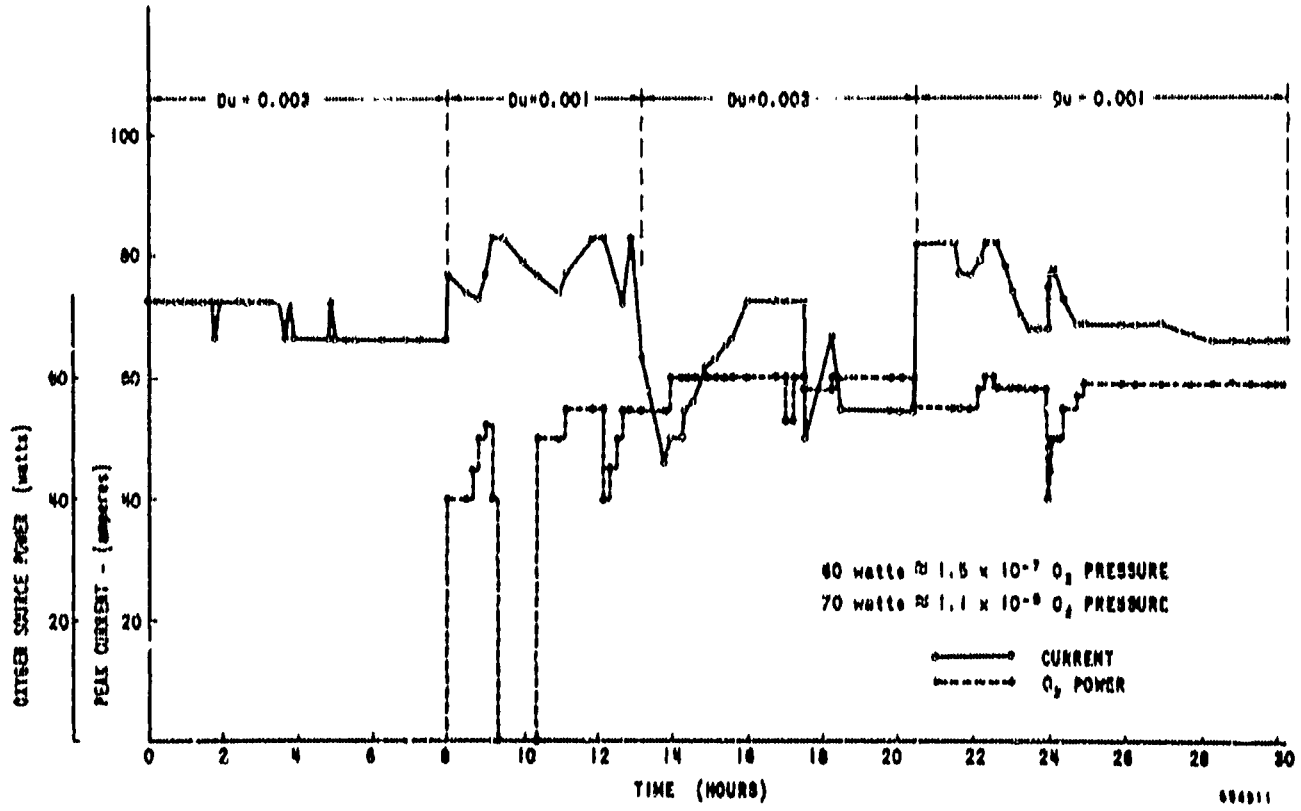

Figure 6-12 (Sheet 1) QKS1397 No. 8A Life Test - Solid Aluminum Cathode

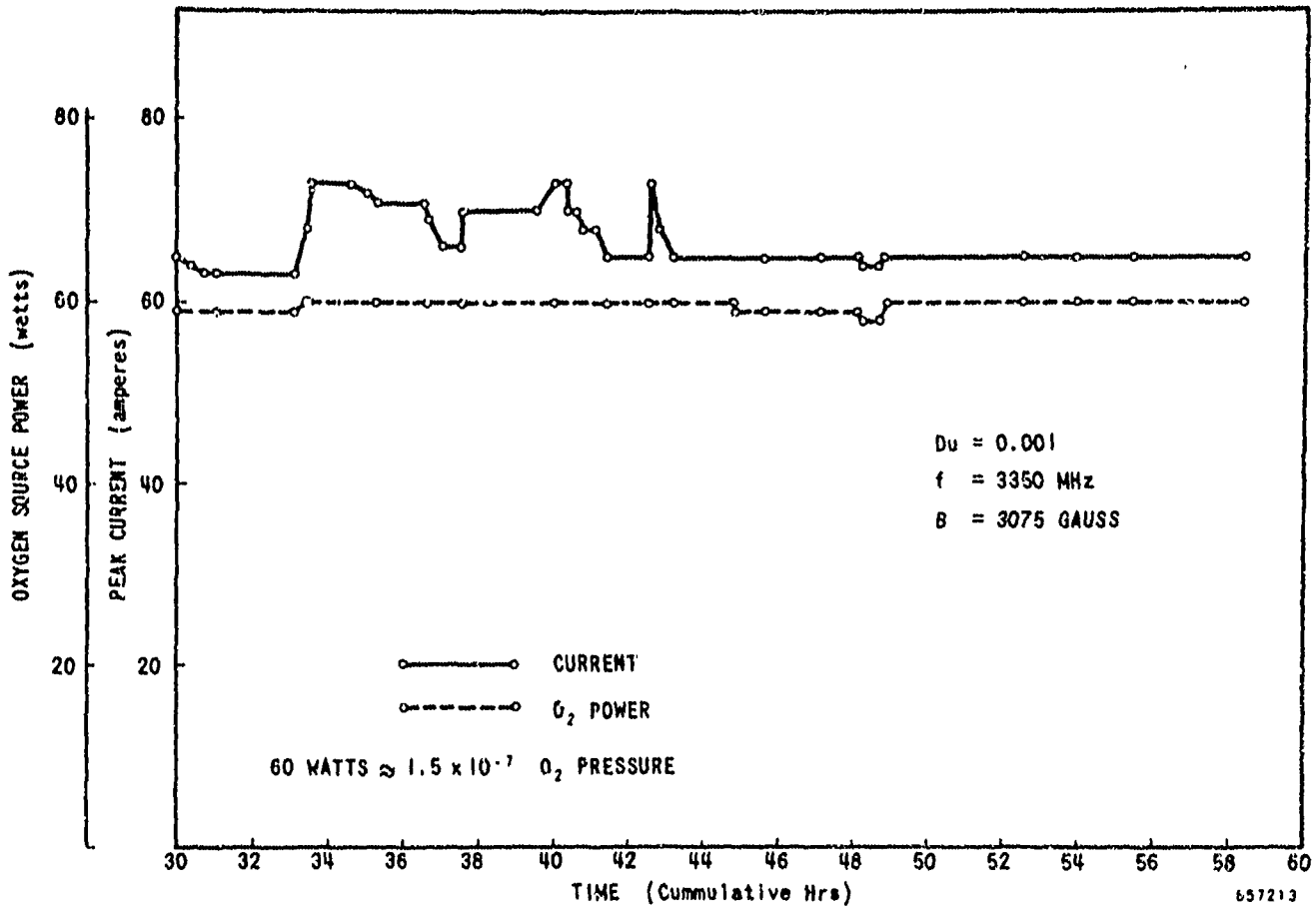

Figure 6-12 (Sheet 2) QKS1397 No. 8A Life Test - Solid Aluminum Cathode

level, resulted in a decreased cathode emission. Hence, cathode emission life evaluation was continued (at du = .003) with the oxygen source heater power initially at 55 watts. Only after the oxygen source heater power was increased to 60 watts did the peak cathode emission reactivate to 72.5 A. At this peak current level an average power of 2700 watts was added by the CFA. The tube efficiency had then decreased to 42.5%, while the cathode back-bombardment power remained at 370 watts. After 7 hours of operation at .003 duty factor, the peak current emission had decreased to 54.7 A.

Evaluation of the cathode emission life continued at .001 duty factor, starting at a peak current of 83 A. The oxygen source heater power was initially 55 watts, but was later increased to 59 watts. Figure 6-12 again shows both the peak current emission and the oxygen source heater power as a function of time for this operating condition. After 10 hours of operation at .001 duty factor, the peak current had decreased to 66 A, where it stabilized.

The emission was quite sensitive to O_2 pressure, an increase in O_2 heater power of only 1 watt gave a corresponding increase in peak current.

Cathode emission life test of model No. 8A was terminated after a total accumulated time of 58 hours to rebuild the test vehicle with a modified aluminum cathode emitter and supporting structure for improved performance.

6.2.2 QKS1397 Model No. 8B. Test Vehicle No. 8A was rebuilt as model No. 8B with a smaller diameter (1.680 inches) aluminum cathode. This smaller cathode diameter conformed more closely to the "standard" QKS1397 design, which has shown practically no pi-mode oscillation.

The operating point selected for test evaluation was the following:

f_o	=	3.4 GHz
p_o	=	877 kW peak
P_o	=	1770 W average
B	=	3000 gauss
i_b	=	100 A peak
e_b	=	28 kV

In Figure 6-13, the solid line shows the peak tube current and the dashed line shows the oxygen-dispenser heater power, both as a function of time. With an initial peak drive power of 125 kW, a peak current of 100 A was obtained at .002 duty factor. This level of emission could be maintained for just over an hour, after which it rapidly decayed to 55 A. The peak drive power was then raised to 150 kW after changing to a .001 duty factor. The emission recovered to 88 A, but then a voltage breakdown occurred within the tube (due to temporary loss of rf drive power), and the emission again rapidly fell off to 55A. The oxygen dispenser was then

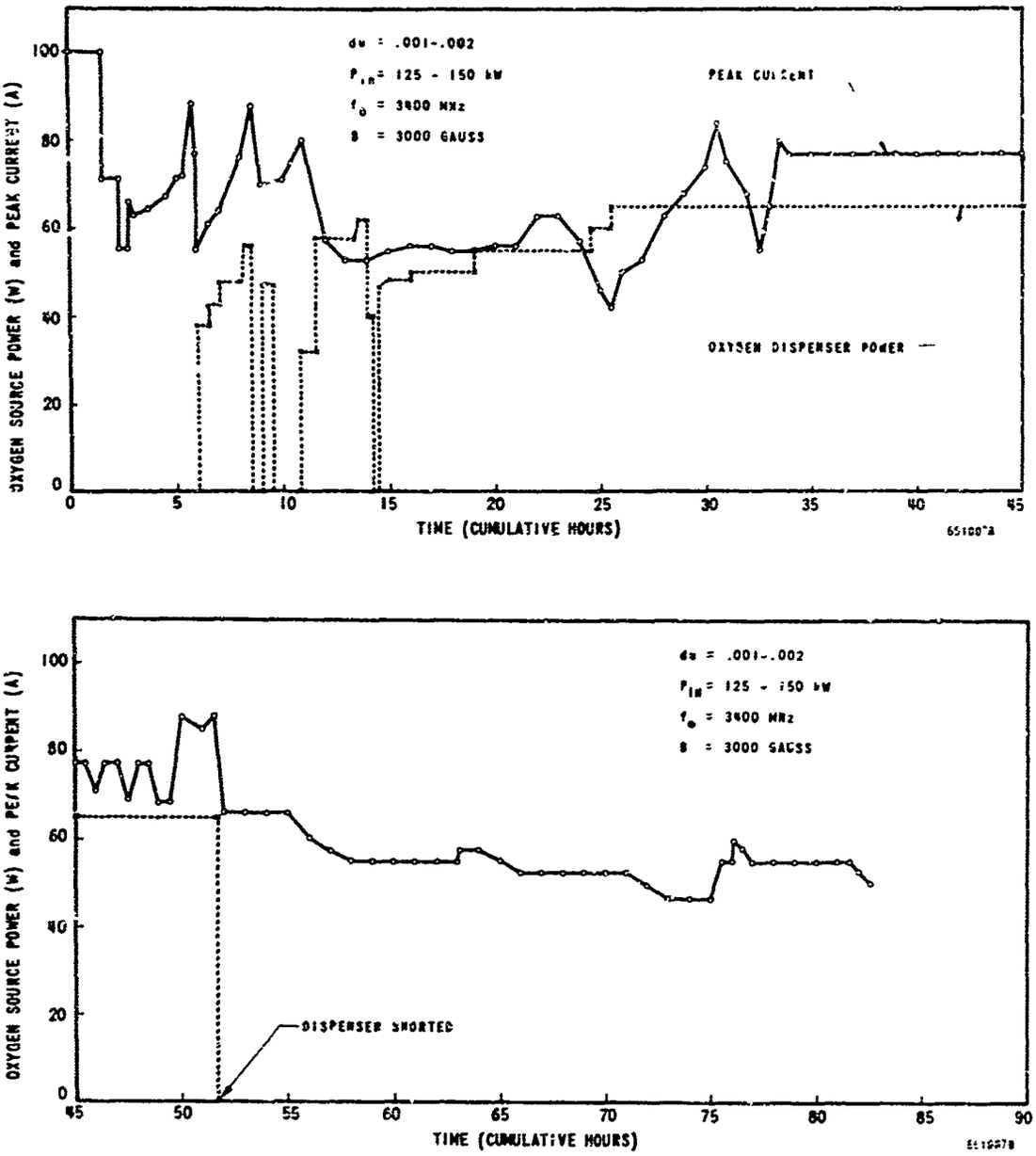

Figure 6-13 QKS1397 No. 8B - Oxygen Source Power and Peak Current vs Time - Solid Aluminum Cathode

activated and again the emission recovered to 88 A. However, the removal of the oxygen dispenser heater power resulted in a rapid decline of the peak tube current. The tube was then "conditioned" for half an hour with only drive power present, after which the emission gradually recovered to 80 A. An internal tube arc (again due to temporary loss of drive power) caused the emission to decline. The emission test continued fairly smoothly (with a few tube arcs) into the 52nd hour, with emission stabilized at approximately 77 A, but at 52 + hours the dispenser heater shorted with 65 W of heater power. Without oxygen dispenser power to maintain a partial pressure of oxygen in the tube, the emission gradually decreased, and the life test was terminated at approximately 82 hours.

6.2.3 QKS1397 Model No. 8C. Model No. 8C was built with a 0.5 mil evaporated layer of aluminum on an OFHC copper base for the cathode. The cathode was 1.645 in. in diameter and 0.670 in. high. The initial operating peak current level was chosen at 54.5 A, at the following operating conditions:

D_u	=	.001
f_o	=	3.3 GHz
P_{in}	=	110 kW
P_o	=	800 kW
e_b	=	31 kV
B	=	3000 gauss

The 54.5 A emission level could not be maintained, however, without the use of the oxygen dispenser. The oxygen-dispenser heater power was therefore gradually increased to 60 watts, at which point the emission had recovered sufficiently for operation at the level initially selected.

In Figure 6-14, the solid line shows the peak current, and the dashed line the oxygen-dispenser heater power, both as a function of time. The maximum emission current available is also indicated in the illustration by X's.

In the 18 to 22 hours operating period, the driver-tube trigger amplifier became unstable, causing the test vehicle to arc, with a resultant loss of emission. After repairs and emission reconditioning, accomplished by increasing the oxygen-dispenser heater power to 65 watts (O_2 pressure approximately 10^{-6} torr), life testing was continued at the initially selected peak-current level through the 73rd hour of operation. At that point the maximum peak current available had decreased to the operating current level.

The operating conditions were next changed to a duty factor of .002 and a frequency of 3.35 GHz. An immediate decline in the peak current available was observed, although it could be recovered by increasing the oxygen-dispenser heater power to 70 watts. However, operation at this heater-power level would have shortened the oxygen pellet life and the heater power was therefore restored within a short time to 65 watts.

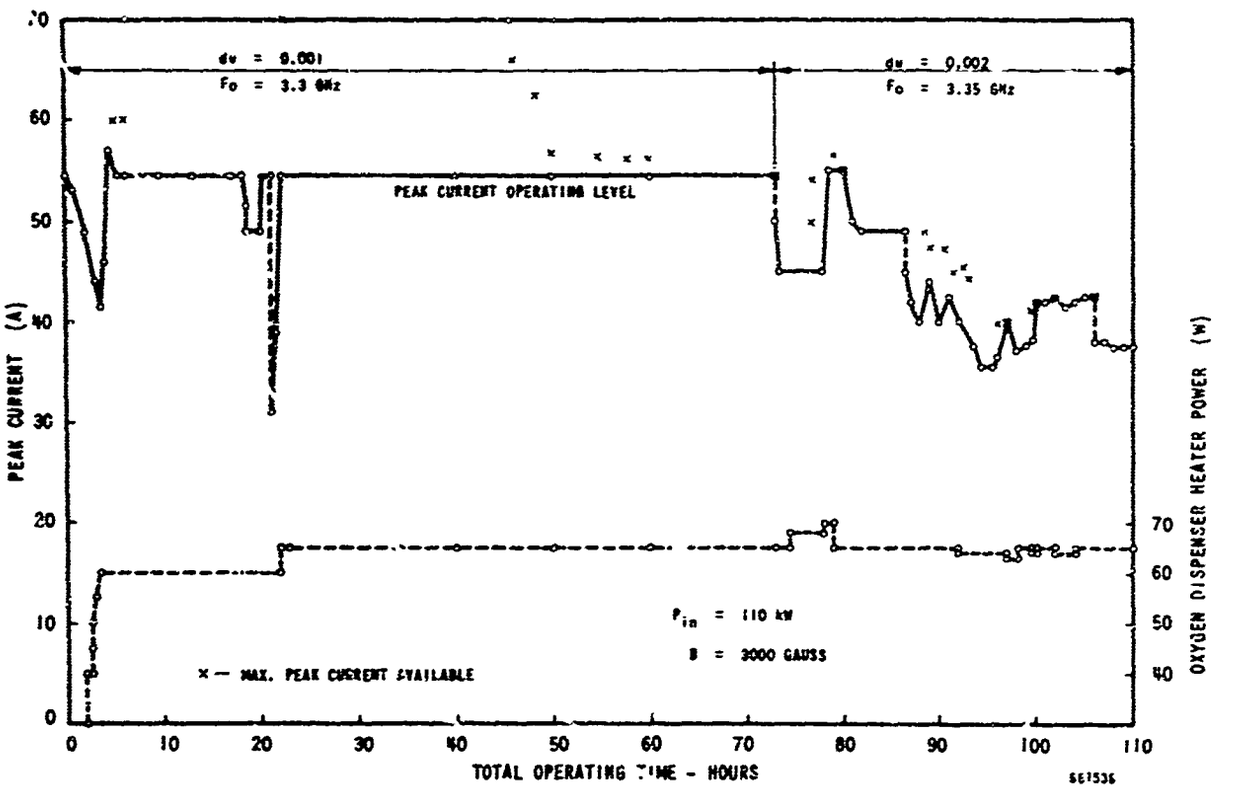

Figure 6-14 (Sheet 1) QKS1397 No. 8C - Life Test - P_{in} = 110 kW, B = 3000 Gauss, 0.0005 in. Evaporated Al on Cu Emitter

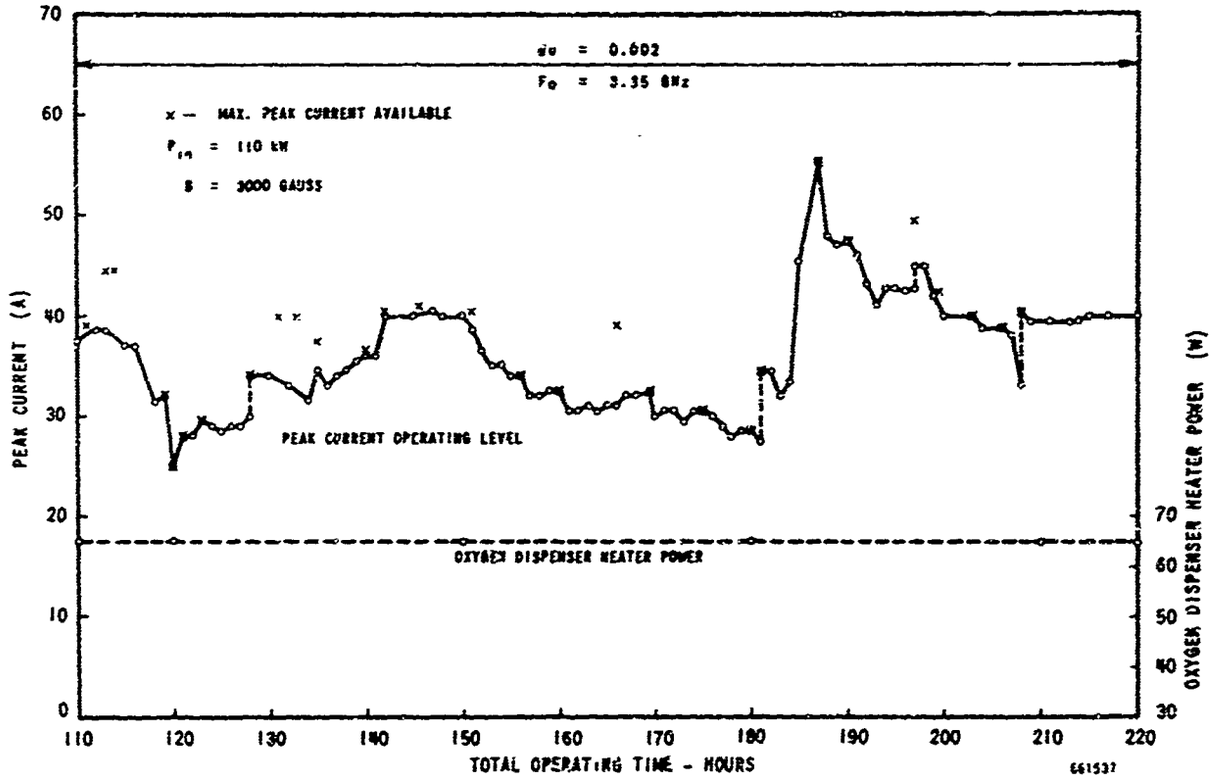

Figure 6-14 (Sheet 2) QKS1397 No. 8C - Life Test - p_{in} = 110 kW, B = 3000 Gauss, 0.0005 in. Evaporated Al on Cu Emitter

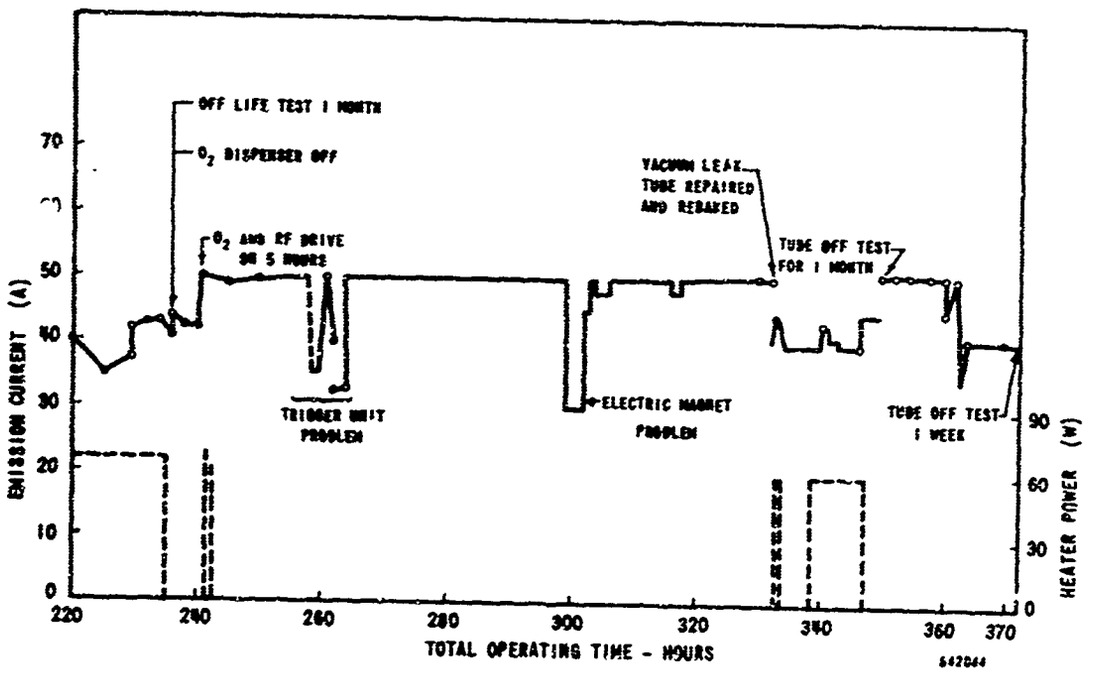

Figure 6-14 (Sheet 3) QKS1397 No. 8C - Life Test - p_{in} = 110 kW, B = 3000 Gauss, 0.0005 in. Evaporated Al on Cu Emitter

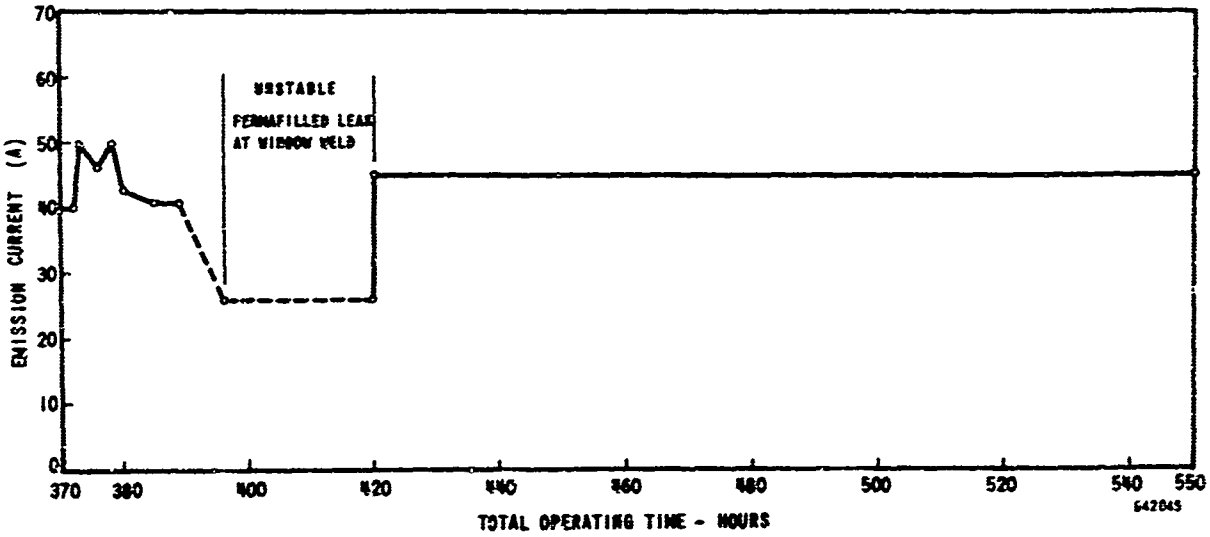

Figure 6-14 (Sheet 4) QKS1397 No. 8C - Life Test - p_{in} = 110 kW, B = 3000 Gauss, 0.0005 in. Evaporated Al on Cu Emitter

Low gauss emission current boundary data taken at 114 hours of life are shown in Figure 6-15. At the operating level of 3000 gauss (I_m = 1.25 A) the ecb was only 44 A.

After approximately 120 hours of operation, the test-vehicle trigger amplifier became erratic, causing the tube to arc, and resulting in a loss of emission. The emission gradually recovered after the trigger-amplifier unit was repaired. At 140 hours of operation, the emission was further improved by increasing the peak drive power to 125 kW. After about 10 hours of operation at this level, the drive power was restored to 110 kW, and the resultant continual decrease in peak-current emission was observed.

At 182 hours of operating time the oxygen-dispenser power supply leads were shortened by eliminating all clip leads. This reduced the lead resistance, and thereby increased the power available for heating the oxygen-dispenser pellet. The peak-current emission available showed an immediate increase to 56 peak A, but again it could not be maintained. The peak-current emission leveled off at around 40 A.

After 235 hours on life the tube was taken off the test set for a month, then restarted without the use of oxygen. The O_2 and rf drive were applied for five hours, and then the O_2 was turned off. The tube then operated for 90 hours at 50 peak A without oxygen. There were some minor equipment problems which momentarily reduced the current, but this was not the fault of the cathode.

During the 90-hour period of operation, a micro leak, which had developed in a window weld, supplied a very limited amount of oxygen in the tube. The vacuum level was initially on the 10^{-8} and finally the 10^{-7} torr scale during this period. The cathode emission had improved, apparently because of the micro leak, such that the tube could operate at 50 peak A, whereas before the peak current was limited to 40 A, even with the O_2 source on. The tube was retubulated and the leaky weld repaired, but the cathode was not removed. The tube was rebaked and replaced in the life test station under the following conditions:

Du	=	.0017
f_o	=	3.3 GHz
P_{in}	=	63 kW
P_{out}	=	700 kW
e_b	=	25 to 30 kV
i_b	=	38 - 44 A
B	=	3000 gauss

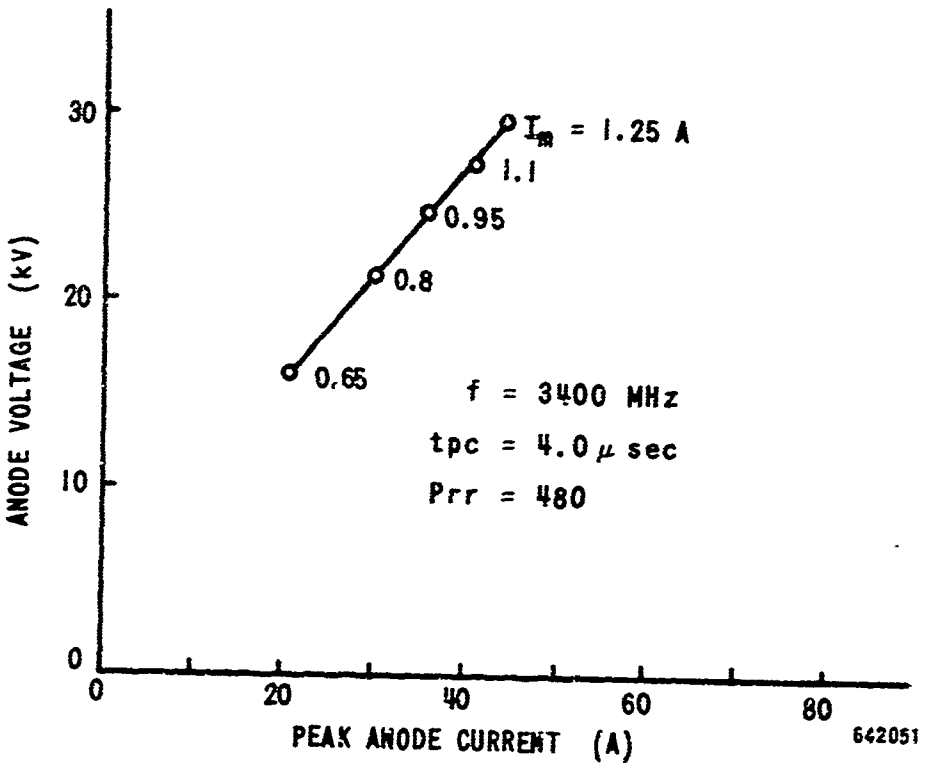

Figure 6-15 QKS1397 No. 8C - Emission Current Boundary after 114 Hours of Life Test - Evaporated Al on Cu Emitter

The initial maximum peak current was 40 to 45 A. The tube had been running at 50 A before the leak developed. An oxygen treatment of approximately 1×10^{-6} torr for 4 hours without the rf on did not show any marked improvement. The tube was run for about 5 hours and then the O_2 source was heated while the tube was operating.

The emission current boundary recovered with the O_2 present, and the tube ran with O_2 for 8 hours. The variation in current during that time was apparently caused by the modulator and was not a tube limitation. The tube was retired from life test for one month and when life test was resumed, the tube ran very well at over 50 A peak current for 10 hours. However, after being off over a weekend, the tube did not immediately function well, but it finally settled down and ran well at 41 peak A. In retrospect the trouble experienced around 360 hours was caused by modulator and/or phasing of the final tube with the driver, and was not an emission limitation.

The tube was then taken off life test for about a week, and when put back on, it ran poorly. At 420 hours on life test it was discovered that the Vac-Ion pump power supply was defective, indicating a pressure low on the 10^{-8} torr scale, while the tube was actually on the 10^{-4} torr scale. The leak was repaired with Permafil and the power supply was replaced.

Life test was resumed at 45 peak A. The tube ran very well here for 130 hours (this was the 550 hour point) without any additional oxygen. The life test was then terminated, and the tube was subjected to high power testing.

6.2.3.1 QKS1397 Model No. 8C - Special tests after 550 hours of life. The tube was subjected to 80 hours of high power testing after the end of the 550 hour life test. Several low gauss e vs i plots were made to determine the actual emission current boundary (ecb). These plots were repeated many times during the 80 hours. Figure 6-16 shows the initial data.

The peak current was increased from 45 to 62 A at .0017 duty cycle. After 9 hours the ecb dropped about 30% as shown in Figures 6-17 and 6-18 and 5 additional hours of operation at 73 A peak had little effect upon the ecb.

Quite often the tube would arc badly as the ecb was exceeded. This would increase the gas pressure in the tube from 10^{-8} to 10^{-5} torr, and the ecb would drop by up to 50%. However, within 5 minutes the ecb would return to its original value.

The pulse repetition rate was increased from 480 to 720 pulses/sec and the tube was aged for 3 hours at the same peak current level. See Figure 6-18. After this, the ecb dropped slightly. To increase the rate of decay, the repetition rate was increased to 1000, producing an ecb of approximately 75 A at $I_m = 0.9$ A. The tube was aged at a repetition rate of 1000 pps at a peak current of 62 A for 63 hours. The ecb data were taken every few hours, but remained unchanged throughout. Figure 6-19 shows the gauss line plots at the end of 80 hours.

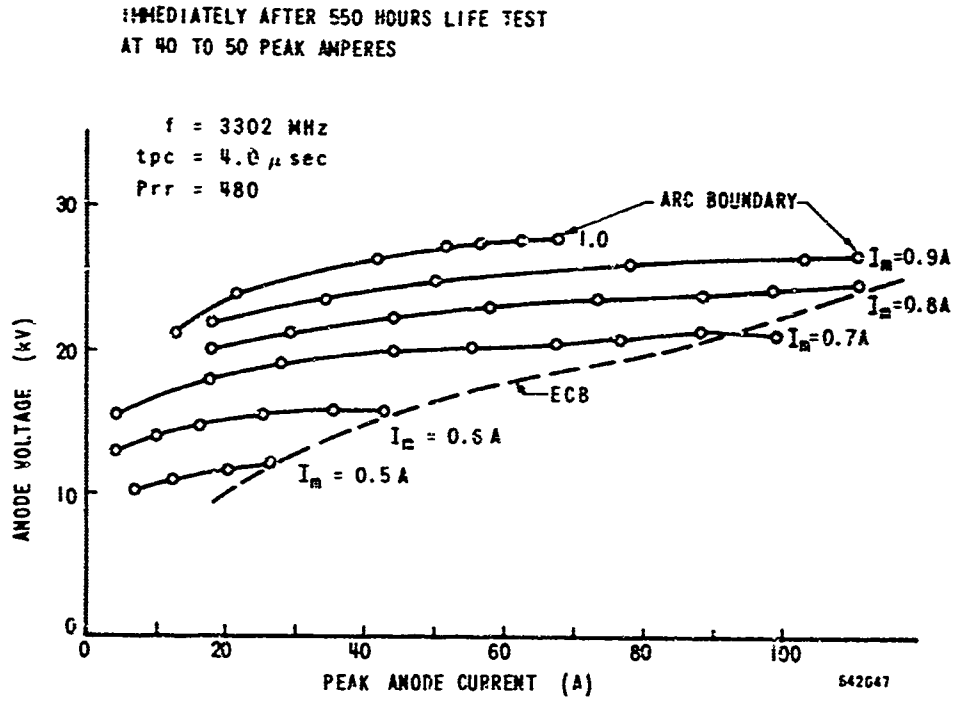

Figure 6-16 QKS1397 No. 8C - Emission Current Boundary - Evaporated Al on Cu Emitter

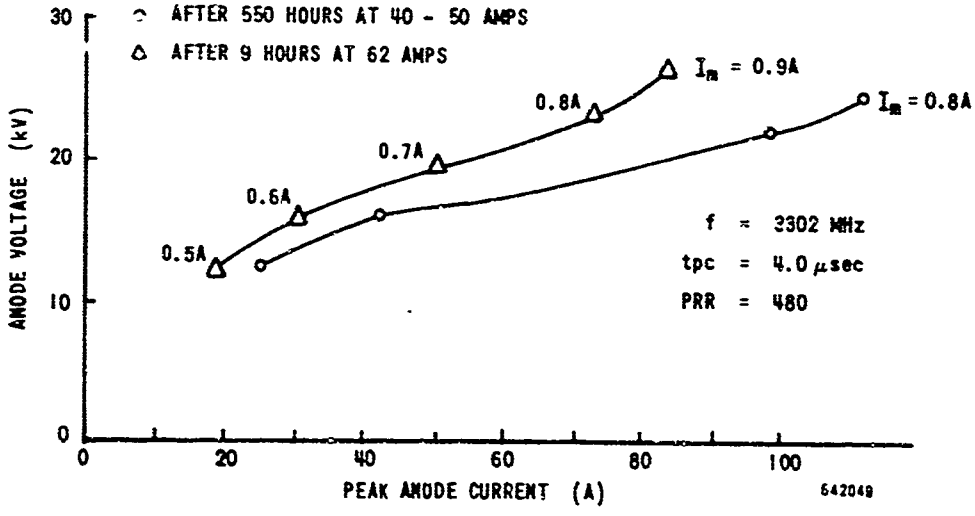

Figure 6-17 QKS1397 No. 8C - ECB as a Function of High Power Testing - Evaporated Al on Cu Emitter

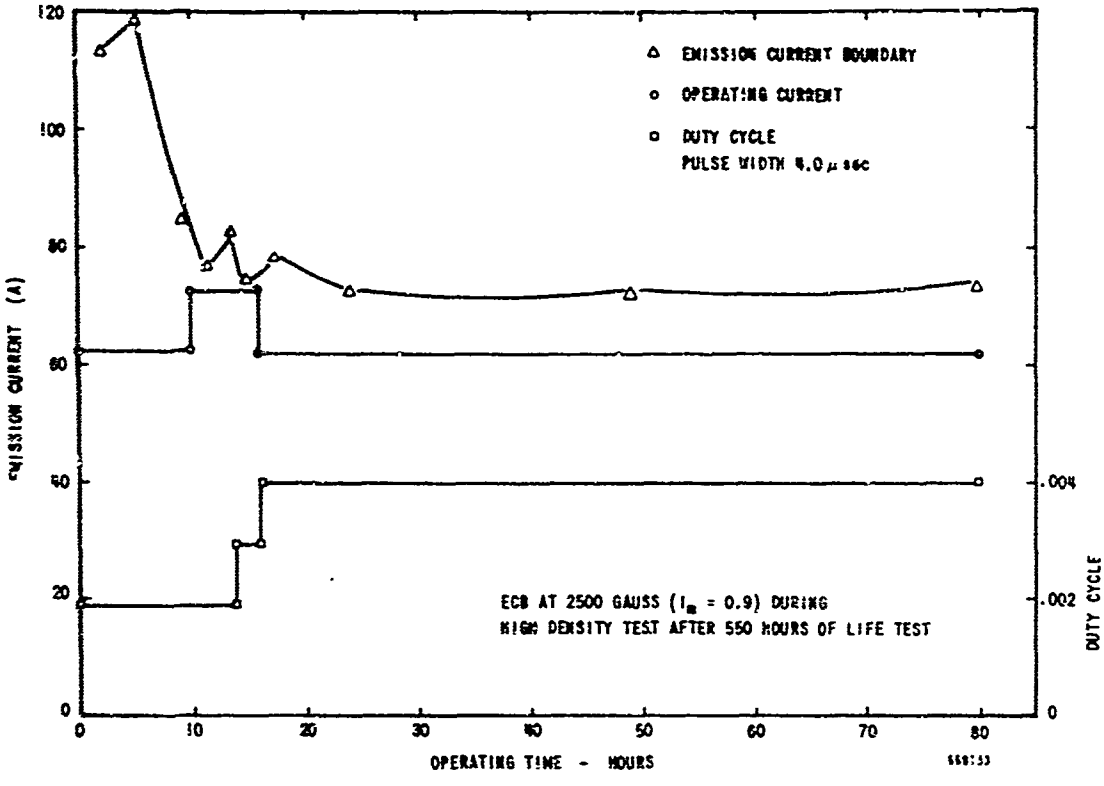

Figure 6-18 QKS1397 No. 8C - Emission Current vs Operating Time - Evaporated Al on Cu Emitter

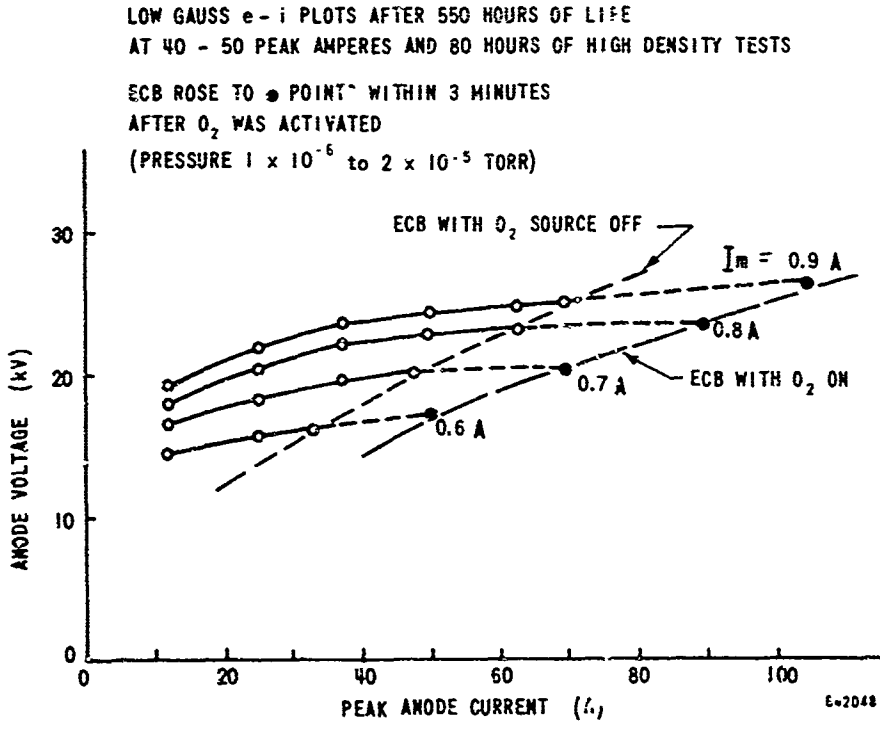

Figure 6-19 QKS1397 No. 8C - Emission Current Boundary - Evaporated Al on Cu Emitter

The oxygen source was reheated after being off for the last 280 hours of test. Immediately the current mode boundary increased 30% and stabilized at this level. (This is also shown in Figure 6-19.) The tube was then removed from test and disassembled.

6.2.3.2 QKS1397 Model No. 8C - cathode inspection. The 0.5 mil aluminum film cathode was in fairly good condition after being operated for over 600 hours. (Figure 6-20). There were several arc marks on it, but less than 5% of the film had been stripped off. However, the beryllium oxide insulator that conducts the cathode heat to the water at anode potential had cracked and it too showed signs of severe arcing. (This is the probable cause of a major portion of the arcing experienced in the last 100 to 200 hours of life at the high voltage levels.)

The initial life test data was taken at 1.25 A gauss current and 32 kV anode voltage and the last 150-hour segment of the 550 hours life test was conducted at 1.0 A gauss current (26 kV anode voltage). The high duty cycle and high peak current tests were conducted at 0.9 A gauss current (26 kV anode voltage). At higher gauss levels the tube would arc excessively because of the broken insulator.

6.2.4 QKS1397 Model No. 8D. The cold cathode test vehicle QKS1397 No. 8C was disassembled and the cathode was completely stripped. The parts were all chemically cleaned and H_2 fired, and the windows were recoated with titanium sub-oxide to prevent multipactor problems. The cathode assembly and oxygen sources were replaced, and a beryllium cathode was installed. The tube was sealed, baked out, etc., with no problems. The O_2 source was degassed up to 60 watts while still on the exhaust station.

The only electromagnet available for this tube would saturate at fairly low gauss levels. Therefore, the gauss levels and ecb data are lower than normal for this cathode. The tube was tested initially without the use of oxygen. Figure 6-21 shows the operating conditions (operating current and duty cycle) and the maximum emission current available at the gauss levels at which the tube was evaluated during life testing. During the first 110 hours, the cathode was evaluated at two gauss levels, 2150 gauss (gauss current 0.85 A) and 2000 gauss (gauss current 0.75 A); during the remainder of the test, only the gauss level of 2150 gauss was used.

The emission current boundary (ecb) dropped by approximately 33% within the first 11 hours of operation (at an operating current of 50A for 6 hours and 31A for 5 hours). The O_2 source was then heated with 60 watts producing a pressure of $\sim 2 \times 10^{-6}$ torr. This did not improve the emission.

After about 40 hours of application of O_2, the O_2 source power was raised to 75 watts. This increased the pressure into the 10^{-5} torr range and immediately activated the cathode. Apparently, the O_2 source was not fully degassed, so that the initial pressure of 10^{-6} torr was not primarily due to O_2, but probably due to desorbed gases.

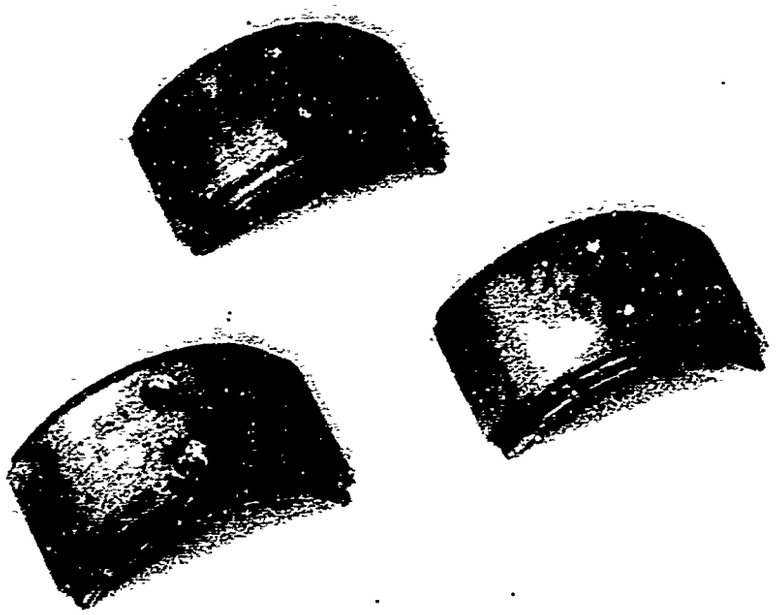

Figure 6-20 Sections of the 0.5 mil Evaporated Al on Cu Cathode of QKS1397 No. 8C after 600 Hours of Life.

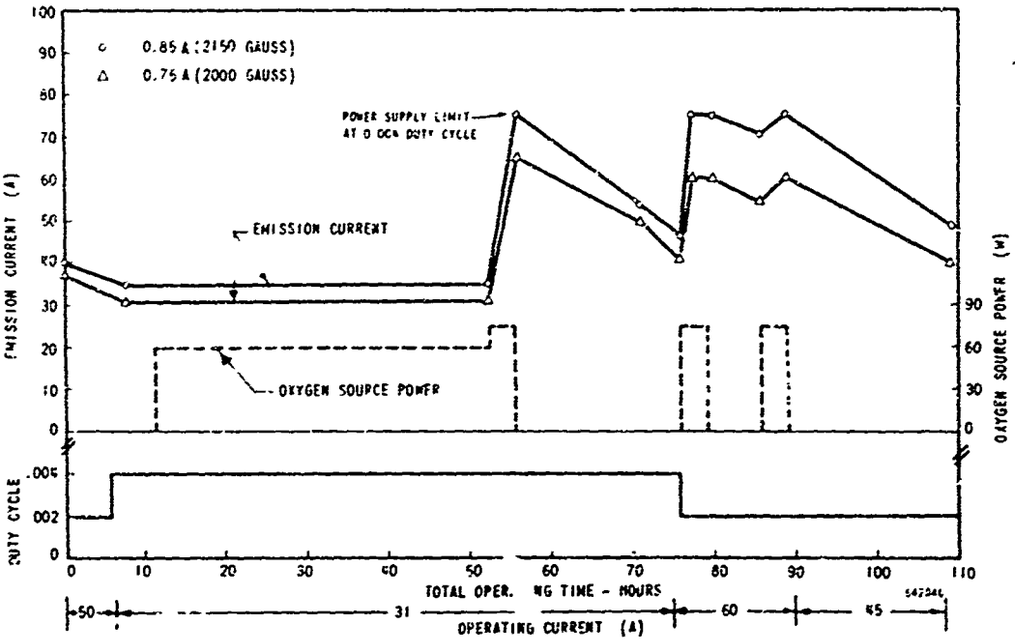

Figure 6-21 (Sheet 1) QKS1397 Serial No. 8D - Life Test Conditions and Emission Current Boundary - Beryllium Cathode

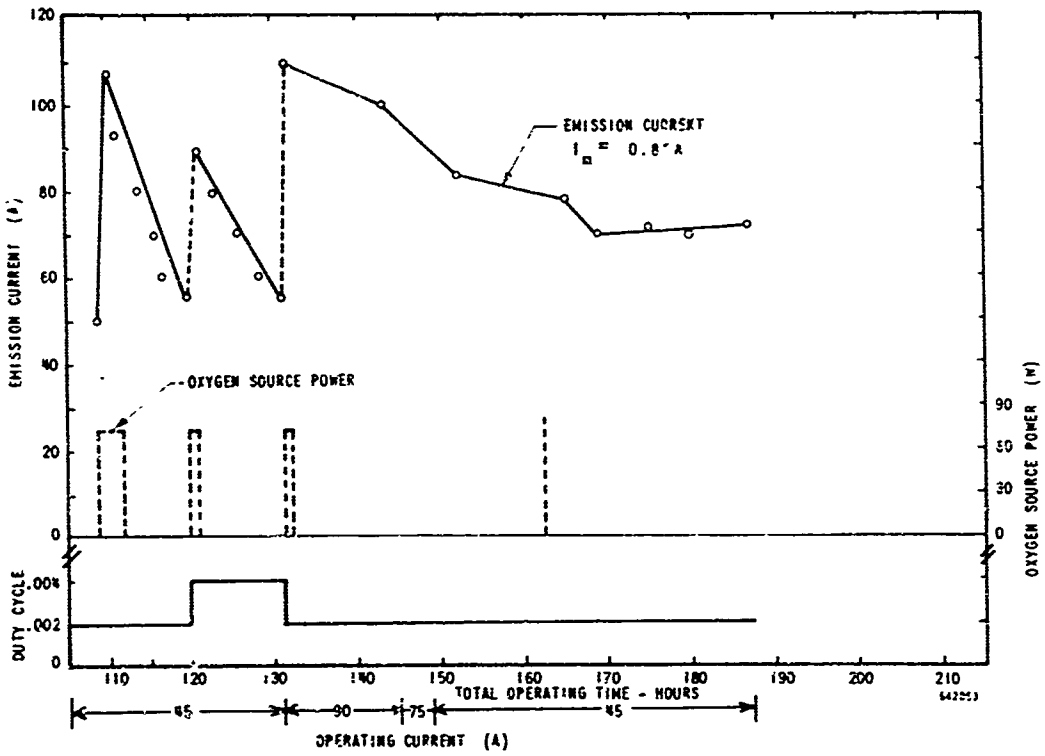

Figure 6-21 (Sheet 2) QKS1397 Serial No. 8D - Life Test Conditions and Emission Current Boundary - Beryllium Cathode

With the O_2 source turned off, ecb dropped by ~28% within 15 hours and by ~40% within 20 hours, i.e., at a rate of about 2% per hour of operation at a .004 duty cycle and an operating peak current of 31A. When the O_2 source was turned on again (heater power 75 watts) ecb improved very rapidly, increasing by 10% in 2 minutes and by 65% in 6 minutes.

Next, the duty cycle was reduced to .002 and the operating peak current was increased to 60A. Operation of the O_2 source was continued for 3 hours, with the result that ecb remained constant during this period (ecb was 75A at 2150 gauss and 60A at 2000 gauss; see Figure 6-21.) Operation of the tube with the O_2 source turned off caused ecb to decay by about 7% within the next 6 hours. If one considers that the duty cycle was reduced to half of its previous value, this is a decay rate comparable to that of ~2% observed after the first O_2 treatment.

The O_2 source was reheated for another 3 hours. The duty cycle and the operating peak current of the tube remained unchanged. This restored ecb to the level observed at the end of the preceding O_2 treatment.

The O_2 source was turned off and the operating peak current was reduced by 25%, i.e., to 45A. The duty cycle (.002) was not changed. The result was that ecb had decreased by ~30% after 22 hours of operation.

The O_2 source was reactivated and operated again for 3 hours without changing the duty cycle and the operating peak current of the tube. The ecb rapidly increased from 50 to 107 A, then leveled off at 95A. This current was 20 A higher than the maximum values achieved after previous O_2 treatments.

With the O_2 source turned off, operation of the tube continued at an operating peak current of 45A and a duty cycle of .002 for 8 hours. The ecb was checked every 15 minutes. At the end of this period, ecb had decreased to 55A.

The duty cycle was then increased to .004, thus doubling the average operating current, and the O_2 source was operated for 1 hour. This increased ecb to 90A. When continuing the operation of the tube without O_2 assistance, ecb was found to have decreased to 60A within 8 hours and to 55A within 10 hours. This decay rate is somewhat lower than that observed after the previous O_2 treatment, even though the duty cycle was twice as high as before.

The duty cycle was next reduced to .002 again, but the operating peak current was doubled (to 90A) so that the average operating current was the same as before. Operating the O_2 source for a period of 1 hour activated the cathode to an ecb of 110 A, i.e., to a value slightly higher than the highest level obtained previously (107A). The decline of ecb during continuation of the operation of the tube with the O_2 source turned off was very slow - only 9% during the first 10 hours (from 110A to 100A). After 14 hours, ecb had decreased to 98A. Plots of ecb made at this point are shown in Figure 6-22. To reduce the danger of arcing, the operating peak current was decreased to 75A.

It was then decided to test the tube again at the low operating current level of 45A, where the decay rate of ecb had been previously quite rapid. The ecb now dropped from 90A to 82A during the next 3 hours, but then decreased more slowly. After the operation of the tube had been continued for an additional 10 hours, ecb was still 78A.

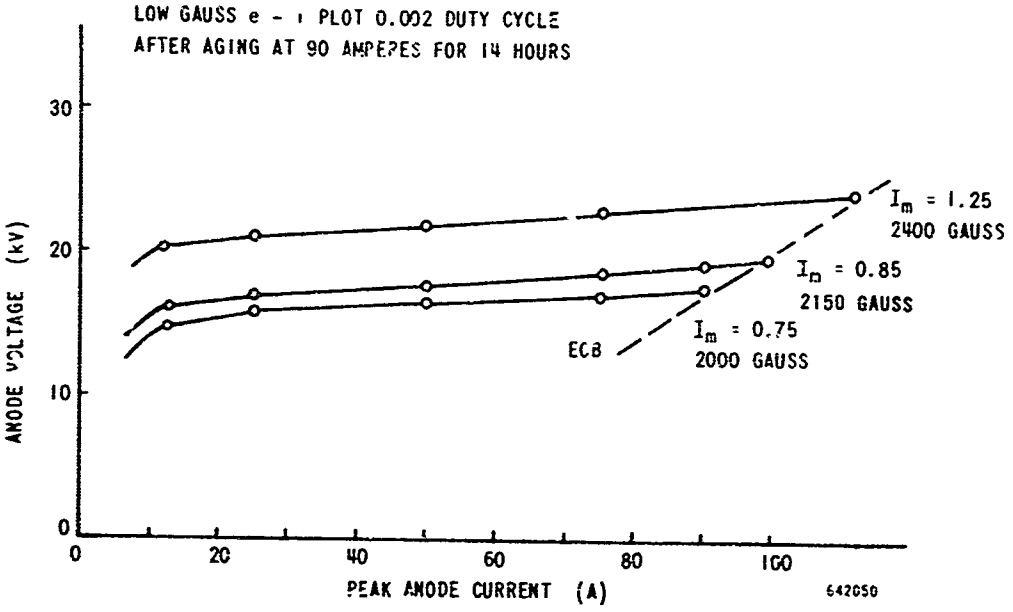

Figure 6-22. QKS1397 Serial No. 8D, Beryllium Cathode

With the tube cold and the rf drive off, the O_2 source was reheated. The O_2 pressure was held at 10^{-5} and 10^{-4} torr scales for 10 minutes and then pumped out for one hour before the tube was started. This was done to check cathode activation by O_2 with the rf off. When the tube was restarted there was no extra cathode activation or emission enhancement as a result of admitting O_2 with the rf power off.

The run was continued for another 25 hours with ecb stabilizing at 70A.

At the end of the program the tube had accumulated 187 hours of life test and was still in good operating condition.

6.3 Test of beryllium oxide emitter for 1000 hours in QKS1267. Life test information was accumulated on a cold beryllium oxide cathode operating in a special model of the QKS1367 Amplitron. While not part of this program, the results are reported here because of their direct relations to the goals of the Cold Cathode Study. The QKS1267 was built as a means of avoiding a difficult heater problem in the normal thermionic cathode arising from an application requiring a tube to operate at both a very low and a very high duty cycle.

In place of the regular emitter, a beryllium emitter was installed in the QKS1267; an oxygen-dispenser was also incorporated. The tube was processed and tested normally. It was established that the oxygen dispenser required about 5.0 V and 7.0 A to maintain stable cathode emi sion for more than short periods of operation in the customer's transmitter. Operation at 3.5 A peak, which is the normal current for the tube's rated 60 kW (peak) output, was maintained uneventfully for 274 hours. It then became necessary to raise the applied dispenser voltage to 5.5 volts to counteract a decreasing emission limit - only 2.8 A peak over part of the specified 2.9 - 3.1 GHz band. This change rapidly increased the emission to normal, and the test was continued for a total of 1000 hours without any trouble attributed by the customer to the tube.

The 1000-hour test was operated 16 hours per day on 5 and 6 day work weeks, with the frequency changed 10 MHz every hour and power measurement made every 4 hours. The operating point was the following:

e_b	=	27 kV (cathode pulsed)
i_b	=	3.5 A peak
I_b	=	95 mA
t_p	=	34 microseconds
PRR	=	800
Du	=	.027
$P_{o\ peak}$	=	60 kW
$P_{o\ avg}$	=	1.620 kW
$P_{d\ peak}$	=	1.6 kW

No performance deterioration was observed during or after this test. The cold cathode emitter stress levels were as follows:

Average Current Density:	15.2 mA/cm^2
Peak Current Density:	0.56 A/cm^2
Average Power Dissipation Density:	30 W/cm^2

The average current and power dissipation levels in the QKS1267 are close to those required in the QKS1397 forward-wave CFA Cold Cathode Study test vehicle at the 5000 watt average power output level (22 mA/cm^2 and 37 W/cm^2, respectively). The peak current density of the QKS1397 (4.5 A/cm^2) and other high peak power CFA's is greater than that in the QKS1267. However, both peak and average back bombardment current densities are probably significant to cold emitter life. It is true that the effective secondary yield required of the QKS1267 emitter is low (δ_{eff} = 1.4) compared to that required of the QKS1397 emitter (δ_{eff} = 3.4 for 1 MW, 2.2 for 0.5 MW) because of the low peak operating current. For another reason, however, the QKS1267 requires very good secondary emission not available from a platinum cathode. This is the low unity -δ crossover energy required to provide reliable jitter-free rf starting at the 1.6 kW peak rf drive level specified for the tube. No trouble was experienced with rf starting throughout the 1000-hour QKS1267 operating test.

The QKS1267 1000-hour test is believed to be significant in establishing that oxygen-stabilized cold cathode emission can be achieved from an oxide-film secondary emitter cathode in a moderately high average power CFA environment.

6.4 The S-band QKS1194. The QKS1194 illustrated in Figure 6-23 is an S-band backward-wave CFA employing a double-strapped vane Amplitron slow-wave structure. The tube provides 1 Mw peak, 15 kW average power output over the 2800 - 3200 MHz range. It features interchangeable cathode heater and coolant assemblies for the initial activation and operation of its thoria-tungsten secondary emitter. This feature made it readily adaptable as a vehicle for evaluating that class of cold secondary emitters which must be thermally activated before tube aging and processing. See Figure 6-24 for the internal hot/cold cathode structure. It operates cathode pulsed at 50 kV and 33 peak with a mean peak current density of 1.5 A/cm^2. The tube dimensions are:

Anode Diameter	1.310 in.
Anode Height	1.350 in.
Cathode Diameter	.815 in.
No. of Vanes	17
Drift Space	1 vane width

The QKS1194 was sealed in with a barium calcium aluminate impregnated matrix cathode. The impregnated cathode is a good primary emitter when operated in the 1000 to 1200°C region. Normally it operates with a thin film of barium and probably calcium (less than a monolayer thick) on oxygen on tungsten. At the operating temperature the alkaline earth aluminate is reduced slowly by a reaction with the tungsten, forming free barium and calcium atoms to replace those lost by thermal evaporation and sputtering.

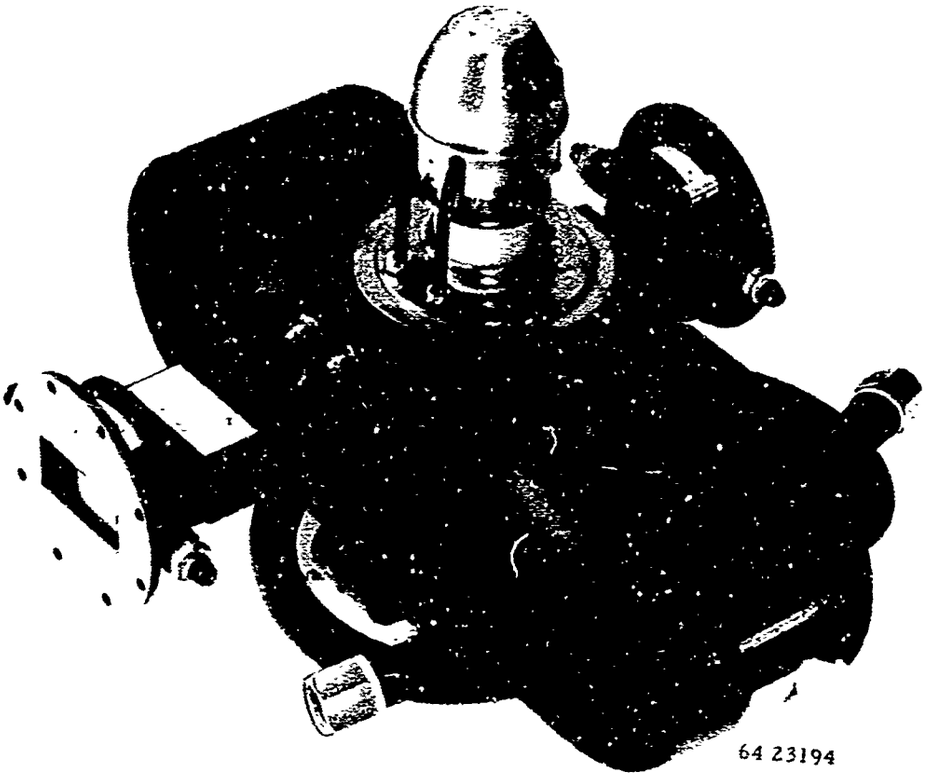

Figure 6-23 QKS1194 - S-band Backward-wave CFA

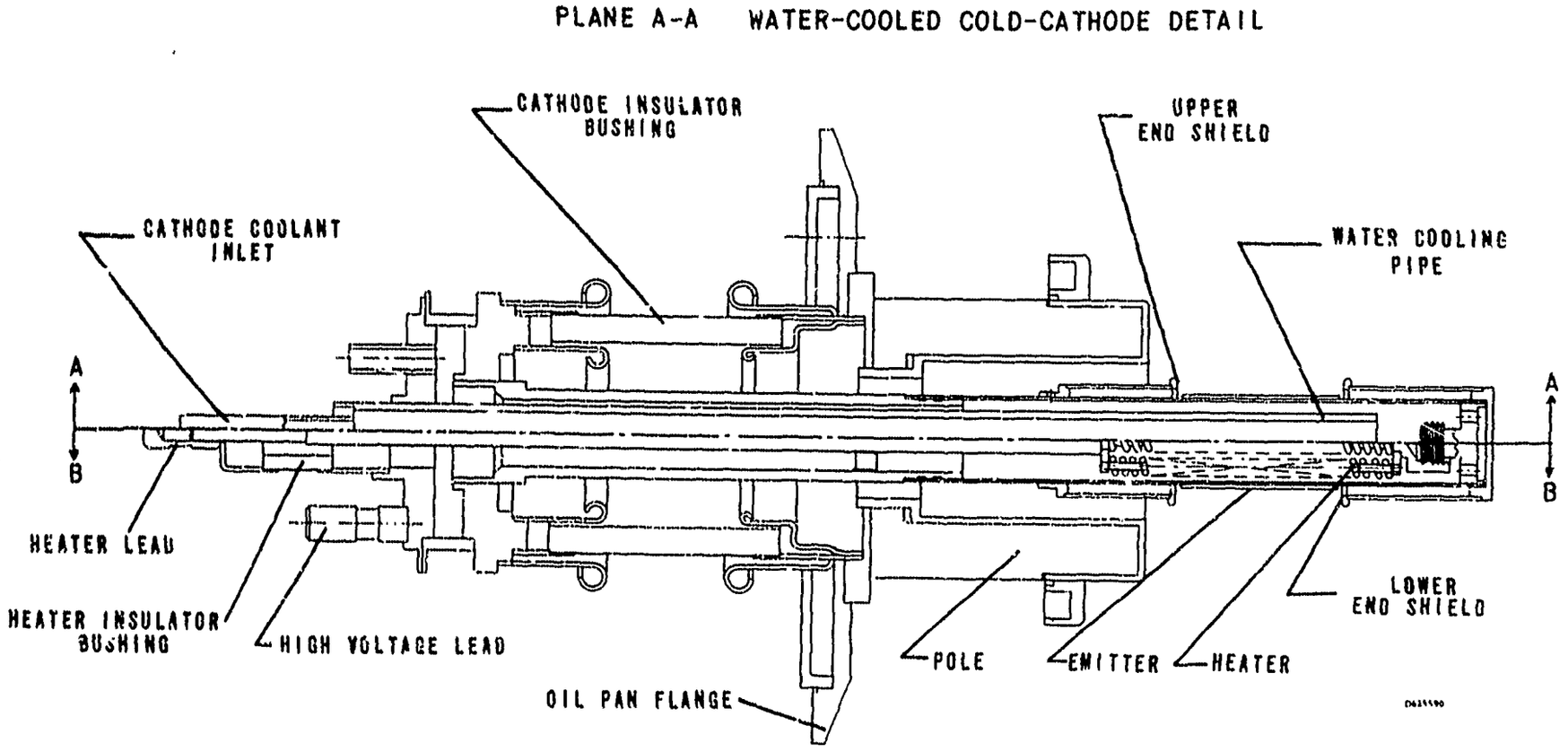

Figure 6-24 QKS1194 Hot/Cold Cathode - Pole Assembly

The secondary electron emission ratio for the impregnated cathode as determined in Phase A of this program is approximately 1.8 before the cathode is activated and rises to 3.5 to 4 upon thermal activation. During life test as a thermionic emitter the δ normally drops to 2.0 to 2.5

Although the QKS1194 had a means for thermally activating the impregnated cathode it was felt desirable to start and run the tube without the use of thermal activation. The information would be useful for tube types that do not have a heatable/coolable cathode structure.

The tube was sealed-in, baked out, and set up as the final amplifier in a S-band chain test setup. The tube was aged with rf drive power only at 20 kW peak at .02 duty cycle. This causes some bombardment of the cathode and some gas evolution. After rf drive processing, the tube started up very easily - without heating the cathode.

Several low gauss e vs i plots were taken during the initial few hours of operation. An initial plot Figure 6-25 indicated a moding condition. Later, low gauss e vs i plots showed single-mode operation (Figure 6-26 and 6-27. The tube was put on life test under the following conditions:

e_b	(Anode voltage-cathode pulsed)	46 kV
I_b	(Average anode current)	600 mA
i_b	(Peak anode current)	33.3 A
t_p	(Pulse duration)	80 μ sec
Du	(Duty factor)	.018
P_o	(Average output power)	20.0 kW
P_o	(Peak output power)	1.1 MW
Gain		13 dB
Peak Cathode Current Density		1.5 A/cm^2
Average-Cathode Current Density		27.0 mA/cm^2

The tube ran very well for 356 hours as shown in Figure 6-28. Operation was smooth and trouble free. Low-gauss emission current boundary data indicated no deterioration of the emission (Figure 6-29).

After 356 hours of life test, the tube started gassing up and arcing. An analysis showed that a leak had developed in the cathode water jacket at or near the copper-to-molybdenum joint. The leak was repaired with Permafil.

The corrosion of molybdenum by water has been experienced recently in other types. A nickel plating on the inside of the molybdenum would have prevented this problem.

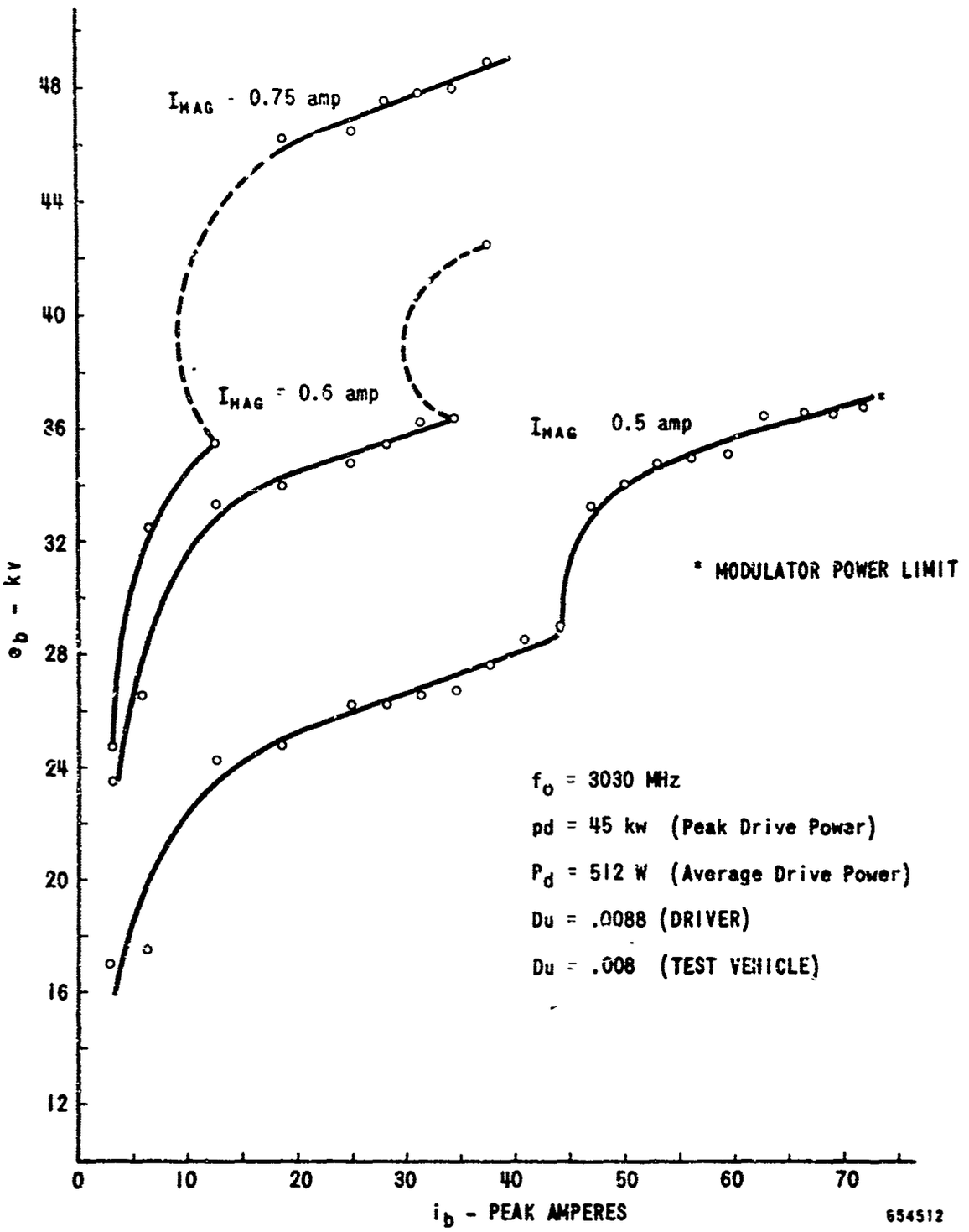

Figure 6-25 QKS1194, (Impregnated Tungsten Emitter)
Low Gauss e_b - i_b Initial Data

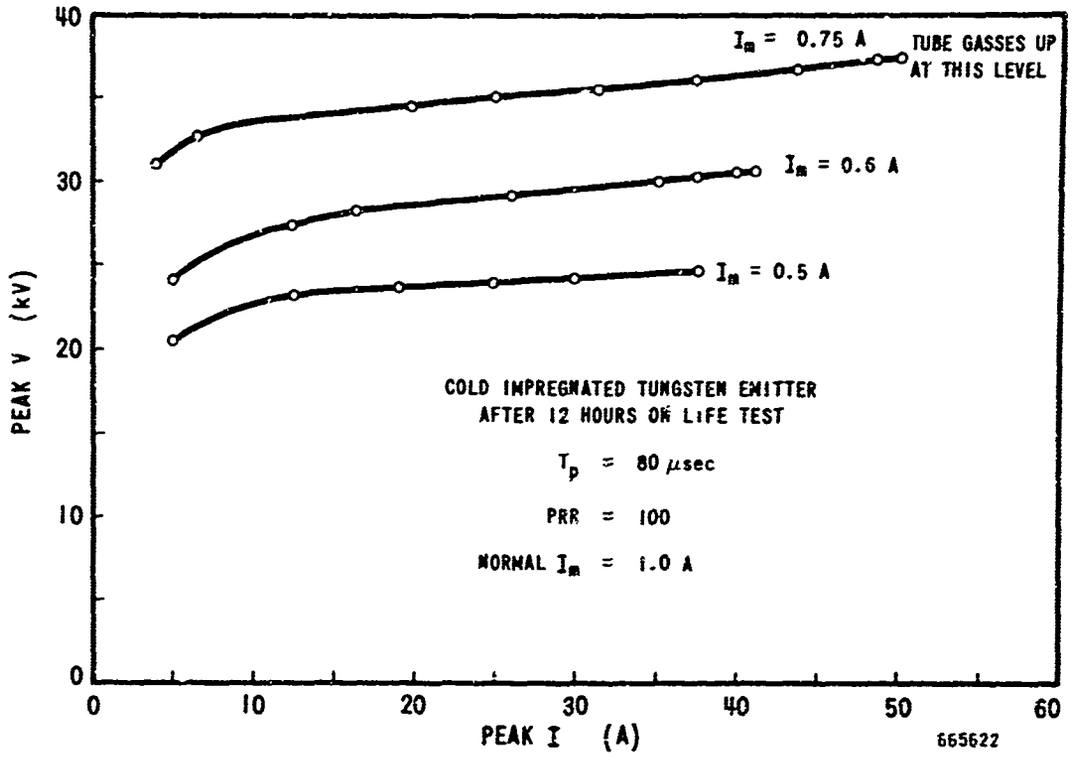

Figure 6-26 QKS1194 - Low Gauss e-i Plots After 12 Hours on Life Test

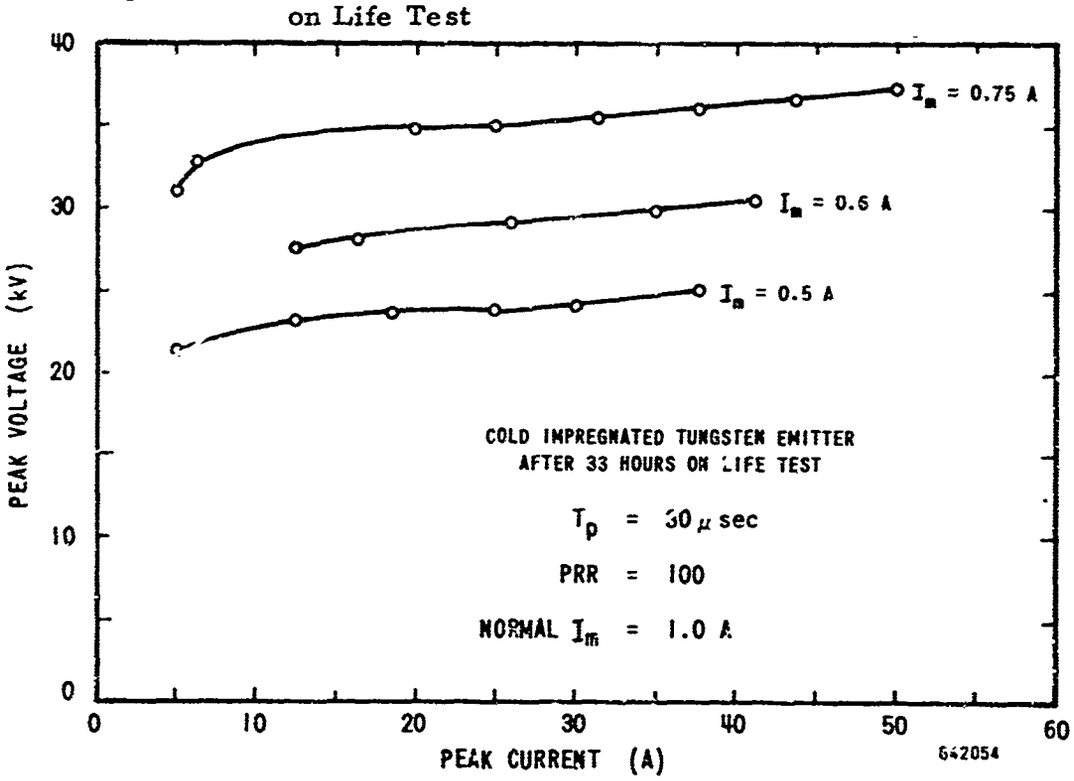

Figure 6-27 QKS1194 - Low Gauss e-i Plots After 33 Hours Life Test

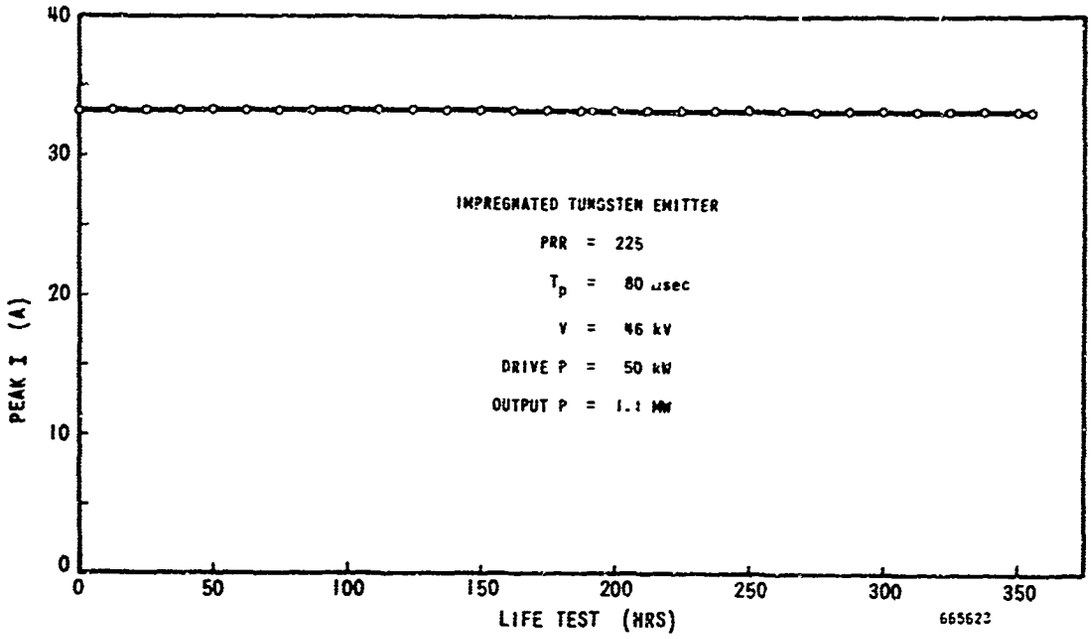

Figure 6-28 QKS1194, - Cold Cathode Life Test

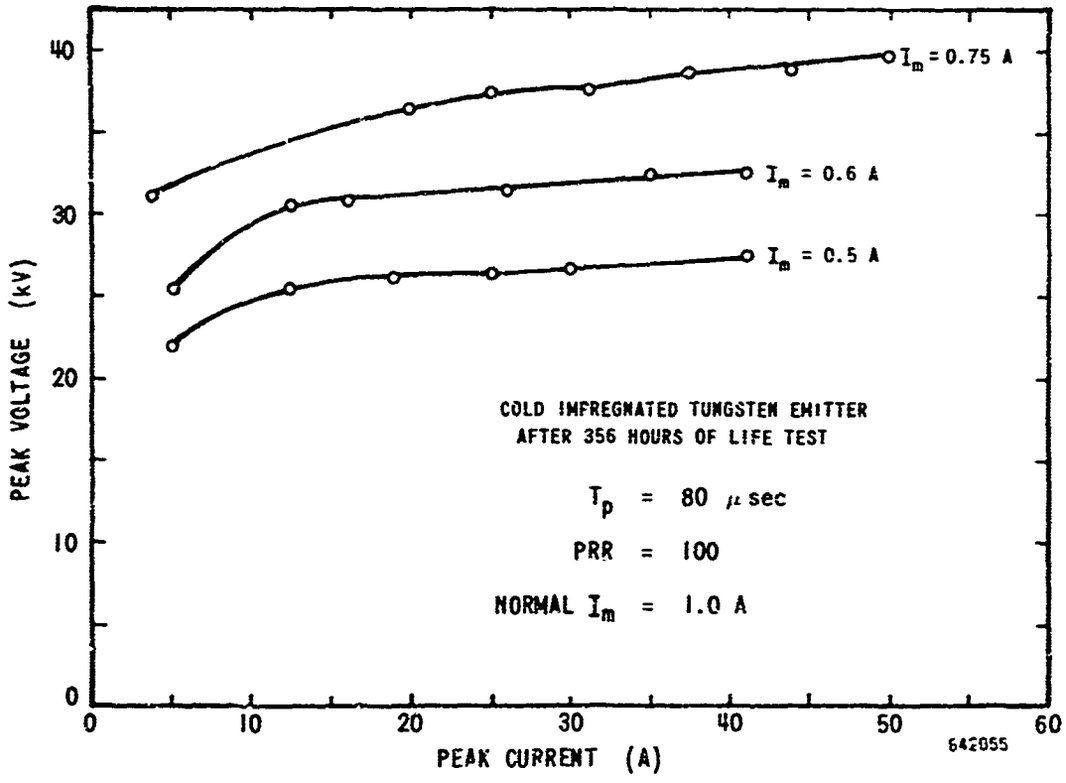

Figure 6-29 QKS1194, - Low Gauss e-i Plots

The tube was off the life test station for 3 months. The vacuum was monitored for the first month and appeared to be holding up, but when the tube was put back in test it had lost its vacuum.

6.4.1 Scrap analysis. After the impregnated cathode was removed from the QKS1194, it was evident that water had corroded the molybdenum to copper joint and had leaked in. Barium calcium aluminate is very hygroscopic. Thus the cathode had absorbed a large quantity of water, had swollen up and cracked, and a white oxide layer had formed over its surface.

6.4.2 Summary of principal results.

a. Aluminum and beryllium:

1. The naturally oxidized surface of solid aluminum or beryllium is in the order of 25 Å thick. These surfaces show a high δ of around 3 to 5, but do not stand up under electron and/or ion bombardment in CFA operation.

2. The dispensing of a low partial pressure of oxygen within the tube, about 10^{-7} to 10^{-6} torr, is effective in restoring Al and Be cathode emission to values near the original levels; emission recovery usually takes place more rapidly when the tube is kept in operation during the administration of oxygen.

3. The emission required for a given peak and average tube power output level can be maintained for prolonged periods of time (over 1000 hours) from an Al or Be cathode with oxygen dispenser heater power adjusted to provide sufficient oxygen to counteract the emission decay mechanism, at least up to the average current levels explored (15 mA/cm^2).

4. The need for O_2 decreases during life.

5. Working limits for oxygen-assisted cathodes have not yet been established, but the observed need for more O_2 pressure at higher duty factors in a given design suggests that the upper limit depends upon the average current density required and the maximum gas pressure that can be tolerated before normal tube amplification is affected or interelectrode arcing is caused.

b. Impregnated tungsten emitter:

1. The impregnated tungsten emitter (impregnant: barium-calcium aluminate) was operated without oxygen at a moderately high average current density (27 mA/cm^2)

for 356 hours without any indication of emission decay. Any emission deterioration mechanism which may exist for this emitter in the QKS1194 must therefore proceed at a very slow rate.

c. Platinum emitter:

The plain platinum emitter evaluated in the QKS1319 showed a very low emission current boundary as expected for a low voltage tube. Other data on an S-band platinum cathode tube at Raytheon [1] showed trouble free CW operation up to 400 KW, where the operating current density was over 600 mA/cm^2 and the cathode bombardment power density was 600 watts/cm^2.

7.0 DISCUSSION OF RESULTS

7.1 Emission current boundaries. The secondary-emission-limited emission current boundary of a CFA employing a cold cathode depends on the effective secondary emission ratio (δ_{eff}) of the cathode surface. The energies and angles of the back-bombarding electrons are unknown, but a means for estimating has been devised. The effective δ in the CFA therefore can be estimated.

In the absence of a thermionic contribution, the available anode current may be expressed as

$$I_a = (\delta_{eff}-1) \quad I_{bb} \tag{2}$$

where I_a is the available anode current

δ_{eff} is the effective δ in CFA taking account of energy and angle spectrum of back-bombarding electrons.

I_{bb} is the back-bombarding electron current.

The dependence of I_a on the anode voltage will depend on the assumption or approximations made for I_{bb}. If we assume that I_{bb} is proportional to I_o, the characteristic current of the crossed-field device, then we obtain the result that I_a is proportional to $V_a^{3/2}$. Thus, the perveance represented by the emission current boundary (ecb) would be proportional to $(\delta_{eff}-1)$. However, it is found that a better fit to experimental ecb data of our own and others is obtained by a linear relation of the form

$$I_a = b\,(\delta_{eff}-1)\,(V_a - V_t)$$

V_t is a threshold voltage and reflects the fact that δ decreases to below 1.0 at the "first crossover" voltage. Figure 7-1 shows emission current boundaries in the QKS1319 CFA test vehicle for several cold cathodes, namely platinum, aluminum, beryllium, and a 1000 Å film of 30% Mo-70% Al_2O_3 on a Mo substrate. If we assume that δ_{eff} for P_t is 1.8, we may compute δ_{eff} for other cathodes in the same CFA by noting that the slope, dI_a/dV_a, of the ecb is proportional to $(\delta_{eff}-1)$. The following values of δ_{eff} are thus obtained:

Cold Cathode Material	δ_{eff}
Al	5.8
Be	4.6
30%Mo-70% Al_2O_3 film	2.2

Secondary emission measurements of an aluminum or beryllium sample, having on its surface a thin oxide film of 25 to 50 Å thick from exposure to 20°C air, yield values of δ_{max} of 2.0 to 2.5. These values are much lower than δ_{eff} in a CFA. Optimally oxidized aluminum or beryllium samples, however, do have δ_{max} values of 4 to 6. Possible explanations of the anomalously high δ_{eff} of aluminum or beryllium cathodes in a CFA are:

a. Special effects of the thin dielectric film at the cathode surface on the back-bombardment current.

b. Enhancement of δ due to tube operation, involving a change in the nature of the oxide film. This has been shown to happen after long time exposure to oxygen during tube operation.

c. Greater preponderance of grazing incidence for back-bombarding electrons in the case of the oxide film.

7.2 Aluminum. QKS1397 No. 8A and 8B showed that a solid aluminum cathode with its natural oxide layer will have good secondary emission initially, but that its lifetime under the condition imposed by the CFA operation is in the order of a few hours.

Tests showed that the electron bombardment will dissociate the thin oxide film and allow the oxygen to escape. If a steady source of oxygen is available to replace that lost by electron bombardment dissociation, the secondary emission level should remain high.

Tube No. 8A and 8B showed that if the oxygen pressure as measured by the attached Vac-Ion pump was approximately 1×10^{-7} torr, a peak emission level of 70 A (4 A/cm^2) could be maintained and when the oxygen is removed, the ecb gradually decreased.

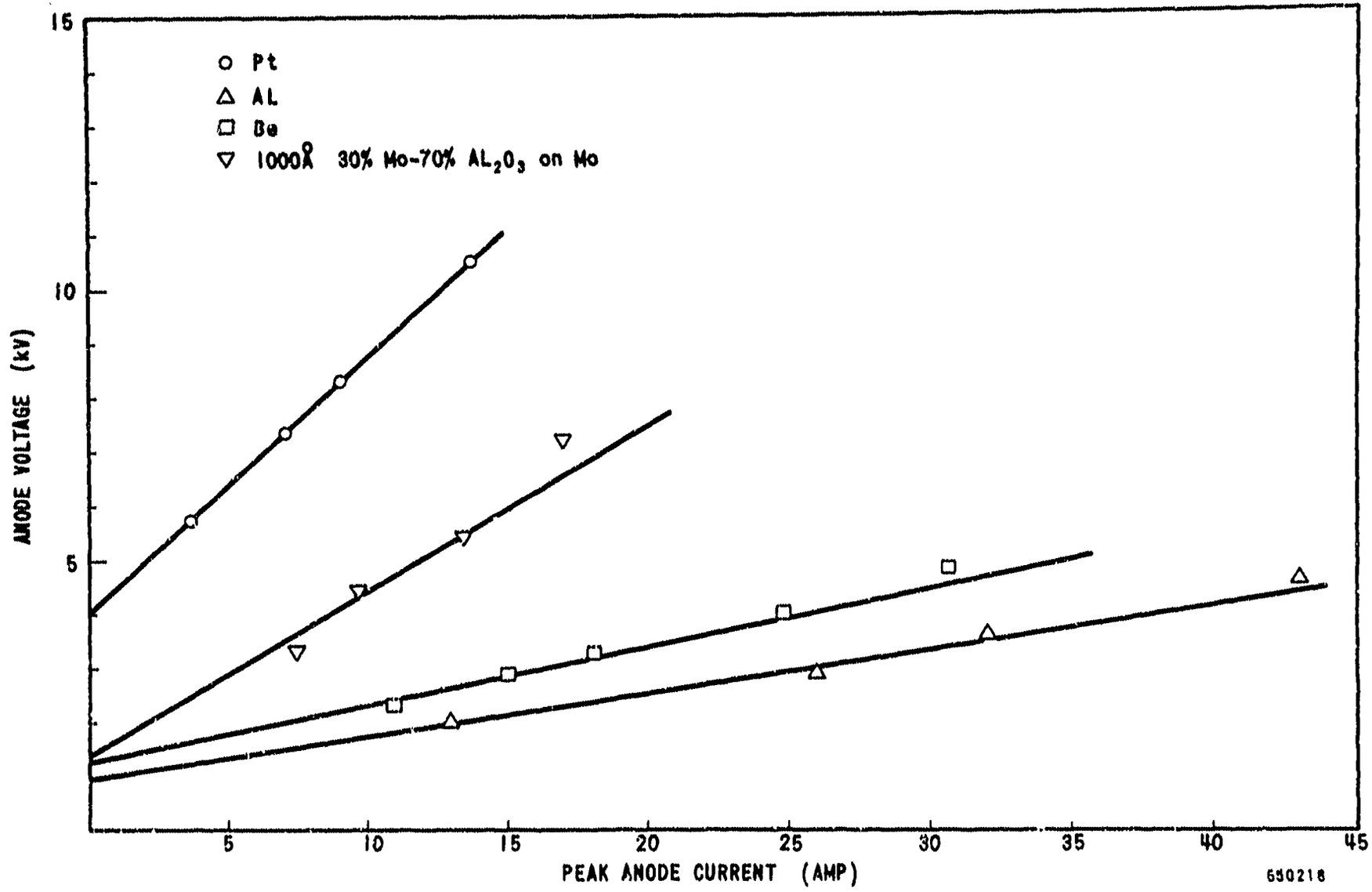

Figure 7-1. Emission Current Boundaries in QKS1319 CFA Test Vehicles for Various Cathode Materials

QKS1397 No. 8C, which had an evaporated layer of Al on a copper base cathode, showed similar results. This cathode required an O_2 pressure high in the 10^{-6} torr range to maintain good emission initially.

After 240 hours of testing, this tube could operate at 50 A peak, even without the use of O_2. A possible explanation is that the cathode became saturated with O_2 as a consequence of the bombardment by O_2 ions with energies up to 30 kev. These high-energy O_2 ions may be implanted several atomic distances deep into the cathode. Since the O_2 is not merely adsorbed at the surface, but is actually buried, it cannot be released easily. Thus the thin Al_2O_3 film on the aluminum surface will undergo a gradual transition to O_2 near the surface of the cathode. The low O_2 pressure of the residual air in the tube may then be sufficient to maintain this configuration.

The ecb tests performed during the special tests of this tube after the completion of the 550-hours of life testing caused periods of arcing which were detrimental to the cathode and resulted in a decrease of the ecb from 110 A to around 75 A. Nevertheless, this ecb level was maintained (without the assistance of O_2) even though the operating peak current was increased to 62 A and the duty cycle was doubled. Furthermore, the addition of O_2 at the end of the special tests increased the ecb, indicating that reactivation of the cathode was possible.

In summary, the results show that a properly processed aluminum cathode will produce a good, stable emission. Optimum processing probably means subjecting the cathode to high energy O_2 ion bombardment and then providing a low partial pressure of O_2 in the tube during life to maintain the cathode at a state of equilibrium.

7.3 Mo-doped Al_2O_3 film. The 1000 Å Mo-doped Al_2O_3 film (30% Mo - 70% Al_2O_3), TV No. 1C and 1D, acted very similarly to a plain aluminum cathode. It had good secondary emission initially, but after 23.5 hours of operation at .002 duty cycle it was nearly depleted.

After the cathode was exposed to air again, the emission recovered, indicating that the thin surface oxide film was the most important and that the remainder of the 1000 Å layer was immaterial.

Since the Mo-doped Al_2O_3 film had no better performance than plain aluminum, there is no apparent justification for using it.

7.4 Beryllium. The behavior of the beryllium cold cathode was very similar to that of the aluminum cathode. Both metals form a very tenacious oxide film in the order of 25 Å thick upon exposures to air. This film is adequate to give good emission for a few hours of life only at low duty cycle.

After 37 hours of operation of the beryllium cathode in QKS1319 No. 2, at .01 duty cycle the cathode emission was depleted (Figure 6-9). Exposing the cathode to air again temporarily restored the initial emission.

With the addition of oxygen, beryllium makes a very good secondary emitter. The life test on QKS1397 No. 8D was carried out with the O_2 source off most of the time after the cathode had become activated. Extra oxygen treatments were used only periodically to reactivate the emission.

The most significant aspect of this life test is the emission decay rate during the last 80 hours of life test. At 45 peak A, .002 duty cycle (5 mA/cm^2 average), the decay rate was rapid - about 50% in 8 hours (Figure 6-21). After rejuvenation by oxygen for one hour at the same peak current, but twice the duty cycle, the decay rate had decreased when the tube was subsequently operated under the same conditions, but in the absence of O_2. Then the peak current was doubled to 90 A at .002 duty cycle and O_2 was admitted for one hour. Upon removal of the O_2, the decay rate was much lower.

One might erroneously assume that the higher peak and average current is less harmful to the emission level, but this is not the case. The peak current was later reduced to 45 A at .002 duty cycle and the decay rate was still very low. This test shows that the nature of the cathode surface has constantly changed during life, such that electron bombardment dissociation was suppressed. The mechanisms involved may be assumed to be the same as those suggested in the discussion of the aluminum cathode of Test Vehicle QKS1397 No. 8C.

7.5 Impregnated tungsten cathode. The impregnated tungsten emitter in the QKS1194 worked very well. The fact that it did not require a thermal outgassing and activation cycle was very surprising. At an average current density of 27 mA/cm^2, and a moderate duty cycle of .018, the tube ran very well for over 350 hours. The emission current boundary stayed practically constant after the initial few hours of processing.

This cathode consists of a tungsten matrix with the pores filled with a molten mixture of barium-calcium-aluminate compounds. During activation as a thermionic emitter, the barium-calcium-aluminate is reduced very slowly by a reaction with the tungsten. The tungsten surface becomes covered with barium and calcium on oxygen about one atomic layer thick. Probably, the aluminate becomes rich in metallic ions also, which should increase its conductivity and the emission level.

The secondary emission ratio of an impregnated cathode is usually low initially, approximately 1.8, then rising to 3.5 to 4.0 with thermal activation, and later dropping to 2.0 to 2.5. In the CFA, the electron bombardment apparently caused sufficient activation without heating to produce very good secondary emission. After 12 hours of test and up through the 356 hours, the low gauss e vs i plots were very stable (Figures 6-26, 6-27, and 6-29). At 25 kV over 35 A were available. The tube operating level for 1.1 MW output was only 33 A at 46 kV.

The impregnated cathode in the QKS1194 may be compared with the tungsten-thoria cermet and platinum cathodes that were used in the same tube type on other programs. At the normal operating gauss level, the platinum cathode had an emission current boundary of 23 A at 46 kV. The tungsten-thoria cermet had an ecb of around 60 A, which is according to general experience about the same as that for the impregnated cathode.

The secondary emission ratio of platinum is 1.3. Although more ecb data would be desirable at lower gauss levels for the platinum emitter, one can use the 1.8 figure to estimate the δ of the impregnated cathode during life as being around 2.2. This is the same value found in the secondary emission test vehicle in Phase A for the impregnated cathodes.

The initial high activation seen with the matrix cathode indicated a δ of over 3.5. At this time, the tube was moding, which makes the data difficult to interpret, but the δ value of 3.5 compares with the phase A secondary emission value of 3.5 to 4 found upon initial activation of the impregnated cathode. By twelve hours the emission level and tube operation had stabilized at 2.2 and remained so throughout life test.

The initial high emission level for the impregnated cathode without thermal activation was not expected. Also, the maintenance of the high secondary emission level for over 350 hours with the cathode cold was still more surprising. It is assumed that the primary mode for emission enhancement is the dipole layer on the surface. The dipole layer (B_a-O-W) is retained by much higher energy levels than those associated with the binding energy of an oxide. Also, the dipole layer should be fairly transparent to the high energy bombarding electrons.

Even though only one CFA life test was performed on the impregnated cathode, its excellent operation warrants further testing.

In the use of the cathode as a thermionic emitter even a very small trace of oxygen will cause severe poisoning.[40] A trace of oxygen will destroy the electro positive dipole layer needed to lower the work function of the cathode surface. The QKS1194 test vehicle incorporated an oxygen source, but it was not used. A high secondary emission ratio is partly dependent upon an electropositive layer also, (but not nearly as much as a thermionic emitter), so that

the use of oxygen with this type of emitter might decrease its secondary emission ratio. However, the contribution of the Ba-Ca-aluminate impregnant to δ might be enhanced by O_2.

7.6 Platinum. Smooth platinum has a δ of 1.8 and a low voltage unity crossover of approximately 350 volts. This δ was not high enough for the QKS1319 with its relatively low operating voltage (10 kV). However, for higher voltage tubes where the peak power requirements may be satisfied by an emitter with a δ of 1.8, platinum is the ideal choice.

Platinum is a noble metal. It will not form stable oxide films at the surface. It can become contaminated only by physically covering it with a foreign solid material - such as sputtered copper from the anode. Tests on some very high power CFA's at Raytheon have shown that a platinum cathode can be poisoned by tube arcing when the platinum is physically covered by copper sputtered from the anode. However, if the cause of the arcing is removed, subsequent tube operation at a reduced power level will cause the copper layer to be eroded and full power can be restored.

7.7 Guideline for choice of CFA cold cathode materials. Guidelines for the choice of cold cathode emitter materials for crossed-field tube applications are suggested by the available CFA data. These guidelines are summarized below.

δ Required	Average Emission Current Density Required	Recommended Emitter Type
> 2.4	< 15 mA/cm^2	Oxygen-assisted Al or Be impreg. W
1.9 - 2.5	< 30 mA/cm^2	
$\leq$ 1.9	----------	Pt

The tentative limits suggested above are shown relative to average emission current density in the crossed-field amplifier. Normally this current density is probably (within a factor of two) equal to the back-bombardment electron flux experienced by the emitter surface. Actually, it is these electrons and their energy level which probably determine the rate of emission deterioration.

The available CFA cathode current is directly dependent on the Slater interaction space parameter "I_o" and the quantity (δ - 1); where δ is the "effective" secondary electron yield required to achieve the operating current

in a given CFA design when the available rf drive level and tube operating voltage are moderately high. Rf drive levels of less than 1 - 2 kW peak and operating voltages less than about 10 kV may require use of a more active (high δ) emitter than would be expected.

No average current density limitation is anticipated for the Pt emitter. Such a limitation may exist for the oxygen-assisted type of emitter if the oxygen pressure required is detrimental to tube performance. However, that level was not reached during testing up to 15 mA/cm^2. Further testing may establish such a limit, while further developments may raise or eliminate it.

As a conclusion drawn from the above tests, we have demonstrated with several cold cathode CFA's a life performance of up to 1000 hours with no indication of a life limitation. Oxygen stabilization can indeed achieve very long life. Oxygen source life of 10,000 hours in a high stress level CFA (such as the QKS1397) is believed to be achievable. Both platinum and impregnated-tungsten cold cathodes can be employed in applications and tube designs requiring δ's of up to 1.8 to 2.5, but higher δ requirements call for oxide-film cold cathodes.

BIBLIOGRAPHY

1. QKS1224 Super Power CW Amplitron, USAF Contract No. AF30(602)-3449 Semi-annual Report Dec. 1965.

2. J. W. McNall, H. L. Steele Jr., and C. L. Shackelford - "Secondary Emission Cathodes for Magnetrons", Research Report BL-R-929-7C-1, Westinghouse Electric Corp., Bloomfield N. J. (Nov. 9, 1945).

3. R. Jepsen and M. Muller, "Enhanced Emission from Magnetron Cathodes", J. Appl. Phys. 22 No. 9, 1196-1207 (1951).

4. C. W. Hartman - Production and Interaction of Electron Beams in Crossed Fields, Electronics Research Lab. Report No. 10, Univ. of California (October. 31, 1960).

5. K. G. McKay, Advances in Electronics 1, 65 (1948).

6. J. H. deBoer and H. Bruining, Physica 6, 941 (1939).

7. E. A. Coomes, Phys Rev, 55, 519 (1939).

8. L. R. G. Treloar, Pro Phys Soc (London) B49, 392 (1937).

9. K. G. McKay, Phys Rev 61, 708 (1942).

10. Bruining "Physics and Application of Secondary Emission", Pergamon Press, London, 1954.

11. E. J. Sternglass, Phy Rev 80, 925 (1950).

12. E. M. Baroody, Phys Rev 78, 780 (1950).

13. A. J. Dekker "Secondary Electron Emission" in Solid State Physics (ed Seitz and Turnbull), vol. 6 (see figure 5, p. 266 and discussion which follows).

14. J. R. Young, Phys Rev, 103, 292 (1956).

15. V. A. Alekseyev and V. N. Lepeshinskaya English Translation. "Radio Engineering and Electronic Physics", No. 3. p. 502, March 1965.

16. V. A. Alekseyev and V. N. Lepeshinskaya. English Translation. "Radio Engineering and Electronic Physics", No. 3. p. 500, March 1965.

17. J. J. Scheer and J. Van Laar, Solid State Communications 3, 189 (1965).

18. L. Bl Hedrick and E. A. Lederer, Phys Rev 50, 1094 (1936).

19. Harold Jacobs, J. Appl. Phys. 17, 596-603 (1946).

20. G. H. Metson, Proc Phys Soc, 62, B, 589-591 (1949).

21. D. A. Wright, Brit. J. App. Phys. 5, 108-111 (1954).

22. L. S. Nergard, RCA Rev. XIII, 484 - 485 (1952).

23. S. Deb, J. Brit. Inst. Radio Engrs 14, 157-167 (1954).

24. T. Imai, Vide, Paris, 55, 384-393 (1955).

25. D. K. Das, 7th Annual Tube Techniques Conference, N. Y. (1960).

26. Yoshida, Shibata, Igarashi, Arata, J. Phys. Soc. Japan, 9, 640 (1954).

27. P. Wargo, W. G. Shepard, Phys. Rev. 106, 694-703 (1957).

28. G. E. Moore, J. App. Phys. 30, 1086-1100 (1959).

29. R. V. Stuart and G. K. Wehner, J. Appl. Phys. 33, 2345 (1962).

30. G. S. Anderson, W. N. Mayer and G. K. Wehner, J. App. Phys, 33, 2991 (1962).

31. G. K. Wehner, Annual Report on Sputter Yield, General Mills Inc. to Dept. of Navy Office of Naval Research Report No. 2136 Project 85037 Nov. 1960.

32. G. V. Jorgenson and G. K. Wehner, J. App. Phy 36, 2672 (1965).

33. O. Almen and G. Bruce, AVS Symposium p. 245 (1961).

34. C. Spindt and K. R, Shoulders, Rev. Sci, Instr., 36, 775, (1965).

35. K. W. Dudley, Secondary Electron Emission of Power Tube Materials, 7th National Conference on Tube Techniques, (Sept. 1964).

36. L. H. Germer and A. H. White, Phys. Rev., 60, 447-454 (1941)

37. P. Rapport, "Journal of Applied Physics", Vol. 25, No. 3, p. 288, March, 1954.

38. Private communication with M. C. Wittmer, Bell Telephone Laboratories, September, 1963.

39. G. J. Ogilvie, "The Surface Structure of Silver on Argon Ion Bombardment", J. Phys. Chem. Solids 10, 222-228 (July 1959).

40. The Effect of Various Gases upon the Emission of Impregnated Type Cathode. Vaughn, J., Dudley, K. and Lesensky, L., Report on Twentieth Annual Conference on Physical Electronics, March 1960 (M.I.T.)

Security Classification

DOCUMENT CONTROL DATA - R & D

(Security classification of title, body of abstract and indexing annotation must be entered when the overall report is classified)

1. ORIGINATING ACTIVITY (Corporate author)	2a. REPORT SECURITY CLASSIFICATION
Raytheon Company Microwave and Power Tube Division Waltham, Massachusetts	Unclassified
	2b. GROUP N/A

3. REPORT TITLE

Long-life Cold Cathode Studies for Crossed-Field Tubes

4. DESCRIPTIVE NOTES (Type of report and inclusive dates)

Final Report: 15 October 1965 to 31 December 1968

5. AUTHOR(S) (First name, middle initial, last name)

L. Lesensky; K. Dudley; H. Miller; M. Arnum; D. Das;
C. McGeogh; R. Handy.

6. REPORT DATE	7a. TOTAL NO. OF PAGES	7b. NO. OF REFS
September 1969	133	40

8a. CONTRACT OR GRANT NO.	9a. ORIGINATOR'S REPORT NUMBER(S)
DA28-043-AMC-01698(E)	PT-2202
b. PROJECT NO. 7900-21-223-12-00	
c.	9b. OTHER REPORT NO(S) (Any other numbers that may be assigned this report) ECOM-01698-F
d.	

10. DISTRIBUTION STATEMENT This document is subject to special export controls and each transmittal to foreign governments or foreign nationals may be made only with prior approval of CG, U.S. Army Electronics Command, Fort Monmouth, New Jersey, Attn: AMSEL-KL-TD

11. SUPPLEMENTARY NOTES	12. SPONSORING MILITARY ACTIVITY
Advanced Research Project Agency ARPA Order No. 345	U.S. Army Electronics Command Fort Monmouth, New Jersey 07703 AMSEL-KL-TD

13. ABSTRACT

The evaluation of prospective material for long life cold cathodes in crossed-field tubes has involved a materials investigation (Phase A), and the testing of cold cathodes in crossed-field amplifiers at medium to high power levels (Phase B).

The main thrust of the program has been to respond to the life-limiting characteristics of the oxide-containing cold cathodes in the electron and ion bombardment of a CFA. The pure (unoxidized) metallic cold cathodes have a longer life expectancy but a lower secondary emission ratio (and therefore lower available current) in a CFA.

Both the materials investigation phase and the tube evaluation phase of the program have demonstrated the advantages of thin films of Al_2O_3 and BeO, and impregnated tungsten, although exploratory experiments were also performed on other materials of interest, such as semiconducting diamond, boron nitride, silver-magnesium, and beryllium-copper. It was shown that dissociation of the oxide films caused by electron bombardment in an operating CFA can be overcome by providing a low pressure atmosphere of O_2 and that δ can thereby be stabilized at an acceptably high value over extended periods of time. CFA life tests of up to 1500 hours have confirmed the feasibility of this approach.

Our experiments indicated a tendency of δ to stabilize at a value intermediate between the maximum and minimum values found as a result of repeated electron bombardment dissociation and O_2-assisted regeneration of the surface oxides. This may be tentatively explained by assuming that, after much surface manipulation, a metal-rich film of only 2-3 atom layers forms at the surface, thus protecting the δ-enhancing oxide layer underneath from further dissociation.

The effects of typical tube gases other than O_2 on Be and Al cold cathodes were also investigated. The beneficial effects of H_2, CO_2, and N_2 on δ, observed particularly on Be cathodes, reminded one of the behavior of many metals which show a higher δ prior to degassing. The non-specific nature of the effect leads one to discount surface dipole effects but rather to suspect a connection with the known lowering of the photoelectric work function due to gas absorbed perhaps to some depth into the metal.

The work performed on the barium-calcium-aluminate impregnated tungsten cathode demonstrated its stability under electron bombardment and in actual CFA operation. During a 350-hr CFA test the emission current boundary stayed practically constant, the cathode not requiring any initial thermal outgassing and activation. The tungsten cathode impregnated with barium-calcium-aluminate is therefore believed to be activated by electron and/or ion bombardment by releasing Ba from the aluminate and enhancing its diffusion along the tungsten surface. The high stability of the impregnated tungsten cathode implies adequate reactivation kinetics.

Based on the results of this investigation, the following guidelines are presented for the optimum selection of CFA cold cathode materials.

δ Required	Average Emission Current Density Required	Recommended Emitter Type
> 2.4	< 15 mA/cm^2	Oxygen assisted Al or Be
1.9 - 2.5	< 30 mA/cm^2	Barium-Calcium-Aluminate impreg. Tungsten
≤1.9	- - - - - - - - - -	Pt

DD FORM 1 NOV 65 1473

Security Classification

Security Classification

14 KEY WORDS	LINK A		LINK B		LINK C	
	ROLE	WT	ROLE	WT	ROLE	WT
Secondary Emission						
Cold Cathode						
Crossed-Field Amplifiers						
Electron Bombardment						
Ion Bombardment						
Thin Films						
Aluminum Oxide						
Beryllium Oxide						
Barium-Calcium-Aluminate						
Dissociation						

INSTRUCTIONS

1. ORIGINATING ACTIVITY: Enter the name and address of the contractor, subcontractor, grantee, Department of Defense activity or other organization *(corporate author)* issuing the report.

2a. REPORT SECURITY CLASSIFICATION: Enter the overall security classification of the report. Indicate whether "Restricted Data" is included. Marking is to be in accordance with appropriate security regulations.

2b. GROUP: Automatic downgrading is specified in DoD Directive 5200.10 and Armed Forces Industrial Manual. Enter the group number. Also, when applicable, show that optional markings have been used for Group 3 and Group 4 as authorized.

3. REPORT TITLE: Enter the complete report title in all capital letters. Titles in all cases should be unclassified. If a meaningful title cannot be selected without classification, show title classification in all capitals in parenthesis immediately following the title.

4. DESCRIPTIVE NOTES: If appropriate, enter the type of report, e.g., interim, progress, summary, annual, or final. Give the inclusive dates when a specific reporting period is covered.

5. AUTHOR(S): Enter the name(s) of author(s) as shown on or in the report. Enter last name, first name, middle initial. If military, show rank and branch of service. The name of the principal author is an absolute minimum requirement.

6. REPORT DATE: Enter the date of the report as day, month, year, or month, year. If more than one date appears on the report, use date of publication.

7a. TOTAL NUMBER OF PAGES: The total page count should follow normal pagination procedures, i.e., enter the number of pages containing information.

7b. NUMBER OF REFERENCES: Enter the total number of references cited in the report.

8a. CONTRACT OR GRANT NUMBER: If appropriate, enter the applicable number of the contract or grant under which the report was written.

8b, 8c, & 8d. PROJECT NUMBER: Enter the appropriate military department identification, such as project number, subproject number, system numbers, task number, etc.

9a. ORIGINATOR'S REPORT NUMBER(S): Enter the official report number by which the document will be identified and controlled by the originating activity. This number must be unique to this report.

9b. OTHER REPORT NUMBER(S): If the report has been assigned any other report numbers *(either by the originator or by the sponsor)*, also enter this number(s).

10. AVAILABILITY/LIMITATION NOTICES: Enter any limitations on further dissemination of the report, other than those imposed by security classification, using standard statements such as:

(1) "Qualified requesters may obtain copies of this report from DDC."

(2) "Foreign announcement and dissemination of this report by DDC is not authorized."

(3) "U. S. Government agencies may obtain copies of this report directly from DDC. Other qualified DDC users shall request through _____."

(4) "U. S. military agencies may obtain copies of this report directly from DDC. Other qualified users shall request through _____."

(5) "All distribution of this report is controlled. Qualified DDC users shall request through _____."

If the report has been furnished to the Office of Technical Services, Department of Commerce, for sale to the public, indicate this fact and enter the price, if known.

11. SUPPLEMENTARY NOTES: Use for additional explanatory notes.

12. SPONSORING MILITARY ACTIVITY: Enter the name of the departmental project office or laboratory sponsoring *(paying for)* the research and development. Include address.

13. ABSTRACT: Enter an abstract giving a brief and factual summary of the document indicative of the report, even though it may also appear elsewhere in the body of the technical report. If additional space is required, a continuation sheet shall be attached.

It is highly desirable that the abstract of classified reports be unclassified. Each paragraph of the abstract shall end with an indication of the military security classification of the information in the paragraph, represented as *(TS), (S), (C), or (U)*.

There is no limitation on the length of the abstract. However, the suggested length is from 150 to 225 words.

14. KEY WORDS: Key words are technically meaningful terms or short phrases that characterize a report and may be used as index entries for cataloging the report. Key words must be selected so that no security classification is required. Identifiers, such as equipment model designation, trade name, military project code name, geographic location, may be used as key words but will be followed by an indication of technical context. The assignment of links, rules, and weights is optional.